

University of Michigan
Department of Mechanical Engineering
Cavitation and Multiphase Flow Laboratory

UMICH 014456-9-I

Liquid Jet and Droplet Impact

by

F. G. Hammitt

Supported by ONR Contract N00014-76-C-0697

March 1977

A. Liquid Erosive Wear: Theory and Test Devices

1. Introduction

Erosive wear of a solid surface can take place in a liquid or gaseous medium even without the presence of another phase in the fluid continuum.

However, it can be greatly accelerated by the presence of additional phases.

For the present purpose, we define "erosive wear" to be that provoked by fluid flow, and other than corrosion.

It includes particularly, then, the phenomena of solid and liquid particle

impact, where the particles may be carried by gas, vapor, or liquid, and liquid

"cavitation", which is essentially a phenomenon involving vapor "particles", i.e., pockets or bubbles, in liquid. Cavitation is not entirely analogous, however, to the

other droplet or particle impact phenomena, as will be discussed later.

The main purpose of this section is

to clarify "erosive wear" and its various facets. A more comprehensive review of the same subject is found elsewhere (1).

2. Mechanisms and Types of Erosive Wear

a. Erosive Wear Mechanisms

Since we have above excluded chemical or corrosive effects from the category of phenomena here dubbed "erosive wear", it seems reasonable to suppose that material removal for this category of phenomenon must be due to the imposition on the surface of shear or normal stresses of sufficient magnitude to cause material failure, either through single blows or through fatigue-type effects. Of course in most real situations chemical effects are not completely absent, although there are certainly many cases where their effects are relatively negligible. Further, in most cases of "erosive wear" the existence of a potentially damaging level of stresses can be rationally justified, as explained in the following.

b. Erosive Wear Phenomena

1) Single-Phase Flow

a) General - In the interest of a logical presentation, single-phase flow phenomena will be considered before multi-phase, even though the most important erosive phenomena for reasonably strong materials appear to require the presence of more than one phase of the fluid. Of course single-phase liquid flows are capable of river bank or beach erosion, e.g., but phenomena of that type are not the subject of this section. It is concerned rather with the erosive wear of engineering materials such as structural metals, plastics, ceramics etc. We are here considering such phenomena as liquid droplet impact in wet steam, e.g., to be a two-phase phenomena; similarly liquid or solid particle impact in an air or gas continuum. The jetting action of a fire-hose on the other hand, we would consider here to be a single-phase phenomenon, provided it did not involve entrained solid particles, vapor bubbles to provide cavitation, or other auxiliary wear mechanisms.

In the nature of possibly erosive single-phase phenomena, there is the possibility of either very high velocity flows of liquid, vapor, or gas, the latter two being relatively similar in their damage capability. Damaging stresses to be provided on a surface can be included within the categories of shear and /or normal stress. Solid surface shear should equal fluid shear at the fluid-solid interface, and would thus equal the product of viscosity and wall velocity gradient, i.e.,

$$\tau = \mu \left(\frac{\partial u}{\partial y} \right)_{\text{wall}} \dots \dots \dots (A-1)$$

where u is velocity component parallel to the surface, and

y is the distance from it, and μ the absolute viscosity.

Normal stress in the surface is numerically equal approximately to the fluid pressure at the surface. In the case of a steady-state impinging jet the maximum value this could attain would be the "stagnation pressure" in the fluid, i.e.,

$$\Delta p_{\text{stag}} = \rho V^2 / 2g \dots \dots \dots (A-2)$$

where V is the total fluid velocity, and

Δp_{stag} is measured above the ambient pressure.

In the case of a non-steady liquid jet, the pressure at certain points can attain the approximate magnitude of the "water-hammer" pressure, i.e.,

$$\Delta p_{W.H.} = \rho VC/g \dots\dots\dots (A-3)$$

where C is velocity of sound in the liquid. Of course "water-hammer" type phenomena are important with gas or vapor flows only if the ambient pressure is very large.

For relatively low velocity liquid flows, water-hammer pressure can reach values sufficient to cause material surface failure, and hence erosion.

A numerical example at this point may be useful. Suppose a flow of cold water of 500 f/s, which is a very high velocity for water flow. For the case where this flow is assumed parallel to a wall, assume the "boundary layer thickness" to be 10^{-4} ft., which seems about a likely minimum. Then the surface shear stress, stagnation pressure, and water hammer pressure are approximately as listed in Table 1, along with values for 1000 f/s.

	<u>500 f/s</u>	<u>1000 f/s</u>
Shear	1 psi	2 psi
Stagnation Pressure	1670 psi	6700 psi
Water-hammer Pressure	30,000 psi	60,000 psi

Table 1 - Numerical Example of Fluid Stresses ^{at} High Velocity in Cold Water

It is apparent from Table 1 that surface shear stress cannot be a damaging mechanism at velocities of interest unless the viscosity were extremely high. It also appears that in most cases the stagnation pressure is not sufficient to be damaging to most structural materials, so that high velocity

impacting liquid jets should not be damaging in most cases of engineering interest unless non-steady-state behavior is involved, in which case fluid pressures could attain values of the general order of the water hammer pressure. Another possibility exists if relatively large asperities exist on the surface. Stagnation pressure, rather than shear stress, could be exerted against these. The bending moment against an asperity of sufficient aspect ratio could cause a surface failure.

Examination of Table 1 and Eq. 1 and 2 indicate that it is most unlikely that either shear stress or pressure induced by gas or vapor flows could be sufficient to damage materials as structural metals, though gas velocities in some applications up to several thousand f/s are possible. The wall shear stress is \propto linear with velocity, so that even very high gas velocities would not raise this stress to damaging values. In addition the viscosity of most gases is much less than that of the cold water used in the Table 1 calculations. The pressure with gases or vapors is not likely to be damaging either, since they are proportional to density, which for gases or vapors is very much less than the cold water used for Table 1 (factor is $\sim 10^3$ between atmospheric air and water).

2). Actual Single-Phase Applications - Several single-phase flow applications in which erosive wear has sometimes occurred will be considered. For the most part these involve high-velocity water flows. However, even for these cases, a consideration of the possible normal and shear stresses induced by liquid flow seem to indicate that erosive wear is impossible in the absence of either corrosive effects, or multiphase phenomena such as cavitation, droplet impact, etc. Thus, in cases where erosion has in fact been observed in these applications, it is the author's opinion that one or more of these "extraneous" effects must have been involved.

i. Pelton (Hydraulic) Turbine

In this application water jets with velocity up to the order of 600 f/s impinge upon a rotating turbine wheel equipped with suitably designed "buckets", usually of hardened steel, perhaps of the 400 series. If the design is correct, no significant erosion occurs, at least for thousands of hours of operation. In some cases, however, prohibitive erosion does occur quickly. This is presumably due to such factors as improper blade design leading to cavitation on the blade surfaces, or perhaps to entrained sand in the impinging water. In any case, it is not, in the writer's opinion, single-phase erosion.

ii. Boiler Feed Pump

Modern boiler feed pumps also involve liquid velocities of the order 500-600 f/s. With proper design, again, no substantial erosion occurs. However, there are many cases on record where large erosion has resulted (Fig. 1, e.g.) in such pumps. This is usually presumed to be due to cavitation, even though it has occurred in some cases in the discharge casing, usually of the first stage. Cavitation in this region is possible, at least for off-design conditions. Again there is no plausible mechanism for erosion of these materials (probably 400-series steels) under the existing velocity conditions, except through cavitation and/or corrosion.

iii. Valve Seats

Very high velocities can exist across valve seats in some cases at least of the magnitudes previously discussed. Resultant erosion, sometimes called "wire-drawing", has been reported for both liquid and steam valves. The materials are often hardened steels. Again no plausible mechanism for erosion exists unless there is either substantial corrosion (unlikely for proper material choice), or multiphase phenomena are involved such as cavitation (for liquid-handling valves) and possible water droplet impingement for steam valves, assuming that wet steam may be involved.

3. Multiphase Flow

a) General - As indicated in the foregoing it seems most probable that in most engineering cases involving erosive wear, multiphase flow phenomena must be involved. These can involve a liquid gas or vapor continuum with solid or liquid particles (droplets), or a liquid continuum with entrained vapor (cavitation), or entrained gas. These cases will be discussed briefly in the following with reference to the stress-raising mechanisms involved.

b) Solid Particle Impingement - High velocity solid particle impingement can certainly provoke erosive wear in many well-known cases, e.g. dust erosion of helicopter blades, propellor blades, helicopter drive gas-turbine compressor blades, etc. In these cases, the phenomenon involved is that of the rapid motion of the eroded material through a continuum of gas with entrained solid particles. Other less clearcut cases involving erosive solid particle impingement are liquid or gaseous slurry flows. Applications are involved in the beneficiation of coal, ore-bearing pipelines, etc. Tests have indicated that such flows are far more erosive than single-phase flows of the same velocity but the precise mechanism of erosion at this point is not entirely clear.

The state of the art at this time does not provide methods for specifying the state of stresses on the eroded material surface (even to the extent possible for liquid impact) resulting from impact by particles of irregular shape, which is the usual case of interest. It is of course obvious that both shear and normal stresses of substantial magnitude will be provoked by such impacts, but no generalized governing relations are as yet available to the author's knowledge.

The situation for slurry erosion is even more obscure than that for direct solid particle impact with respect to being able to specify the material or the detailed mechanisms causing the erosion. This is particularly true for liquid slurries, since the velocities are normally relatively low so that stresses

from direct impact should not be of damaging magnitude. An extremely damaging situation, nevertheless, is that provided by cavitating slurries which have sometimes occurred in pumps (dredging pumps, e.g.) or in solids-bearing transport pipelines (ore-bearing, e.g.).

c) Liquid Droplet Impingement - Liquid droplet impingement erosive wear applications usually involve the rapid motion of the eroded material through a gaseous or vapor continuum with entrained liquid droplets. Important examples are the motion of high-speed aircraft or missiles, or propellor or helicopter blades, through air, or the motion of steam turbine blades through a vapor continuum including relatively large water droplets. A somewhat similar situation can occur for aircraft gas turbine compressor blades under atmospheric rain conditions. Inverse cases, where the droplets are projected against relatively stationary target materials, are not usual because it is not generally possible to accelerate liquid droplets of potentially damaging size to damaging velocities without droplet disintegration, i.e., a critical Weber number from the viewpoint of droplet stability is involved.

The stress regimes applying for liquid droplet impact erosion can be estimated much more closely than those applying for the solid particle or slurry cases discussed above. In general, the order of magnitude of normal stresses can be obtained from the water hammer relation (Eq. 3). Some improvement can be made if the result is corrected for the non-rigidity of the target material and for the effects of liquid compression on liquid sonic velocity and density. Droplet shape also affects the stress regime, as shown by various recent numerical and experimental studies, some from our own laboratory (2-4, e.g.). The last of these is a numerical study where the target material was assumed elastic rather

than rigid as in the earlier cases, so that realistic target material stresses could be computed (4). However, the precise state of the analysis of liquid droplet impact is beyond the scope of the present chapter, and will not further be discussed here. Suffice it to say that the general level of stress magnitudes computable (and measured) for this case is sufficient to explain and justify the erosion observed.

Another interesting point which can be made with regard to droplet impact erosion is that radial velocities along the impacted surface are generated by droplet impact which can be several times the original impact velocity. It has been ~~suggested~~ that the shear stress caused by this high-velocity flow parallel to the surface might contribute importantly to the damage. However, this hypothesis seems unlikely considering the numerical results in Table 1 and the form of Eq. 1. Even though the radial velocity in an extreme case might be 10 times that used for the example of Table 1 (500 f/s), the shear stress induced by this flow would still be very small, since it is proportional only to velocity to the first power. However, the impingement of this high-velocity radial flow against a small asperity raised from the surface could create failure stresses. This process as well as that of the droplet impact in general is well-illustrated in Fig. 2 (from ref. 5). This handbook article co-authored by the present writer summarizes the droplet impact and cavitation processes here discussed.

d) Cavitation - Whereas droplet and solid particle impact involve liquid and solid particles respectively in a gas or vapor continuum, cavitation involves vapor (with some gas content) "particles" in a liquid continuum. However, since these "particles" involve only relatively low density material with little mass, their "impact" with target material is not in general a likely cause of erosion; rather it is a case of the highly-specialized phenomenon of bubble collapse, discussed in Chapter IV. Of course, this statement may not apply to the combined phenomenon case of a cavitating slurry (mentioned

Though particle impact per se is not the presumed cause of cavitation erosion, a combination of shock waves in the liquid, and liquid "microjet" impact upon the eroded surface, seem ^{to} represent at this time, the most likely detailed mechanism for cavitation erosion. This problem is thoroughly discussed in Chapter IV of the present work as well ⁱⁿ ~~as~~ the book Cavitation (6) and summarized in ref. (5), as well as in numerous research articles too numerous to mention here. Bubble collapse adjacent to a surface with development of liquid microjet is shown in Fig. 3 (ref. 5). The shock waves emitted during the bubble "rebound" (7, eg) which often follows original collapse (Fig. 4) are believed to provide in many cases important assistance to the damaging process originating from the microjet impact. At least the liquid pressures upon a neighboring wall during bubble collapse appear to be considerably less than those during rebound (8,9, eg), and appear to be in fact of sufficient magnitude to contribute to damage for most materials.

Actual calculation of the stress regime applied to an eroded surface by cavitation is not possible in the present state of the art. This is not surprising when one considers the complex mix of processes which are involved (not to mention the important contribution of corrosion in many cases). The problem of stress calculation appears even more difficult, as compared with that of droplet impingement, when it is realized that the size and position of the collapsing bubbles, to which the damage is presumably due, is not fixed or well known in most cases. Natural cavitation fields include bubbles covering a large range of diameter. In the usual engineering case, neither range of diameter, distribution over this range, or number of bubbles involved is known to any degree of precision. Hence, for the general engineering case, estimation of the stress regimes to which a cavitated surface will be exposed by a given flow regime is essentially impossible, whereas for the droplet impact case quite

reasonable estimates can be made, as previously discussed. For laboratory cavitation erosion test devices, the situation is only slightly less obscure (depending upon the type of test device) as will be discussed later. While from numerical analyses (6,8-10, eg) it can be shown that the potentialities for sufficient stress magnitudes to account for the observed damage exist, it is still true that the best evidence of the stress regimes to which cavitated surfaces have been exposed can be obtained from examination of the damaged surfaces themselves. or (more difficult to achieve) damage debris. Since the damaged surfaces from cavitation and droplet impact often have very similar appearance, it can be presumed that the two processes are quite similar in their effects upon surfaces. Of course in most cases the attack by cavitation is on a smaller and finer scale so that individual-blow craters from cavitation have a diameter typically of only a few mils (11, e.g.), and it appears that the microjet diameter is typically only a few microns (12, e.g.). Typical individual-blow cavitation craters on stainless steel are shown in Fig. 1. In a typical case such craters presumably cover the entire surface by an essentially "random" bombardment, until large scale fatigue failure eventually occurs, producing eventual large-scale failure (Fig. 1).

3. Erosive Wear Testing Devices

a. Applications

The applications for erosive wear testing devices can be sub-divided in the following manner. This division is not entirely parallel to that based on erosion phenomena previously discussed, since the test devices attempt in general for practical reasons, to model one primary factor of the application involved, rather than the phenomenon itself.

1) High fluid velocity devices where "single-phase" erosion only is to be evaluated. If cavitation or droplet or particle impact occurs, it is unintentional, but may be instrumental in the results. Such devices are intended for the study of erosion in steam or liquid ("non-cavitating") valves, i.e., "windrawing", boiler feed pump casings, etc.

2) Solid particle or droplet impact devices wherein the material to be eroded traverses rapidly a field of essentially stationary particles or droplets. In most cases the target material is whirled through a field of falling particles or droplets, but in some cases translational motion rather is used. In some cases liquid jets rather than droplets are impacted. Impacting liquid devices can sometimes generate secondary cavitation, which may contribute importantly to the damage, but usually this is not intentional.

3) Flowing cavitation devices wherein cavitation is caused by converting pressure "head" into kinetic "head". Numerous geometries have been used for this purpose as will be discussed later. In general these could be characterized under the terms "venturi", "rotating disc", and "miscellaneous". These devices are meant to obtain cavitation erosion under flow conditions as realistic as possible, since damage modelling laws are highly uncertain.

4) Vibratory cavitation devices wherein cavitation is provoked in an essentially static fluid, as opposed to the flowing cavitation devices discussed above. Such a device, sometimes called "magnetostriction" or "ultrasonic" tester, relies usually on the rapidly reciprocating motion of a submerged test plate, at relatively high frequency, to provoke cavitation by pressure oscillation in an essentially static liquid. The necessary pressure oscillation is due to the very high acceleration imposed upon the liquid ^{by the vibration.} This type of device is used for the study of cavitation damage, since it is the most economical, both for purchase and operation, of the possible cavitation damage test devices. It also is a strongly "accelerated" device in that it can provide substantial damage on even the most resistant of materials within relatively short test periods. However, its major disadvantage is that it does not, by its nature, relate cavitation damage to flowing system parameters such as velocity and pressure, so that the conversion of "vibratory" results to projected performance in field devices is extremely uncertain if not impossible.

b. Actual Test Devices

1) High-Velocity Single-Phase Erosion Wear Test Devices

Various tests have been made at ^{various} times to evaluate high velocity single-phase erosion in cases where this has occurred in field machines, so that laboratory tests seemed warranted. However, no relatively standardized machine of this type appears to exist. A case in point was the work at Detroit Edison in the 40(s) to evaluate erosion in boiler feed pump casings and regulating valves (13,14, eg.) which were exposed to relatively high velocity but, supposedly not cavitation. Some corrosive contribution no doubt was also included with some of the materials used (carbon steels, etc., but also including the 400 and 300 series later used in this application). High velocities (~ 60 m/s) were attained by accelerating the pressurized water through a small slit formed by the materials to be tested. Back-pressure was limited by the equipment available for the test, so that although the absence of cavitation was one of the test objectives, it is nevertheless quite likely, in my own opinion, that it contributed importantly to the results, which included considerable erosion of most materials tested. As previously discussed, without cavitation (or corrosive attack, probably not important for the stainless steels tested), there is no plausible mechanism to explain the erosion observed.

Other partially pertinent cases in point are the "rotating wheel" devices developed originally in the 1930(s) probably first by Ackeret and de Haller (15). This device is shown schematically in Fig. 6 (from Ref. 6), and consists of a rotating "wheel", to the periphery of which the specimens to be eroded are attached. These are rotated through a relatively low velocity water jet with direction parallel to the wheel axis. Since the impact velocity for these devices is typically no more than 100 m/s, it is difficult to explain the rapid erosion of some of the hardened materials tested without the contribution of

local cavitation, as well as liquid impact. According to Table 1, the "water hammer" pressure for this device at 100 m/s would be $\sim 29,000$ psi (2000 bar), but even materials such as stellite are rapidly eroded. These devices were originally developed to study erosion of impulse hydraulic turbines such as "Pelton wheels". It was assumed then that this erosion was of similar nature to that encountered in large steam turbines (which is now clearly known to be a case of liquid droplet impact). Actually the Pelton wheel erosion is probably mainly due to cavitation, but involves a very high liquid velocity parallel to the blading surfaces, as previously discussed. Thus, since this rotating wheel test device was developed to study Pelton wheel erosion, which at first glance appears a case of high-velocity single-phase erosion, its introduction in this article at this point is pertinent.

2) Solid Particle or Droplet Impact Erosive Wear Test Device

Various devices of this type have been developed and used over the years, including the relatively low velocity "rotating wheel" device discussed above (Fig. 6). In recent years, solid wheel devices for rotating speeds up to perhaps 500 m/s have been built in various laboratories throughout the world, particularly for the study of the droplet impact problem existing in the low pressure end of large steam turbines. These more modern wheels are generally enclosed within a strong steel casing, both for protection in case of failure, and to allow operation under vacuum, both to model more closely the steam turbine problem, and to reduce drive power for the device. Relatively low velocity liquid droplets or jets are caused to impact the rotating test specimens. Various test facilities of this type, existing in England, are well described in ref. 16, e.g. Somewhat comparable facilities also exist in this country and in Russia, but little descriptive data has yet been published.

In addition to the wheel devices described above, designed particularly for the steam turbine application where the materials to be tested are generally of highly resistant nature such as stellites, hardened steels, etc., another group of facilities has been developed in recent years for droplet impact erosion testing, both in this country and Europe, of aircraft and missile component materials where the application is "rain erosion", i.e., the erosion encountered when such components are flown through rain storms. For applications where the flight velocity exceeds Mach 1 (~ 350 m/s) particularly, erosion can occur very rapidly, since the materials involved are not optimum for erosion resistance, but are rather chosen for other prerequisites, i.e., for radomes, propellor or helicopter blades etc. For this application, rotating arms rather than disks are normally used. Relatively large diameters, and hence low rpms usually required for such a test device, since very large "g" loads must not be imposed upon the test materials. This requirement is obviously not of such great importance for the very strong metallic alloys to be tested in the turbine application. Also required test times for the aircraft type device is obviously much shorter. The largest and highest speed such device (~ 900 m/s), is that at Bell Aerospace (17). The diameter of the rotating element is ~ 7 m. The rotating arm at WPAFB* is shown in Chapter VIII.

Another type of device for the study of air and missile component rain erosion resistance at very high velocity is the rocket sled, where test materials can be driven through an artificial rain field. The largest such device to the writer's knowledge is that at Holloman Air Force Base (18,19, eg) where test velocities up to \sim Mach 5 (~ 1700 m/s) have been utilized. This type of device allows higher velocities than do rotating arm devices, which are limited by centrifugal stresses in the arm. The rocket sled has the advantage of allowing the test of many material specimens in a single run, and hence under precisely identical conditions. However, the test is relatively

expensive, and has the disadvantage that intermediate observation of the progress of erosion is not practical.

Many of these aircraft component test devices have also been used for dust erosion tests, which is an important present day problem for such applications as helicopter blades.

3) Flowing Cavitation Devices

a) General and Miscellaneous - Flowing cavitation erosion test devices include machines involving both rotating elements and translatory flows. In general, these are well described in ref. 6 from which some of the illustrative figures here used will be taken. No really standard device has yet devolved in this field, and a variety of devices have been used. These can be considered under the main headings of "venturi" and "rotating disc" devices. However, there exist several miscellaneous devices such as test specimens submerged in large water tunnels (used by Knapp - ref. 6) and a vibrating reed in a flowing stream (20), e.g. However, since these and other miscellaneous devices are not of major importance to present-day cavitation damage evaluations, they will not be discussed further here.

b) Venturi Devices - Venturi devices are here taken to include all those flow devices employing a flow restriction to convert pressure into kinetic head, creating a cavitating region when the static pressure falls to the level of the vapor pressure. For damage studies, relatively standard venturis (Fig. 7, University of Michigan, e.g.) as well as several quite special designs have been used. Of these the earliest is probably that of Boetcher reported in 1936 (Fig. 8 from ref. 6, see also ref. 21. As will be noted from Fig. 8, the arrangement is such that the cavitating jet impinges upon the test specimen. Such a venturi geometry does in fact provide a very intense damaging regime, as compared, for example, to the University of Michigan design (11, Fig. 7), which, however, does model more closely the usual flow conditions found in hydraulic machines. (Table 2, from Ref. (22).

Another special damage venturi design which has been used fairly broadly in various countries since its introduction in 1955 (23) is that of Shal'nev (Fig. 9) in Moscow. The flow geometry consists of a rectangular throat of constant flow area across which a small cylindrical pin is placed. Cavitation occurs in the wake of this pin, and the damage specimens are located flush with the wall and downstream of the pin (Fig. 9). The damaging intensity induced by this geometry is also much higher than the University of Michigan design (Fig. 7). However, the flow regime is that of separated vortices which may model a relatively special type of cavitation quite closely, but is not particularly similar to the more usual flow regimes encountered in flow machinery.

c) Cavitating Disk Devices - A "rotating disk" device developed for the study of cavitation damage was reported (24) in 1955 by Rasmussen (Fig. 10). The flow geometry consists of a flat disk, fitted with pins or through-holes at various radial locations. The disk is caused to rotate in the test liquid which is contained within a circular casing. The casing is fitted with radial baffles to prevent gross rotation of the overall fluid. The traverse of the disk pins or holes through the relatively quiescent surrounding liquid causes cavitation clouds which follow the rotating disk and collapse upon test specimens fitted flush with the disk surface. Figure 11 (from ref. 6) is a schematic of a more recent rotating disk facility built by Pratt and Whitney Aircraft for eventual use with liquid metals (25). Eroded specimens of refractory metal are also shown in Fig. 11.

This type of facility also produces damage very rapidly, more so than the Boetcher and Shal'nev types of venturi (Table 2). In all these cases, however, the flow regimes involved are really quite different. By its very nature that provided by the rotating disk resembles closely that involved for regions of separated flow in turbomachines.

Another valid comparison between these flowing damage tests is the expense of the facilities involved. The venturis obviously require a loop facility with driving pump and much other instrumentation and controls. The rotating disk, however, is not a simple or cheap facility in itself, as can be seen from Fig. 11 which shows the actual design drawing for the Pratt and Whitney device (25). An accurate statement comparing the cost of rotating disk and venturi damage facilities is not possible at this time, since too many unknown and complicating factors are involved. However, it is certainly true that the vibratory type of damage devices, to be discussed next, are considerably more economical, certainly in first cost. Operating costs, primarily that of operator salary, are probably similar. Length of test required for a given material, i.e., damage intensity (Table 2), for the vibratory device covers the same general order as the others.

4) Vibratory Cavitation Devices

The vibratory type of cavitation damage test, already described, is certainly the simplest, cheapest, and most common of all presently known cavitation damage test devices. It is also capable of providing erosion rates of the same general order as the flowing systems already discussed. It is also the only one for which an ASTM Standard Method has been promulgated (26). Figure 12 (from ref. 6) is the schematic of the University of Michigan device of this type which is designed for a variety of liquids, temperatures, and pressures. This unit is somewhat more complex than the standard ASTM device (26), since the open beaker is replaced by a sealed tank. This type of test device is most useful for comparison of material resistances, evaluation of effects of different fluids, temperatures, and pressures, but it is not suitable for evaluation of probable cavitation erosion in the usual fluid-handling machine, since the very important flow parameter of velocity is not modelled. In the present state of the art it is thus not possible to predict damage in a flowing situation from vibratory test results. Recent work in the writer's laboratory and elsewhere (27-30, eg) to correlate the damage rate from such a device with bubble collapse pulse counts measured by an acoustic probe show some positive correlation. (discussed later)

Variations of the vibratory device have been used (but not yet standardized), wherein a cavitation field is provided by the vibrating horn, but the specimen to be tested is held stationary in the cavitating horn. The specimen to be tested is held stationary in the cavitating field rather than attached to the end of the vibratory horn, as in the standard arrangement. This arrangement is useful for the testing of materials which cannot be vibrated by the horn without deleterious extraneous effects. Since the stationary specimen is usually located with only a small clearance from the vibrating horn, this stationary specimen test geometry is useful for the testing of materials for bearings, since the bearing geometry is well modelled even though the effects of velocity are absent.

4. Conclusions

Fluid-induced erosion, both single and multi-phase, has been considered according to the various phenomena from which it may be generated. These include both simple high-velocity single-phase flows, and also liquid and solid particle impact, as well as cavitation. These latter phenomena are considered as multi-phase in nature. It is concluded that in cases of engineering interest there is no plausible mechanism for single-phase erosion of relatively strong materials unless essentially multi-phase phenomena as droplet or particle impact and/or cavitation are present. Finally, the various types of erosion testing devices are considered and described as to their range of utility, limitations, and relative merits. Further discussions of these test devices is provided in Chapter VIII.

B Basic Cavitation Damage Mechanisms and State of Art

1. INTRODUCTION

It is generally recognized today that the flow phenomenon called "cavitation", involving a generally heterogeneous mixture of vapor and gas pockets or "voids", some of which can be approximately described as bubbles, frequently causes a rapid erosion of adjacent material structure. ^{This is} often much more rapid than would be expected for single-phase flow erosion or corrosion for the same conditions of velocity, temperature, and turbulence. While rapid erosion or damage is only one observable result of this flow condition, it is the one with which this chapter is primarily concerned.

There is at present an enormous body of research literature concerned with the processes of bubble collapse and cavitation damage. This has accumulated at an increasing rate since the pioneering work of Rayleigh⁽³¹⁾ in 1917. It is the purpose of the present section to briefly summarize the significant results of the very considerable research which has been concentrated on this problem over the years, both from the viewpoint of basic understanding of the phenomenon and of practical information of use to the designer of fluid machinery.

In spite of more than half a century of research there is still only a very incomplete understanding of the mechanisms by which a "cavitation field" causes rapid damage to adjacent solid material. Hence, it seems logical to start this discussion by listing those points which seem to be clearly and directly based upon observations or experimental measurements, and thus appear at present to be essentially indisputable. These basic experimental observations lead to simple theoretical concepts from which apparently clear and incontrovertible ideas are generated. From this point of common agreement, more complex theory and

less definite experimental observations lead to more speculative concepts regarding the detailed mechanisms of cavitation damage, until an area is reached where no general agreement exists. For previous partial summarization of similar material see refs. 6 and 3.

The foregoing relates primarily to the basic understanding of the phenomenon of cavitation damage, considered primarily from the viewpoint of fluid mechanics rather than material reaction. So far, this basic approach has produced only scattered practical information of utility to the fluid machinery designer. Hence, as in many fields of engineering, it has been necessary to formulate semi-empirical relationships and general rules for the use of the designer, using the specialized test results which have become available. Generally these attempt to predict, with varying degrees of precision, the effect of various independent variables upon cavitation damage in real situations. In a fully-developed form such relations must involve both fluid and material behavior, since significant coupling between these often exists in the real situation. This body of semi-empirical knowledge will be very briefly reviewed and avenues for use of future research in these areas discussed.

2. COMMONLY AGREED BASIC PRINCIPLES RELATED TO CAVITATION DAMAGE

a. Primary Experimental Facts and Conclusions

It is first necessary to review various well-known indisputable experimental facts upon which the ^{consideration} of cavitation damage must be based. These are primarily the following:

1) General Observations

Rapid pitting and erosion often occur in flows where cavitation is observed to exist. Its existence can be determined audibly, by acoustic instrumentation, visually if windows in the containment systems are provided machine vibrations, or through decrease or other change in performance from the single-phase flow condition. For example, a

measurable decrease in head is produced from a cavitating centrifugal pump for a given flow and rotating speed. If the cavitation region in a fluid machine is observed visually, it appears as a "frothy" region. If optical instrumentation of suitable time and space resolution is used, it is found that the "frothy" region is actually composed of a heterogeneous mixture of odd-shaped "voids", many of which are roughly spherical bubbles. In some cases a relatively clear cavity attached to the structure is found, but this is then often ^{and followed} surrounded by a "frothy" region of traveling "voids". In a cavitating flow the rate of attack can be many times that due to erosion and corrosion alone in the absence of cavitation.

ii) Cavitation can damage, under certain conditions, even the strongest of materials such as stellites, tool steels, and any other known structural materials. This damage can occur rapidly even in cases where chemical corrosion in single-phase flow with the same liquid-material combination would not be significant, e.g. cavitation in petroleum products on metals or glass.

iii) Cavitation pitting shows the characteristics of mechanical attack. Such well-known mechanical manifestations as e.g., slip lines in metals, have frequently been observed. The single craters which are formed in the early portion of the attack appear under a low-power microscope as "moon craters", ^{i. e.,} more or less symmetrical craters often with a raised rim, as if formed by single impact rather than corrosion. In fact, damage to materials from liquid impact tests closely resembles cavitation damage both qualitatively and quantitatively.

iv) Mechanical cavitation attack and corrosion can supplement each other through obvious mechanisms resulting in a damage rate increase, in cases where both are important, to many times the sum of damage rates from corrosion and cavitation acting separately and independently.

v) An important theoretical contribution to the development of the concept of the mechanical cavitation damage mechanism was given by Rayleigh.⁽³¹⁾ He showed^(see also Chapter IV) that a collapsing spherical vapor bubble has the potential for generating extremely high pressures and velocities in the fluid near the point of collapse. The original analysis, based entirely on ideal fluid concepts including that of spherical symmetry, shows that these quantities, i.e. pressure and velocity, become infinite. Thus, while more realistic assumptions are required to evaluate pressures and velocities quantitatively, it is apparent that the possibility exists for values large enough to be damaging even to very strong materials.

Certain obvious and important conclusions can be drawn from the general observations noted above. They primarily apply to cases where mechanical effects predominate, although as has already been mentioned it is evident that if corrosion effects are significant, they too can add greatly to the overall damage rate.

2) Conclusions from General Observations

1) Since observed cavitation fields usually contain large numbers of essentially spherical bubbles of various diameters, and since as Rayleigh showed⁽³¹⁾ the collapse of such bubbles could create pressures and velocities large enough to be damaging, it is likely that the surface of a material exposed to cavitation will experience a multiplicity of impulse impositions of widely varying intensities and with locally random spatial distribution. The Rayleigh theory⁽³¹⁾ shows that the / ^{duration} of imposition of such impulses due to individual bubble collapses is extremely short. Furthermore, the impulse magnitudes and collapse times are greater for larger bubbles for a given collapsing

pressure differential. Since individual symmetrical craters are observed, it is apparent that some of these impulses are sufficient to cause permanent material deformations. Since the spectrum of impulses varies widely, it is to be expected that individual craters with diameters covering a given range will be formed, (as has been observed (33,34, eg.) and that in fact many "blows" (i.e. impulses) may be of insufficient strength to cause permanent material deformation. A large number of these weaker blows, however, may be sufficient to also contribute to eventual fatigue failure. Thus it is to be expected that cavitation damage will often eventually take the form of fatigue failures, and this is in fact observed. The concept of a spectrum of blows resulting from a spectrum of bubble sizes and locations is well summarized by Fig.13, previously published by the author to describe cavitation damage in a venturi.⁽³⁴⁾

ii) As the surface roughness increases due to accumulated cavitation (or corrosion) damage, the flow pattern near the surface will frequently be importantly altered. In addition the substantial cold-working of the material surface may affect its ability to resist further damage (increased strength and hardness will tend to increase its damage resistance while increased brittleness will have the opposite effect). Thus it is to be expected that the rate of cavitation damage in a given situation will not be constant with time. Often an "incubation period" is observed before substantial material loss occurs, presumably while fatiguing processes proceed to a point necessary to cause failure. The damage rate then often increases to a maximum after which it decreases. Later secondary and tertiary, etc. maxima may occur. This behavior probably depends primarily upon the interplay of flow pattern alteration by virtue of accumulated roughness and material surface property changes which are themselves due to the accumulated permanent deformations and stressings. This general situation is well described in ref. (5).

b. More Speculative Observations and Conclusions

It will be noted that the foregoing generally agreed concepts relating cavitation damage do not attempt to specify the detailed mechanism whereby bubbles collapsing in the liquid continuum can damage materials submerged in or containing the liquid. It has been stated already that a simple ideal fluid analysis (31) shows that very high pressures and velocities may exist for a very short time period over a very small space around the center of collapse of the bubble if this collapse proceeds with spherical symmetry. The detailed mechanisms whereby the material surface of even very strong materials can be stressed sufficiently to cause damage was left ambiguous, since this is an area where at present agreement does not exist. However, certain additional items of experimental and theoretical evidence can be presented to throw some light on the probable mechanisms involved. Some of these additional items are discussed below.

) In typical situations only one out of perhaps ten thousand bubbles seen to collapse close to a surface actually causes a crater (35,36, eg.) though such craters, judging from their symmetry and unchanging contours with additional exposure⁽³⁴⁾, result from individual bubble collapses. However, in very carefully controlled laboratory conditions, even in a flowing system such as a venturi, a one-to-one correspondence between bubble collapses and observed craters can be attained if all parameters are adjusted precisely correctly.^(37,38) These facts seem to indicate that some very selective mechanism is involved in delineating damaging from non-damaging bubble collapses. The model of symmetrical bubble collapse provides only bubble diameter and ^{wall} distance as "sorting" parameters, while an additional sorting parameter exists, i.e., orientation, if the collapse is non-symmetrical.

Intuitively, this latter factor seems more consistent with the very large ratios of damaging to non-damaging collapses ^{which are} observed.

ii) The collapse of bubbles with approximate spherical symmetry through a radius ^{i.e. change in radius,} ratio ⁽³¹⁾ sufficient to generate damaging pressures according to the Rayleigh analysis ⁽³¹⁾, close enough to a material surface so that damage might occur, and in real flow situations involving pressure and velocity gradients, turbulence, etc. seems unlikely. This statement is based upon excellent photographs which generally have been obtained quite recently ⁽³⁷⁻⁴²⁾ as well as theoretical analyses. ⁽⁴³⁻⁴⁶⁾

Wall effects, pressure gradients, gravity, and initial motion are all sufficient to radically change the mode of collapse from one of approximate spherical symmetry to an approximately toroidal collapse wherein the bubble is apparently pierced by a small microjet of liquid before the bubble volume has been reduced by more than a factor of 10 to 100. This type of collapse is shown clearly in recent pictures (Fig. 14) obtained in our laboratory ^(37, 38) for bubbles collapsing in a venturi adjacent to a knife-edge which is aligned parallel to the flow.

iii) Theoretical analyses of bubble collapse assuming spherical symmetry but real fluid parameters such as viscosity, surface-tension and compressibility ^(8, 9, eg) indicate that the pressures around a collapsing bubble at a minimum distance of the initial bubble radius from the center of collapse, i.e. the minimum possible distance from the collapse center to the wall to be damaged if the collapse center is stationary, are not sufficient to explain the damage observed on most materials. However, if the bubble rebounds from a minimum volume condition as it theoretically would if it contained some non-condensed gas or vapor, the calculated

pressures are greater in the surrounding liquid, so that damage from this mechanism becomes more likely. Also, theory indicates that the center of a collapsing bubble will tend to move toward an adjacent wall (or away from a free surface) during collapse. No realistic analysis has yet been made to show how important such movement might be in the consideration of damage mechanisms, though an analysis assuming the bubble to remain spherical during the motion,⁽⁴⁷⁾ shows a significant effect upon the pressures exerted on the wall.

Motion picture sequences of collapsing bubbles often show rebounds, i.e. growth of the vapor mass after passing through the minimum volume condition, though not usually as spherical bubbles.^(37, e.g.) A rebound would be theoretically expected if the bubble contained trapped gas (or vapor which behaves as gas during the very short critical portion of the collapse which may last only about a microsecond.) Also in some cases the pressure distribution around a bubble moving at considerable velocity relative to the fluid,⁽⁴⁴⁾ may have the same effect. However, a rebound is even more likely if the bubble collapses in a toroidal mode, since the centrifugal pressures around the vortex ring provide a restoring mechanism in much the same fashion as trapped gas.

Individual craters caused by cavitation are often very similar to craters generated by the impact of high velocity liquid. This similarity is especially striking if one compares the craters formed by actual liquid droplet impact on plexiglass (Fig.15) with those from cavitation in a venturi (Fig.16),^{obtained in our laboratory} since the damage pattern for droplet impact on plexiglass is rather unique, having an undamaged center area surrounded by an annular failure area. Another crater configuration illustrative in this respect

was obtained in our laboratory from venturi cavitation upon stainless steel plated with a very thin coating of cadmium (Fig. 17). The cadmium is completely removed in the center so that the underlying stainless steel is exposed. This region is surrounded by an annular area where the cadmium is partially removed, suggesting the impact of a liquid jet which then accelerates radially after impact (a common observation for the impact of actual liquid jets⁽⁴⁸⁾), and "washes" away the thin cadmium plate. It is difficult to imagine a similar result caused by the imposition of a spherical shock front which would merely press the cadmium plate deeper into the surface, leaving a crater within which the cadmium plate would remain on the surface. This was confirmed^{here} in an experiment wherein hard steel balls were impacted upon the surface at high velocity (~ 100 m/s)

The foregoing points all tend to indicate the probability that in most engineering situations the mechanical portion of cavitation damage is due more to the impact of a high velocity microjet upon the damaged surface than to the imposition of shock waves in the liquid emanating from the center of collapse of a spherically collapsing bubble, as Rayleigh⁽³¹⁾ assumed. However, even if the bubble does not collapse spherically, the liquid pressures will rise substantially around the bubble as the volume is significantly reduced from the initial value. Intuitively, the pressure rise will be less the greater the departure from spherical symmetry, and the collapse will generally be slower although local pressure rises due to the asymmetry might be greater in the non-symmetrical case. Also, a given diminution of volume in an ideal fluid will produce the same total kinetic energy in the fluid for both symmetrical and non-symmetrical cases, since this is equal to $(p_{\infty} - p_v) \Delta V^*$ for the bubble.⁽⁴⁹⁾ Unfortunately, little quantitative information pertinent to this highly complex problem yet exists. Nevertheless, in real cases if liquid microjet damage appears to be the most important mechanical damage component, it is also likely that the pressure rise

* p_{∞} is upstream pressure and p_v is vapor pressure.

around the collapsing bubble caused by the reduction of bubble volume according to the Rayleigh mechanism may also be an important damaging mechanism. It must be admitted that both schools of thought on the relative importance of likely damage mechanisms exist at present.

An indication that very high pressures (and hence temperatures) do sometimes exist within collapsing bubbles is afforded by the observation of "sonoluminescence". An indication that thermal effects are of substantial importance in this phenomenon has been provided.^(50,51) However, there is no indication^(52, 53) that bubble collapse through the large radius ratio required to compress trapped gas to the extent necessary to cause luminescence can occur near enough material surfaces to cause damage, since such a collapse requires a highly symmetrical environment. Schlieren and interferometric pictures have succeeded in showing strong density gradients or shock waves in the liquid around collapsing bubbles.^(52, eg)

Another manifestation of cavitation damage which is sometimes observed that is difficult to either in terms of shock wave effects or microjets is that of "worm-hole" pits, i.e., very deep curving pits of a large length/diameter ratio. While chemical effects are probably predominant in this phenomenon, ^{they} / may also be the result of (a) a wave-guide effect⁽⁶⁾ which tends to amplify shock wave pressures generated in the liquid, or (b) a microjet mechanism wherein the jet is repeatedly generated across a liquid-gas interface at the bottom of the pit where a vapor-gas mixture may be trapped. A concave surface, conducive to the generation of such jets, would be formed if the liquid wets the walls of the "worm-hole". The jet would be triggered by the imposition of pressure loading either from shock waves or jets at the outside end of the worm-hole.⁽⁵⁴⁾

The foregoing items indicate that many points relating to the actual mechanism even of mechanical cavitation damage remain unresolved, and that there is no general agreement even on the type of event which is occurring. However, certain apparently relatively firm conclusions can be drawn.

i) It seems obvious that mechanical cavitation damage is the result of the highly transient imposition of very intense and highly local forces on the surface. Since these are associated with bubble collapse rather than bubble nucleation, it is apparent that the damage occurs in the collapse region. Hence, modification of the flow geometry in a damaged region of a fluid machine to prevent further damage will be usually ineffective in eliminating the cavitation since the bubbles initiate at some point upstream, and only collapse in the damaged region. Obvious as this appears today, it has at times been disputed in the past literature.

The fact that cavitation loading on a surface is very transient and local is important in the selection of protective coatings or surface treatment. It is also important in the attempt to correlate cavitation damage rates with material properties, since the mechanical properties of materials measured in the ordinary fashion do not reflect accurately the resistance of the same materials to the highly transient loading encountered in cavitation.

ii) According to present evidence the cavitation-induced loading on a material surface results from a combination of liquid shock wave effects generated by the volume reduction of a bubble, with the impact of a high-velocity liquid microjet directly on the surface to be damaged. Such a microjet is generated when the bubble collapse becomes substantially non-symmetrical, and in such cases the magnitude of shock waves is probably reduced. Photographic evidence shows that approximately symmetrical collapses are the exception (or perhaps even an impossibility) in the vicinity of solid surfaces and/or in regions of strong pressure and

velocity gradients. Since these conditions are almost necessary prerequisites to cavitation damage in an engineering device, it is this author's opinion that the microjet damaging mechanism is probably predominant in most engineering situations. Considering the jet-impact mechanism in further detail, it is clear that shock waves within the jet itself are important in the impact phenomenon and local cavitation around the point of jet-impact may also be a damage mechanism. This appears to be so for large jets which damage relatively strong materials at surprisingly low impact velocities.* This damage may be at least partially the result of local cavitation as the jet is deflected around the target specimen.

c. Additional Research for Basic Understanding of Damage Mechanisms

It is apparent from consideration of the foregoing that many years of additional research may be required to fully delineate the presently rather sketchy picture of the cavitation damage mechanisms. Such basic studies could well consider the following areas in which more precise information is required.

i) Detailed bubble collapse behavior. Powerful tools are becoming increasingly available today which are useful in this respect, such as ultra-high-speed photographic equipment and other sophisticated optical techniques. Since the critical part of bubble collapse requires only a few microseconds and involves an object only a few mils in diameter, it is clear that extremely sophisticated photographic equipment is required. Another possible method for obtaining much new and useful information is holographic photography with a nanosecond light pulse. This technique can be combined with Schlieren photography or differential interferometry, hopefully to show density gradients or shock waves in the liquid. Such shock waves have already been shown by Ellis (52) and Lauterborn (53), for example

*Type 316 stainless steel was quickly eroded by a 5 mm. water jet impacting at only about 100 m/sec. (55) in tests conducted for an ASTM study.

Other important measurements which could be made around a collapsing bubble include local temperature distributions using a microthermocouple probe, ⁽⁵⁶⁾ or acoustic output from bubble collapse / ^{discussed in more detail later}. Several measurements of this general type have been made, but more precise information and correlation with other conditions of the experiment would be useful. Another good possibility which has been employed to some extent is the direct measurements [^] of the peak pressures exerted upon a specimen by an adjacent bubble collapse. Some excellent measurements of this last type have been reported ^(57,58, etc) but additional information would be desirable.

ii) The effect of fluid properties, flow field parameters, and wall effects ^(discussed later) including deflection under bubble collapse loading on bubble kinetics. It would be very desirable to know the effects of pressure and velocity gradients, boundary layer parameters, etc. on the very complex chain of events apparently necessary to produce a damaging bubble collapse. If more detailed information of this type could be achieved, it might become possible to modify the design of fluid-handling machines in such a way that cavitation damage would be largely avoided or reduced. Along this same line, it might eventually become possible to measure the size and number distribution of the gas nuclei upstream of a cavitating region, and knowing the flow patterns approaching the region, predict the cavitation bubble distribution within the region. If the damage mechanisms were understood to the extent necessary to predict the required size, location, and orientation of damaging bubbles, it would then be possible to predict the rate of damage to be incurred from a given flow situation

If this were possible, it might then be only a small additional step to modify the flow path design in such a way that damage would be grossly

reduced or avoided entirely. A few studies have appeared attempting to predict the trajectory and distribution of bubbles from an initial distribution and given flow regime. (59,60, eg).

3. SEMI-EMPIRICAL RESULTS OF UTILITY TO DESIGN ENGINEERS

Various groups of information have^{been} accrued through the many years of cavitation experimentation which can be summarized in a form useful to the design engineer. Some of these are discussed below.

a. Basic Information

1) Effects of Flow Velocity and Pressure. In many flowing devices such as rotating discs, jet impact devices (which have been used to study "cavitation", since it was observed that damage produced by such impact and true cavitation damage were very similar), tunnel devices using separated flow past a pin such as that pioneered by Shalnev^(61, e.g.), or flow over an ogive as used by Knapp^(6,36), it has been observed that damage rates are proportional to a relatively high power of the velocity. The 6th power was suggested by Knapp⁽³⁶⁾; and this seems fairly representative for the damage obtained with these types of devices. Later tests have shown that the exponent varies with many factors such as accumulated damage^(33,34). It appears that no general rule is possible, since there is an interrelation involved between velocity and pressure in the collapse region that depend upon the actual flow regime. It seems clear theoretically that pressure is actual the primary variable. If pressure in the collapse region increases rapidly with velocity so that collapse intensity is strongly increased, then damage rates should be very sensitive to flow velocity. On the other hand, if the pressure in the collapse region is not affected by velocity, as in a conventional venturi, then damage may not increase strongly with velocity. Such a condition was observed in our own laboratory⁽³⁴⁾. Nevertheless, from the designer's viewpoint it must

be recognized that damage rates may increase very rapidly with velocity, so that a small increase in velocity may convert an otherwise non-damaging, but nevertheless cavitating flow, into one of substantial damaging capability. In cases where there is little or no cavitation, a very small increase in velocity may cause a cavitation field to form, with subsequent significant damage. In such a case, the "velocity exponent" could be very large. Although cavitation damage is primarily pressure dependent, it is the velocity fields which are directly under the control of the designer.

2) Effects of Gas Content in the Fluid. There appear to be two opposing effects. If total gas content is increased it is likely that entrained gas, generally thought to be most important (as compared to dissolved gas) for bubble nucleation, will also increase. In this case there should be more cavitation bubbles produced for the same pressure, temperature, and velocity, i.e., "cavitation number", conditions. Thus damage should increase. On the other hand, if the cavitation bubbles actually contain a higher quantity of non-condensable gas, the bubble collapses are restrained and reversed at a larger radius than otherwise, so that the resultant pressure waves in the liquid are reduced in amplitude. The analogous effect on the microjet collapse mechanism is less clear, and intuitively appears to be less important. Still, for either mechanism damage would be reduced. The interplay of these opposing trends is uncertain in the general case, but experience appears to indicate that large quantities of injected gas do indeed substantially reduce cavitation damage. These trends are discussed in further detail in ref. 62, and also elsewhere of this book.

3) Effect of Cavitation Number. The effect of cavitation number ($\sigma = \frac{2(p_{\infty} - p_v)}{\rho v_0^2}$) upon cavitation damage rates is similar to that of gas content in that much the same opposing trends are evident. If cavitation number is increased for a given flow situation (e.g. by raising the pressure and maintaining constant velocity), the number and mean diameter of bubbles will be decreased, but their collapsing

pressure differential increased. Thus collapse violence will be increased, although the number of bubbles will be reduced. Hence, it is conceivable that a slight raise in the cavitation number, if accomplished by raising pressure at constant velocity, could cause an increase in damage. This has in fact been reported for ^{various} vibratory test facilities⁽⁶³⁻⁶⁶⁾. It is of course clear that a sufficiently large pressure increase will cause a reduction in damage, since cavitation will cease entirely if the pressure is raised sufficiently.

If cavitation number is increased in a given situation by reducing velocity and maintaining constant pressure, the general evidence related to a velocity effect, already discussed, indicates that the damage will probably be decreased.

4) Effect of Fluid Temperature at Constant Cavitation Number. If fluid temperature is raised at constant cavitation number, the density of vapor within the bubbles is increased. Due to thermal restraints bubble growth and collapse are inhibited. Thus ^{the} mean diameter of bubbles may be reduced, tending to reduce cavitation damage. Due to the thermal restraints upon collapse velocities, damage is also reduced. The overall mechanism, described as the "thermodynamic effect",^(67,68) involves a thermal restraint upon bubble collapse and growth due to a potential alteration of the vapor temperature in the bubble. This will become actual, and affect the pressure in the bubble, if heat transfer in the vicinity of the bubble is not adequate to transfer quickly enough the latent heat component involved in either bubble growth or collapse. The resultant vapor pressure change within the bubble is in such a direction as to inhibit either growth or collapse.

The effect of increased fluid temperature in reducing cavitation damage has been adequately demonstrated in vibratory cavitation damage tests ^{(63-66, 68, 69,}

where it is shown that damage decreases rapidly for temperatures larger than the approximate average of melting and freezing temperatures for the liquid.

Figure (18-a) demonstrates the effect from tests in our laboratory, though somewhat similar data was also reported earlier (71). The

decrease of damage rate at temperatures approaching the boiling temperature in

such a test is of course also partially a result of the decrease of collapsing though the same effect is observed when static NPSH is maintained constant (63-66,68,69, pressure differential as the fluid vapor pressure is increased appreciably, (Fig.18-b)).

11 cases the decrease in damage rate becomes significant at temperatures below those for which the increase in vapor pressure seems significant.

A study in this laboratory of this effect using a variety of fluids including water and high temperature liquid metals, but conducted at constant pressure with a vibratory cavitation damage device, showed that damage was not affected by thermal restraints as long as a modified "thermodynamic parameter" was in a range typical of low vapor pressure fluids, but that damage became very strongly reduced when this same parameter reached values typical of fluids such as hot water (70). The correlation presented in that paper is not entirely

satisfactory, and somewhat more complex relations have since been presented by Bonnin (69, eg) using two "thermodynamic parameters."

5) Material Property Effects. Cavitation damage rates are of course very a) General strongly affected by material properties, but no generally applicable relations

appear to exist. The subject is extremely complex and cannot be treated in although more detailed information is given in other section adequate detail here. While any body of damage data on various materials can be

adequately fitted by a sufficiently complex expression combining various material properties, there is little likelihood that such an expression will fit new data unless it is based on adequate physical reasoning. In addition such complicated empirical expressions are likely to be too complex for general utility. On the other hand, relatively simple expressions do not adequately fit the data, unless a

factor

probable error on the order of x^3 is considered satisfactory. This general problem has been explored recently here (70,73, eg) and elsewhere (48-50, eg), using very comprehensive sets of data generated both in vibratory and venturi facilities. As a result of these studies and others, it appears

that the statistically best overall correlation with a single mechanical property for metals is obtained in terms of "ultimate resilience"

= (Tensile strength)²/Elastic Modulus, as originally suggested by Hobbs⁽⁶⁶⁾, or with other relatively similar combinations of these terms.

Ultimate resilience is the energy per unit volume necessary to cause failure if the failure

were of the brittle type, so that ductility apparently does not play a very effective

Since the earliest days of cavitation damage investigations, it has been the practice to use hardness as a simple indicator of probable cavitation resistance for a material. For brittle materials, particularly, hardness still seems perhaps the most suitable

index. Furthermore, it appears to be relatively generally applicable within groups of materials of the same general type. It is further recommended by the fact that it is comparatively easy to measure for a given material. It is probably still the most widely used parameter for this purpose, and, as a result of the relatively complex statistical studies mentioned above, its predicting value is not substantially worse than that of any other mechanical property parameter. The questions are further discussed in Section C of this chapter.

b. Complicating Factors

Further complications in the attempt to predict cavitation damage resistance of a new material in terms of easily measurable mechanical properties exist as a result of the following facts, even if the effect of corrosive influences are completely neglected.

i) Cavitation damage is created by a very transient impulsive loading while the standard mechanical properties are measured under semi-static conditions. Time dependence of mechanical properties differs significantly between materials.

ii) The response of a given material to pressure waves or liquid impact involves some coupling between fluid and material properties. A suitable coupling parameter is presently not known and perhaps must await the development of a more precise understanding of the cavitation damage mechanisms.

iii) The material to be damaged in most operating machines is under substantial stress in its normal mode of operation. The cavitation-induced stresses are thus superimposed on the already existing stresses, so that the resultant stress regime depends upon its initial state of stress. Thus damage rates in operating components may not be entirely predictable from tests on unstressed specimens. Some initial work on this problem has been done by this laboratory^(76, 77) and also by Shalnev.⁽⁷⁸⁾

In addition to the above, and perhaps even more important, are the possible effects of corrosion on the otherwise mechanical damage problem. It is primarily this effect which often renders laboratory cavitation damage tests inapplicable to prototype field conditions, since scaling of the correct "mix" of mechanical and corrosive effects in accelerated laboratory tests is almost impossible to achieve. The problem of prediction of erosion resistance from laboratory tests will be discussed in more detail in another section of the book.

c) Useful Additional Research. It is clear from the foregoing discussion that there are many avenues for additional research which would be useful in assisting the equipment designer. However, it is difficult to list a limited number of especially desirable studies as was done in the case of basic research, since the results to be expected from applied research of the type involved here are generally highly specialized to the actual geometry, etc. which was used. While the gap between the basic understanding of the cavitation damage process remains as large as it is at present, so that the practicality of predicting engineering results from basic principles remains small, it is clear that many applied investigations will continue to be necessary

C. MATERIAL PARAMETER EFFECTS

1. INTRODUCTION

Over the past half century very much experimental data upon cavitation and liquid droplet impingement erosion rates for numerous materials and with various liquids over a range of temperatures and pressures has been accumulated. This is reported in articles too numerous to list here, but summarized up to the mid-sixties in the previous book, Cavitation (6). However, in general it had not been possible over this [redacted] extended period to provide good and usable correlations between measurable material and/or fluid properties and measured erosion rates. It has also not been possible to predict with reasonable engineering precision erosion rates in field devices from laboratory tests. While this is still generally the case, some meaningful progress has been made, and this will be reported in the present section. A [redacted] portion of the ^{pertinent} research [redacted] was done in this laboratory (32).

One of the major objectives of much past and present erosion research, either cavitation or impingement, ^{must} be to establish a mathematical model with fluid-flow and material parameters as input data which would allow the engineering prediction of erosion rates for given, as yet untested, materials. A precise model of this sort has so far ^{however} eluded investigators. This appears to be inevitable in view of the highly complex and varied natures of the erosion processes, even though produced by droplet impingement or cavitation, for example, alone. Nevertheless, it is desirable, using a large and diverse group of data, to attempt to determine optimum correlation relationships, and also to determine roughly what degree of precision can be expected from correlation models using easily measured standard engineering parameters as input data. A

fairly complex sets of data, including both impingement and cavitation results has been used for the study here reported. This combination of data seems reasonable due to the presumed basic similarity of the erosion phenomena in impingement and cavitation, as discussed elsewhere in this book. The model chosen for further investigation has been made dimensionally-consistent and as simple as possible, in hopes of obtaining maximum generality and applicability. This objective is also enhanced by the use of a diverse data set including items generated in different impact and cavitation-type tests.

2. MATHEMATICAL MODEL

The relatively poor fit achieved so far in correlating measured erosion data with material properties indicates the desirability of a predicting model based closely on the details of the physical processes involved. However, such a desirable resolution has not yet been attained.

A model similar to that suggested by Hoff et al(79), relating the rate of erosion (MDPR = mean depth of penetration rate) to the kinetic energy impacting the target, the efficiency of energy transfer between drop and target (η), and a material parameter (ϵ) with dimensions of energy per unit target material volume, has been used. The resulting equation relates MDPR to the impinging kinetic energy and the energy necessary to remove material:

$$\text{MDPR} = \left(\frac{\eta}{\epsilon} \right) \left(\frac{A_p}{A_e} \right) \left(\frac{\rho_{\text{eff}}}{2} \right) (v^3) \quad \text{----} \quad \text{(C-1)}$$

This equation attempts to compartmentalize and rationalize the effects involved. It also shows the real complexity of the phenomenon and the extreme difficulty of a reasonably rational analysis. The evaluation of the material parameter ϵ in terms of mechanical material properties, as well as of the effect of the energy transfer efficiency term η which depends upon material and fluid parameters are areas in which some progress may be possible.

Incidentally, for implementation of Eq.(C-1) it is necessary to use only data wherein the total MDPR vs. exposure curve is available so that only comparable portions of this curve will be compared. It is by now well recognized, as / perhaps first emphasized by Thiruvengadam (80) eg), but now well recognized that damage is not linear with time. For the present purpose, data from various types of facilities, both impact and cavitation , have been compiled together and used to evaluate and generate "best fit" erosion predicting equations.

The best hope of achieving a relationship of the generality necessary to allow possible applicability over a broad range of materials, requires a relation which is directly related to a physical model of the erosion process, is dimensionally consistent, and is as simple as possible. While it will be possible often to achieve a better fit for a given data set with more complex mathematical expressions, its utility in fitting other data sets has always been poor. Following this line of reasoning, the basic energy flux model suggested by Hoff et al. (79) may be useful. This assumes simply that the product of the rate of volume loss per unit exposed area (MDPR) times the exposed area (A_e) is proportional to the product of the impacting kinetic energy per unit projected area times the projected area. The constant of proportionality is the quotient of the efficiency of energy transfer between impacting drop and material damage processes (η) and a material parameter (ϵ) describing the energy per unit material volume absorbed in the material in such a way as to cause damage. This relation is expressed by eq. C-1

The efficiency, η of energy transfer is influenced by several factors, and may perhaps be considered as a product of several separate terms reflecting each of these mechanisms. Considering the details of the jet impact process (assumed applicable to both cavitation and droplet impact) between a liquid drop and a material surface,

η should be a function of (a) material and liquid properties perhaps as reflected by the acoustic impedance ratio (82, eg.) (b) geometrical factors involved in the collision, i. e., shape of impacting drop, angle of impact, surface roughness, etc., and (c) velocity of impact which will affect the pressure applied to the surface and hence the degree of surface deformation and the departure from the concept of an elastic material.

Since material and liquid properties involve no other parameters of the collision, we have lumped their consideration into that of the energy parameter \mathcal{E} , assuming as a first approximation that this portion of the efficiency term may be some function of the acoustic impedance ratio. No comprehensive attempt has yet been made to evaluate the remaining portions of η ; but some discussion of possibilities will be presented later.

3. Evaluation of Energy Parameter, \mathcal{E}

a. General Remarks

From the foregoing, it is desired to find a material mechanical property with units of energy per unit volume having the characteristic that for a given test (impingement or cavitation) with fixed test

parameters (velocity, fluid conditions, geometry, etc.), the product of MDPR x $\bar{\epsilon}$ will be ^{as} nearly constant as possible over a broad range of test materials. The material property must appear only to the first power. Thus a polynomial expression for the energy term will not ^{suffice} / , since this would destroy the dimensional consistency of eq. (1). ^{Also,} to be of use in a predicting equation, the energy term must be measurable in a simple mechanical test. Hopefully it will already be available in the literature for most standard materials. Among the parameters meeting these conditions are those energy terms which can be computed from the standard stress-strain curve. Our own previous work (83, e.g.), primarily that of Hobbs (84, and Rao ^{et al}(75) (all, incidently for cavitation tests) and Heymann (74,85) for a combined data set suggest that the best single parameter correlation is to be found with "ultimate resilience = $T.S.^2 / 2E$, i.e. the area under the elastic portion of a stress-strain curve if elastic* strain were continued up to the full tensile strength (T.S.). Thiruvengadem (80, e.g.), on the other hand, has reported that the best fit is in terms of strain energy (area under the complete stress-strain curve of a material). This latter ^{parameter} can be evaluated either as the "engineering strain energy" (SE), i.e., area under the conventional stress-strain curve where tensile strength is computed from the observed breaking-load without consideration of reduced area) or "true strain energy" (TSE) where actual breaking stress is used. Approximations of both have been used for the present purpose.

For ultimate resilience ^(UR), for simplicity ^{has} the observed breaking load only been used, since for many materials, reduction of area data is not available. Also, our previous work (83) indicated this to be preferable.

*E = Elastic (Young's) Modulus

Another parameter which can be considered approximately energy per unit volume, and which is easily available for most materials, is hardness. This also has been considered (Table 3) as a possible correlating parameter in the form of Brinell hardness, but is difficult to use in a "rational" damage equation.

b. Selection of Data for Evaluation

For maximum applicability and generality as broad a group of data as possible has been used for evaluation of the "material coefficient" of, ϵ/η_a from Eq. (C-1),

including some from cavitation tests, and some from impingement tests. It was also necessary that accurate stress-strain curves for the materials used be available. Also

the damage data must be such that the entire MDPR vs. time curve be available so that a comparable portion of this curve could ^(83, eg.) be used in all cases. Consistent with our own previous practice and that of Hobbs (85) as well as following fairly we have used

maximum MDPR as the characteristic value for the material.

The largest single portion of the present data set is that generated by our own vibratory cavitation facility in water following the present ASTM standard conditions (86), i.e., 24°C. 20 kHz, 2 mil double amplitude. Other

data has been incorporated into the analysis only when tests were available for at least one common material, preferably from identical material ^{specimens} from same bar stock, if at all possible.

A ratio between maximum MDPR for the common material in the differing tests or facilities was established, and the additional materials tested in the other facility (or test condition) normalized to the common material in our ^{own} vibratory facility.

Thus values of these comparative amplitude constants are relevant to our particular vibratory facility. In this manner, it is possible to incorporate data from various types of tests, since the efficiency factors involving test geometry and velocity are thus removed from consideration. Data from the following sources, in addition to our own vibratory cavitation data have been used:

→ Generally adopted procedure today (86, eg)

Impact tests by King of RAE (87) in Dornier rotating arm facility

Impact tests by Electricité de France (55,88) on rotating wheel

Venturi tests by Rao et al (75)

Vibratory cavitation tests in our laboratory (77) using stationary specimen arrangement in close proximity to vibrating horn (same unit also used in standard set-up).

The materials and their mechanical properties are listed in Table 3.

c. Best Fit Results Attained

Predominant Mechanical Property

Previous work here and elsewhere led to the conclusion that the most likely form for an energy parameter \mathcal{E} would be a combination of ultimate resilience and strain energy so arranged that the resultant term would have the units of energy/volume. To attain reasonable flexibility within this limitation, the following relation was assumed:

$$\mathcal{E} = C_1 \left(\frac{UR}{ESE} \right)^a UR + C_2 \left(\frac{UR}{ESE} \right)^b SE \quad \text{--- (C-2) ---}$$

where C_1 , C_2 , a , and b are constants to be computed by a least square fit regression analysis of the data. Investigation of this relation showed that the best values for a and b were close to zero, so that the simpler relation of eq(C-2) was indicated. An additive constant, C_0 , was used since this improved the data fit. The physical interpretation of C_0 is that of a threshold energy necessary to cause measurable damage, i.e., a concept analogous to that of threshold velocity.

$$\epsilon = C_0 + C_1 UR + C_2 SE \text{ - - - - - (C-3)}$$

Using the least mean square fit analysis with eq. (C-3) or the following special case versions of it:

$$\begin{aligned} \epsilon &= C_0 + C_1 UR \text{ - - - - - (a)} \\ \epsilon &= C_0 + C_1 SE \text{ - - - - - (b)} \\ \epsilon &= C_0 + C_1 TSE \text{ - - - - - (c)} \\ \epsilon &= C_0 + C_1 UR + C_2 SE \text{ - - - - - (d)} \\ \epsilon &= C_1 UR \text{ - - - - - (e)} \end{aligned} \text{ - - - - - (C-4)}$$

it was found that the best correlation coefficient and the smallest percent standard error of estimate resulted from eq. (4 -d), although (4-a) was in all cases nearly as good, indicating that ultimate resilience was the material parameter of major importance. This was further verified by the dominance of the second term over the third in eq. (4-d). The statistics of the correlation with either eq. (4-b) or (4-c) were relatively very poor with TSE, worse than ^{for} SE. Hence SE is used in eq. (4 -d). This data is summarized in Tables 4 and 7. While the correlation with eq. (4-d) is better than that with (4-a), it is only slightly so. Hence for simplicity it is permissible to use eq. (4-a) in preference to (4-d),

so that the only mechanical property involved in the correlation becomes ultimate resilience.

Since the best value of C_0 in eq. (4-a) is relatively very small, it is justified to use (4-e) where this threshold energy term is neglected.

The standard error of estimate (72) was computed in such a way that it is always approximately proportional to give equal weight to both weak and strong materials in the correlation, and allow the reasonably accurate prediction of MDPR for materials of low ϵ .

2) Determination of Efficiency Factor, η

It seems reasonable that one factor of an overall energy-transfer efficiency term in the basic eq. (C-1) i.e. η_a , may be represented to a first approximation as a function of the acoustic impedance ratio (AI) between liquid and material ($AI = \rho_L c_L / \rho_S c_S$)

The "water-hammer equation", discussed in detail in another section of this book, is usually assumed for materials of finite elasticity to give a reasonable approximation of the pressure applied to the material surface under droplet impact (77, e.g.). Examination of this equation indicates the importance of AI in determining this pressure, and in fact suggests a functional ^{form} \wedge of AI, $f(AI)$, which might be tried.

$$\Delta p = \frac{\rho_L c V}{AI + 1} \quad \text{--- -- -- -- -- (C-5)}$$

so $f(AI) = AI + 1$

$f(AI)$ is taken as a direct factor in the relation describing the pressure generated at the point of impact. Since pressure has units of energy per volume, its use here is dimensionally consistent with the general model assumed. Another possible form of $f(AI)$ is the "transmission coefficient" giving the ratio of absorbed to reflected energy for the case of a shock wave impinging upon a solid surface in a continuous medium (which is not identical to the present case).

$$\text{Then } f(AI) = \frac{(AI + 1)^2}{4AI} \quad \text{--- -- -- -- -- (C-6)}$$

The best fit correlations have been investigated for both forms. It was assumed that:

$$\eta_a = f(AI)^n, \text{ where } n = \begin{matrix} + \\ -1, -2, -3 \end{matrix} \quad \text{--- -- -- -- -- (C-7)}$$

Table 5 summarizes the results. It appears that there is no substantial improvement in the correlation to be attained by the use of $f(AI)$ in any of these forms. This is surprising in the light of Heymann's result (74,85) that the fit with UR was improved by using $UR \times E$, since $E^2 \cong \rho E = \rho^2 c^2$ for the metals used. As also suggested by Heymann (74) it seems necessary that η_a differ substantially between materials, since the ratio between

of
 the extremes/ material erosion resistance is orders of magnitude
 greater than that between the corresponding material energy propert
 Nevertheless, in light of the present results η_a must be
 assumed unity, and omitted from subsequent relations. Further disc
 of efficiency factors is provided in section E.

3) Non-Linear Parameter Fits

i. Polynomial Energy Parameter Fit

The postulated basic Eq. C-1 requires a first
 power energy term for dimensional consistency. In order to
 verify that the assumption of such a linear relationship with
 energy is reasonable, polynomial data fits of the type

$$\Sigma = C_0 + C_1(UR) + C_2(UR)^2 + C_3(UR)^3 - - - - - (C-8)$$

were investigated. (Table 6 While there was some improvement over th
 linear fit in "correlation coefficient", the "standard error of estimat
 becomes worse. Thus it appears that the linear relationship, being
 physically reasonable, is most suited for the present purpose,

where the maintenance of dimensional consistency is important.

ii. Fit with UR x E²

Heymann's study (74,85) showed some improvement by usin
 UR x E² rather than UR x E. However, the statistical fit for either of the
 terms according to the present data set is not as good as that with UR alon
 and of course is dimensionally inconsistent with the assumed model (Table 6

4) Recommended Relations

The following relations seem most useful (in "English
 engineering units") for common metals and alloys.

$$\begin{aligned} \mathcal{E} &= C_0 + C_1 UR \quad \text{--- (C-9-a)} \\ \mathcal{E} &= C_1 UR \quad \text{--- (C-9-b)} \end{aligned}$$

	(9-a)	(9-b)
where $C_0 =$	0.463	-

$C_1 =$	1.999	2.330
---------	-------	-------

Coefficient of Correlation = 0.808 0.808

Standard Error of Estimate = 1.981 2.007
(multiplicative factor)

Since the improvement due to the inclusion of the threshold energy C_0 is small, the simplest form (9-b) is perhaps most useful.

Tables ^{+8.} 7 list the full data set used along with measured and predicted values of \mathcal{E} (which is equivalent to MDPR for data normalized in the fashion here used), according to Eq. C-9.

The predicted and measured values are tabulated for both eq. (9-a) and (9-b) along with the deviations for each material. Fig. 19, presents the same information graphically for the recommended eq. (9-b) where the "triangular" standard error of estimate band is shown. Table 6 summarizes statistically various best fit equations including those which are non-linear (2).

Figure 20 shows information very similar to Fig. 19 from a different but also very comprehensive data set, provided by Heymann (19) in a discussion to our earlier paper (2). Heymann plotted his and our data together (Fig. 20) and the very close agreement between these two correlations based upon independent, but large, data sets is heartening. Heymann's analysis leading to Fig. 20 is further discussed in his article (20) at the same ASTM symposium.

The amplitude constants apply to the UM vibratory facility only. Constants for other facilities are found by multiplying the given constants by the ratio between maximum damage rates in the other facility and the UM facility.

4. Interplay of Corrosion and Mechanical Effects

a. General

All the previous discussion, as well as the mathematical model proposed, has considered only the mechanical aspects of cavitation erosion of materials, i.e., possible corrosive effects have not been considered. However, it is obvious that with certain liquid-material combinations corrosive effect will also be significant, and of course corrosion-induced erosion is a major topic in its own right. Corrosion per se is not within the scope of this book; it is treated in detail in various other works. However, there are many important applications which include cavitation effects but also substantial corrosive attack. The most obvious case may be marine propellers fabricated of corrodible materials, or other machines operated in sea water. Other cases are hydraulic turbines in some cases even in fresh water, machines operating with other corrosive liquids, and numerous other similar applications. An important case, usually involving only very mild cavitation combined with strong corrosive effects, are diesel engine coolant "liners". In this case the cavitation is apparently of vibratory, rather than flow origin.

b. Mechanism and Results of Combined Cavitation-Corrosive Erosion

Numerous experimental observations clearly indicate that the combined erosion due to a combination of cavitation and corrosive effects is often very much greater than the summation which would be obtained if the two effects were to act

singly. This multiplied combined effect is usually attributed to the following interactive mechanisms.

i) Mechanical cavitation removes the protective layer which normally inhibits rapid corrosion with most materials, thus continually exposing fresh metal for renewed corrosive attack.

ii) Corrosion roughens the surface causing increased local cavitation, beyond that which would be incurred in the absence of such surface roughening.

These interactive mechanisms often result in a much greater overall attack than would result from their separate application.

c. Cathodic, Anodic and Other Effects

1) Cathodic and Anodic Voltages

"Cathodic protection", i.e., application of a negative electric potential, to a material under corrosive attack in water, particularly sea-water, has been used for many years to reduce or prevent ordinary corrosive attack. Experiments have also been made to evaluate the effect of cathodic protection upon cavitation damage (89, 90, eg.). It has been found that cavitation damage is thus reduced for various metallic materials (89, eg). However, it was later stated (90, eg.) that this was primarily a result of electrolytic gas evolution at the eroded surface, which then "cushioned" cavitation bubble collapse, rather than of the expected inhibition of the corrosive component of the overall attack. Presumably either of these mechanisms is oversimplified in general; both, as well as perhaps other presently unknown mechanisms, are involved in many real applications.

Recent experiments have also been made to include the effects of both positive and negative voltages applied to cavitated metallic specimens (91, 92, eg). Generally it seems to be indicated that for vibratory horn cavitation damage tests there is a continuous progression toward increased damage as the applied voltage is increased from strongly negative, through zero, into the positive range. Much greater damage rates are observed for positive (vs. zero) voltage. This observation does not appear consistent with the concept of reduced damage due to "gas cushioning" (90), since approximately similar rates of gas evolution are observed at either positive or negative applied voltages. It thus appears at this time that the effects of applied voltages are not well understood, and that additional careful research is required.

2) Gas Effects

As discussed in the foregoing, "gas cushioning" has been proposed in the case of "cathodic protection" as a possible mechanism for reduced cavitation damage. This mechanism also presumably explains the reduction of damage observed for large gas contents with various liquids as discussed in ^{more} detail in Section V-D. Also air injection is used in some field applications for the purposeful reduction of cavitation damage. However, in some cases there may be a partially countering effect due to the increase in corrosion which would be expected with higher oxygen content. Again this is a region in which very little quantitative information exists at this point.

3) Stress Corrosion

The phenomenon of "stress corrosion" represents an obvious interplay between applied mechanical stress and corrosion. In those cases where liquid-handling components encounter "stress corrosion", there is also a possible interplay between cavitation and corrosion effects, if cavitation is in fact present. Again this appears to be a field wherein very little quantitative information is available.

4) Cavitating Slurries

Cavitating slurries involve erosion which may result from both corrosive and particle impact effects, in addition to ordinary cavitation mechanical attack. While some field experience shows that very high rates of erosion may result from cavitating slurries, there is virtually no qualitative information available at this point.

5. SUMMARIZATION

The most likely form for an equation relating material, liquid, and test parameters with cavitation or impingement erosion rates with good hope for general applicability, is one which is based on a simple physical model with dimensional consistency. For the evaluation of impingement erosion rates, consistent with the previous suggestion of Hoff, et al (6) the equation

$$\text{MDPR} = \frac{(\eta_i \eta_a)}{\epsilon} \left(\frac{A_p}{A_e} \right) \left(\frac{\rho_{\text{eff}} V^3}{2} \right) \quad \text{--- (C-1)}$$

has been chosen

A statistical evaluation of ϵ , which must have units of energy per volume, has shown the best fit with a comprehensive data set, generated in various laboratories with various types of test devices and various test materials, including both impingement and cavitation data in the form

$$\frac{1}{\text{MDPR}} \propto \epsilon = C_1 UR \quad \text{--- (C-9-b)}$$

(terms previously defined)

Neither higher power terms in UR nor terms in SE improved the statistics of the fit substantially, and the fit in terms only of SE was relatively very poor. It is thus concluded that for the large group of metals here used the best linear energy per volume mechanical property correlation for volume loss rate under droplet impingement or cavitation attack is the expression eq.C-9-b) in ultimate resilience alone.

Traditionally hardness has been used as the indicator of cavitation or impingement liquid erosion resistance. This parameter at least has the merit of extremely easy laboratory determination, where values are not already available. In terms of a predicting equation, BHN (Brinell hardness) requires an exponent of ~ 1.8 (Table 6) as opposed to ultimate resilience where the best exponent is essentially unity (Eq. 9-6). Another very useful predicting equation is then:

$$\frac{1}{\text{MDPR}} \propto E = C (\text{BHN})^{1.8} \quad \text{-----} \quad (\text{C-10})$$

The statistical fit of Eq. C-10 is not quite as good as that of Eq. C-9-b), but it is not very much worse (Table 6), and BHN is much more easily determinable than is UR, in most cases.

For these, or any correlating equations, there are certain materials (Stellite, eg) which lie very far from the predicting line. In any case, a standard error of the order of $\times 3$ must be expected. Since there is a range of $\sim \times 10^4$ between the resistances of weak materials such as soft aluminum and strong ones as Stellite 6-B (eg), this apparently large standard error may not be too surprising.

Liquid impact erosion in particular is discussed in further detail in Chapter VI of this book.

D. Cavitation Damage Scale Effects

1. Introduction

A review of the state-of-the art for cavitation damage "scale effects" is ^{here} made. [▲] Nucleation scale effects were discussed in Chap. III. [▲] The most prominent such damage scale effects (for constant sigma) occur with variation of velocity, pressure, or size, but no precise prediction of the magnitude of these effects is as yet possible.

A relatively comprehensive bibliography of pertinent literature is included, but ^{this} is by no means complete.

"Cavitation damage scale effects" are here taken to include all those phenomena which result in a change in cavitation damage rates in a given flow regime occurring as a result of changes in operating conditions such as velocity, pressure, machine size, fluid and fluid condition (temperature e.g.), all at constant sigma, with geometric and nominal similarity maintained. In most cases the operative mechanisms, and the fact that such changes in damage rates exist at constant sigma, are fairly clear. However, it is in general not possible in the present state of the art, to estimate the changes to be expected other than empirically. In most cases, reliable empirical information is also not available, although in many ^{cases} it is at least possible to know the direction of the trends to be expected. Hopefully within the next decade or two, these matters will be substantially clarified as a result of continuing research. For the present purposes, it is best to divide the overall subject into several portions according to the type of effect to be considered, although in many applications several of the mechanisms operate simultaneously. The various separate effects will be considered in the following sections. The operative mechanisms will be described as they are presently understood and important literature sources will be cited. More detail on this

subject is found in the survey report (93) prepared by Working Group No. 1 of Hydraulic Machinery Section of IAHR,^{*} and a subsequent summary article (94).

2. Velocity and Pressure Effects

The most prominent and well-known cavitation damage scale effects are probably those due to variations of velocity or suppression pressure. Assuming, however, that "scale effects" presuppose the maintenance of constant σ , it is obvious that velocity and suppression pressure cannot be varied arbitrarily and independently, if σ is to be maintained constant. It is also obvious that tests at varying pressure and/or velocity, but with varying σ , will result in large changes in cavitation damage rates. However, these are not "scale effects".

a. Pseudo-scale effects

Considering cavitation damage tests wherein suppression pressure is varied but velocity held constant, σ varies as determined by the variation of suppression pressure. In such cases it is obvious that as suppression pressure (and σ) is reduced from a very high value at which cavitation is completely suppressed, cavitation damage rate will increase from zero toward a maximum. As suppression pressure is further reduced, experience and theory show that damage rate will decrease again toward zero. This general behavior is clearly indicated in tests using a vibratory type facility (95-99, e.g.) and in flowing tests such as in venturi-type devices (11,100-104, eg). However, these results are not, strictly speaking, damage "scale" effects, since σ is varied.

*International Association for Hydraulic Research

Other related tests in which the effect of velocity variation has been examined at constant suppression pressure are those using liquid jet or droplet impact devices. While these are not basically cavitation tests (though local cavitation may be involved), it has been assumed for many years, and demonstrated experimentally to some extent, that cavitation and liquid impact erosion are very similar phenomena, perhaps governed by the same parameters. In these tests, damage exponents vary over the range ~ 5 to ~ 10 (10^5 - 10^8 e.g.). The same is approximately true for cavitation tests using rotating disc devices in which the nominal pressure is held constant, but the velocity varied (24,25,109, e.g.). This, and other somewhat anomalous results, may be due to the highly complex three-dimensional nature of these flows.

3. "True" Damage Scale Effects

True damage scale effects are those encountered at constant σ with variation in velocity (or pressure), while the other parameter is also varied in such a way as to maintain constant σ . Under these conditions, to a first approximation, i.e., neglecting ordinary "scale effects", if the size is also constant, the number and size of bubbles in the collapse region should be very approximately constant, as should the flow regime in general, although the very non-linear nature of bubble growth and collapse equations makes even this approximation hazardous. This is not a good approximation for cavitating wakes, where periodic cavity shedding is involved (110, e.g.). Here the number of bubbles and the cavity shedding frequency may increase with velocity. However, the energy involved in the collapse of a bubble of a given size would then be directly proportional (to a first approximation) to suppression pressure, and hence its damage capability greater for greater suppression pressures. Of course, it cannot be

assumed as a consequence that damage rate will also be proportional to suppression pressure. This general situation, using many idealized assumptions, has been examined by Thiruvengadam (111-114, e.g.)

"True" damage scale effects are then defined as those for which sigma and flow geometry are constant. As pointed out in the foregoing, many tests involving the effects of velocity change upon cavitation damage rates do not meet these conditions, and of course vibratory tests are inapplicable, since velocity is not an important parameter for such tests. However, tests reported in the literature of this type will be discussed in the following.

a. California Institute of Technology (CIT) Tests

In water tunnel tests at CIT in which velocity was varied, but sigma held constant, Knapp (6,115) deduced the ^{now} well-known velocity-damage "exponent law" and assigned the exponent a value 6. His observations were based on counting pits in a soft aluminum specimen of ogival shape immersed in the working section of the large water tunnel at C.I.T. No weight losses were involved, only pit counts. Velocity was varied, but minimum pressure in the working section remained p_v . The variation of pitting rate with velocity on soft aluminum was later confirmed in a test on a water turbine in the field (6,116). A somewhat similar program involving damage comparisons between vibratory, rotating disk, and hydraulic turbine with different test materials has been reported at the Institute of Fluid Flow Machines, Polish Academy of Science, Gdansk, Poland (117-119).

b. Industrial experience

It is generally recognized in the industry that pumps, turbines, propellers, or other machines designed for an acceptable sigma from the

*Damage $\propto V^n$. It is sometimes assumed that Damage $\propto (V-V_0)^m$, where V_0 is a "threshold velocity" below which no substantial damage occurs. Exponent m is then less than exponent n.

viewpoint of head drop, loss of efficiency, etc. will be satisfactory from the viewpoint of cavitation damage, if the velocity is sufficiently low. Thus, in most cases, sigma is fixed from the viewpoint of fluid-dynamic performance, and damage will be negligible (or at least acceptable) if the pressure and velocity are sufficiently low. For fixed sigma, a low velocity of course implies a low pressure, and vice versa. A case in point is the comparison between condensate pumps and boiler feed pumps. It is common practice to design condensate pumps for operation in the cavitating regime, which has been used sometimes as a method of flow control. In this type of pump, operating with very little suppression pressure, the velocities are necessarily low to provide the desired sigma. On the other hand, for boiler feed pumps (operating after the condensate and booster pumps in a powerplant system, and thus provided with much higher suppression pressure) a small amount of cavitation can lead quickly to prohibitive damage. Other similarly related industrial experiences exist, but do not in general lead to quantitative predicting relations regarding the damage scale effect. Examples of related industrial experience are reported from Voith by W. Thuss (120) and from Electricité de France by H. Giraud (121, e.g.).

4. Venturi Damage Tests at Constant Sigma

Tests at the University of Michigan in a cylindrical-conical venturi, wherein damage specimens were inserted through the wall into the region of bubble collapse, have been conducted recently (11,100e.g.). Figure 21 shows the venturi geometry used. Many series of tests have been performed at essentially constant sigma, on various materials. However, the geometry of the cavitating region as viewed through the transparent wall was kept constant so that sigma actually varied slightly. In general of course there should be an unambiguous relation between σ and cavity length.

Test fluids were water and mercury. These tests showed that the "velocity exponent" depended upon the "degree of cavitation", i.e., the extent of the cavitating region into the venturi diffuser, with the exponent being greater for more limited extent of the cavity region. In all cases the exponent was less than had been expected from previous tests such as those of Knapp (6,115 / It ranged for water from ~ 1.7 to ~ 4.9 for a cavity length extending into the diffuser up to the position of the test specimen. In the mercury tests, the increase of damage with velocity was generally small, and in some cases a decrease was found (11,100-102) In these particular tests, a reduced cavitation damage exponent for increased cavity length was generally observed, explainable by the fact that the pressure in the collapse region for this particular geometry (Fig. 21) is insensitive to velocity for the cases of well-developed cavitation, since the damage test specimen is then completely immersed within the cavity region, where the pressure is essentially vapor pressure at all velocities.

On the other hand, for a degree of cavitation near initiation, the pressure in the bubble collapse region increases approximately with the square of the velocity, thus strongly increasing the collapse "intensity" for increased velocity. These results emphasize the fact that, in general, in order to estimate the effect of velocity change on cavitation damage rates, it is first necessary to estimate the effect of velocity change on suppression pressure, both in initiation and collapse regions.

Other recent damage tests in a venturi type geometry (Fig. 22) are those at the Indian Institute of Science at Bangalore (103) While the velocity was varied over a considerable range, tests at constant sigma and variable velocity were not made. In any case the velocity exponent

increased from about 6 to 17 as velocity was increased, but then became negative, i.e., damage decreased with further increase of velocity, with the exponent eventually reaching a negative value of ~ -74 . A large scatter of velocity exponent ^{data} is ^{also} consistent with the University of Michigan tests described above. Again, it appears that the key lies in a knowledge of the behavior of the pressure regime and cavity extent in a particular system.

A summarization of the sigma vs. damage rate effects from the University of Michigan venturi tests is shown in Fig. 23. Here sigma is based upon the minimum wall pressure measured for the various flow conditions. Figure 24 shows the venturi flow path in which these tests were made, and Fig. 25 typical measured wall pressure profiles from which the sigma values used in Fig. 23 were calculated.

The general shape of the sigma vs. damage rate curve (Fig. 23) is as would be expected, i.e., very low or very high sigma produces low damage rate (MDPR mean depth of penetration rate), whereas an intermediate sigma produces maximum damage rate. However, the value of the maximum damage sigma and the detailed shape of the curve depends on other related parameters such as test liquid and material, velocity, temperature, and details of the flow geometry (which differs slightly for the two curves shown in Fig. 23). It can thus be concluded that cavitation sigma is a very important parameter for developing an overall correlation between externally measurable parameters and damage rate, but that it is not alone a sufficient correlating parameter. While it is perhaps the most logical externally measurable parameter with which to start in the formulation of damage rate correlations, it must be considered along with the other related parameters discussed above.

The reasoning leading to the expected shape of the damage-sigma curve is simply that for sufficiently high sigma, cavitation is entirely suppressed; for very low sigma, driving pressure to collapse the bubbles and generate damage is lacking, i.e., "super-cavitation" develops. The case of saturated boiling is obviously very similar. Incidentally, the same pressure-damage relationship is exhibited by the vibratory test, but facility limitations so far limit this to the low pressure part of the spectrum (122, eg.).

A somewhat similar and related investigation, producing relatively similar results, is that by Hutton, et al at the University of Southampton in England (123, e.g.).

Another problem to be considered, aside from prediction of damage rates, is the prediction of the pressure and velocity conditions which correspond to the inception of cavitation damage in a given situation. This approach has been followed by Tullis, et al. (124, e.g.) in a study of cavitation downstream of sudden enlargements. They present empirical equations from which the velocity for inception of cavitation damage can be estimated.

5. Other Parameter Effects

a. Size Effects

The problem of cavitation damage scale effects with change in machine size (as from model to prototype) at constant sigma (or constant "degree of cavitation" from the viewpoint of head loss, efficiency loss, etc.) is highly complex. In the first place, due to ordinary performance scale effects, constant sigma and constant degree of cavitation are not synonymous. Neglecting that rather secondary difficulty for the moment, and assuming that damage scale effects imply constant degree of cavitation (or cavitating regime), in a given machine, the area to be damaged will be

proportional to the square of any characteristic dimension. The average bubble size attained, however, will be greater for increased machine size, since the time of exposure of the bubble to the same underpressures will be greater, and hence the energy of bubble collapse will be greater. Due to the non-linearity of the bubble growth and collapse equations, the total bubble collapse energy (considering all bubbles in the field) will not in general be directly proportional to size scale, but (intuitively) will probably increase with an exponent considerably greater than unity.* A numerical study of this situation by Canavelis (125) predicted an increase of total volume loss on this basis proportional to D^5 . Hence it appears that the volume loss exponent with size lies between 2 (based on the simple area effect) and at least 5. Experimental studies in a venturi by Shal'nev and various co-workers (110, e.g.) indicates a diameter exponent of 3^* , and a velocity exponent of 5. More recent studies by Meier and Grein(126) and Schiele and Mollenkopf(127) also indicate a D^3 and V^6 dependence. Malyshev and Pylaev (128) confirm the D^3 dependence. General experience in the hydraulic turbine industry appears to be that a diameter exponent of about 3 is realistic. Tests by Thuss at Voith (120) indicate a velocity exponent of ~ 4 .

b. Temperature ("Thermodynamic") Effects

The effect of fluid temperature variation on cavitation damage under conditions of constant sigma and similar geometry can reasonably be included in the family of damage scale effects, although it is perhaps not usually considered as such. This effect has been explored in most detail in vibratory horn cavitation damage tests (40,43, 70,71,95-99,122,129). To first approximation, it has been shown that, for a variety of fluids

*In general, of course, collapse energy is proportional to $p \cdot dv \propto pD^3$.

129)

(including liquid metals (70,96,97,122,129) there is a very strong diminution of damage rate as temperature is increased beyond a certain intermediate value for which the damage rate is a maximum. The foregoing assumes no change in material mechanical properties due to temperature variation, i.e., the diminution of damage at increased temperature would be at least reduced if the material were at the same time weakened substantially by the high temperature.

In the vibratory tests there is also a relatively mild decrease of damage rate as the temperature is reduced beyond the temperature for maximum damage rate. The reason for this decrease in damage at low temperature is not fully known, but probably involves increased viscosity, and other changes in the liquid properties with temperature, including gas solubility. The decrease in damage at high temperature, which is much more pronounced, is presumably primarily the result of "thermodynamic effects" /explained elsewhere/ also in this book. The overall result of these effects is the confirmed existence of a maximum damage temperature for all liquids tested.

This general behavior, common for all fluids so far tested, covers the temperature range between the freezing and boiling temperatures corresponding to the static pressure under which the test is conducted. The maximum damage temperature is in general about midway between these limits. There is no reason to doubt that the same trends exist in flowing situations, but there are as yet no pertinent precise data. It is thus likely that cavitation damage is not a serious problem for liquid conditions for which the "thermodynamic effects" are predominant. This is probably true of water at temperatures of the order of 300° F (99 °C) or sodium at high temperature, e.g., ~600° F (122,129) and also for cryogenic liquids such as hydrogen or oxygen, but at much lower temperatures.

These trends have long been recognized industrially, the name "thermodynamic effects" (which is really a misnomer) originating probably from the pioneering paper on this subject by Stahl and Stepanoff (67). The primary mechanism involved is the fact that heat transfer from the vapor in the collapsing bubble to the surrounding liquid becomes a limiting mechanism as the temperature is increased, because of the rapid increase of vapor density with temperature. While very high liquid velocities can be achieved if the collapse is inertia-controlled, this is not the case for thermally-controlled collapses, so that cavitation damage rates are greatly reduced under these conditions. While there have been a great many theoretical and experimental studies of this problem, particularly in recent years (70,122,129-134) it is still not possible to predict "a priori" the degree of reduction of damage to be expected from these effects in a given situation with any fluid.

c. Fluid property effects

Fluid property effects, other than temperature, may also not normally be considered as true scale effects, even though they involve tests conducted at constant sigma and similar geometry. However, as with temperature, they are very important, particularly from the viewpoint of damage.

Aside from temperature, probably the most important fluid property, from the viewpoint of damage, is liquid density. Constant sigma for fixed velocity implies constant suppression "head".* Thus, to a first approximation, bubble collapse velocities would also be fixed. The pressure then generated by contact between the collapsing bubble wall and the structure, i.e., the microjet impact or shock wave imposition, would then be directly proportional to liquid density, if other pertinent properties (such as velocity of propagation of sound in the liquid, e.g.) remained

*Here defined as energy/mass, i.e., ft-lbf/lbm in English "engineering units"

constant. The situation is obviously highly complex, but it seems probable that fluids with higher density, under constant sigma conditions, will produce higher pressures upon neighboring structural walls, and thus be more damaging. However, as yet no directly applicable experimental data appears to exist.

Another fluid property which has in the past been discussed in relation to damage (135) is surface tension. While numerical studies show that it is not likely to affect the collapse process (9), it can importantly affect nucleation, and thus the existence of cavitation itself, in a given situation. If cavitation does in fact exist, however, the number and size of bubbles in the collapse region will be affected, thus having an important indirect effect on damage. The foregoing argument leads to the conclusion that high surface tension will reduce cavitation damage by reducing the number and size of bubbles. No direct evidence is available to our knowledge, since any experiment in which different values of surface tension are involved, also involve changes in numerous other related parameters.

Other fluid properties of probably less importance to damage, (except for extreme variations) are viscosity, sonic velocity, and bulk modulus. Numerical calculations of bubble collapse (9, e.g.) show that even relatively large viscosities do not have much effect upon collapse velocity. Presumably increased viscosity can only reduce damage, but no pertinent tests where only viscosity is varied are available to our knowledge. The same is true of sonic velocity and bulk modulus, although in both cases reduced values should in general reduce cavitation damage.

A final and most important fluid property to be considered is corrosivity. This is certainly not in the nature of a "scale effect", but it can obviously strongly affect damage rates under conditions of constant sigma and similar

geometry. However, its increase certainly leads to increased damage (except for "completely" non-corrodible materials). In the same category might be considered the solids content of the liquid, in cases where this is a factor (as with slurry flows). Little information on this effect appears to exist at the moment, although it can be important in certain solids-transporting pipeline applications (coal or ore-bearing pipelines).

6. Conclusions

One general conclusion is that damage rate can increase very strongly with increased velocity, pressure or size, when sigma is maintained constant. Damage rates are in general more sensitive to these parameters than to any others. The velocity damage exponent is likely to lie in the range 4-6, and the diameter exponent in the range 2-4. Considerable further systematic experimentation is required before these effects can be delineated more closely. Uncertainty in erosion scale effects is also due to the lack of any universally accepted criteria in the measure of damage parameters. Damage intensities from only rather identical eroding environments can usefully be compared at this time.

1. Introduction

One of the major problems at present concerning liquid cavitation and impact erosion is our relative inability to predict erosion rates, or even the likely existence of important erosion, in field devices, from available laboratory tests or theoretical models.

This problem exists for all liquids of interest ranging from cryogenic to water, to liquid metals such as sodium, used as coolants for nuclear fast breeder reactors. Even the relative erosion resistance of materials measured in the same type of facility, but with minor differences in operating parameters, are often not the same even to a useful engineering approximation. In addition, there is no presently known technique for applying this type of test result to field devices. This was illustrated forcefully in a recent "round-robin" conducted by ASTM Committee G-2⁽⁸⁸⁾ for the simplest and most readily standardizable type of cavitation test device the vibratory horn, described in detail in Cavitation (6) and in numerous other papers and articles.

A similar situation exists for liquid impact erosion, for which a second ASTM "round-robin" has also been held (136)

Liquid impact is even more difficult to standardize cavitation because of the present lack of a relatively conventional test device, a situation which is even worse for the case of solid particle impact which is not within the scope of this book.

This section attempts to summarize the status of liquid erosion laboratory testing and its relation to erosion in field machines. In addition, some of the pertinent experimental and theoretical work to improve this situation is here summarized. It is treated more fully in other sections.

One of the major difficulties involved in the prediction of field machine erosion from laboratory tests is due to the fact that liquid erosion involves both mechanical and corrosive effects. In long-term field exposure, the corrosion effects can be relatively much more important than in the laboratory devices which in general are intended to accelerate the mechanical effects, and thus provide tests of short enough duration to be feasible from the viewpoint of laboratory tests. To provide realistic modeling for specific field applications, it is necessary either to accelerate both modes of attack in suitable proportion, or to provide methods of measuring them separately, ie, identify somehow the mechanical and corrosive effects in laboratory tests, so that a more meaningful application to field devices can be made. Work to achieve these goals is described in detail in another section.

One objective then is to measure, with greater precision than has been previously possible, the characteristics of the cavitation or liquid impact regime in both laboratory and field devices, and thus make more meaningful predictions than previously possible of probable prototype field results from laboratory tests. To accomplish this goal, one possibility is to measure and count actual individual pressure pulses from bubble or droplet impact lapse/originating from the flow regime in both laboratory and field devices. This would have the advantage of increasing basic understanding of the cavitation or impact flow regime involved, and providing a comparison of their "intensity" in various field and laboratory devices.

Liquid impingement is now supposed (5,6 , eg) to be a major contributory mechanism in cavitation erosion through the asymmetric collapse of bubbles and the generation of a liquid "microjet" which impinges upon the material surface.

laboratory, and others have, therefore, developed various numerical models of individual droplet or jet impact, with the goal of providing the capability for estimating actual stresses and strains in a material so impacted. These models of course apply to direct droplet or jet impact as well as to cavitation. Hopefully, it may eventually become possible to then compute expected rates of erosion if size, velocity, shape, and number of impacting droplets is known. The likelihood of a realistic calculating capability of this type for droplet impact appears to be much greater than for cavitation erosion because in most cases the details of the attacking flow regime, i.e. "microjet", pressure pulses, etc., are known much less precisely. It is for this reason that many present efforts on cavitation are primarily concerned with providing a technique for measuring and counting bubble collapse pulses. These spectra can hopefully be used as a measure of the "intensity" of the cavitation regime attack. Brief details of the mathematical modelling of liquid impact and bubble collapse will be provided here. However, further details are given in other sections.

2. Computer Modelling of Bubble Collapse and Droplet and Jet Impact

a. General Background

The phenomenon of liquid-solid impact has technological importance in various engineering applications; including steam turbines, rain erosion of aircraft or missile components, and also cavitation through the liquid "microjet" mechanism previously discussed. Its detailed study using sophisticated computer models is thus worthwhile in attempting to promote the ability to predict damage. It has thus been pursued vigorously in this laboratory over the past several years as well as elsewhere. For simplicity, primarily our own work will be here discussed as illustrative (2-4, 137-139). Previously we had also conducted several detailed studies of bubble collapse utilizing both high-speed photography (9, 140, eg.) and computer models (12, 51 eg). Some of these studies (9, 51, eg) considered spherically symmetric bubble collapse, but included all pertinent real-fluid effects, including "thermodynamic" restraints (51, eg). Our other studies considered the effects of non-symmetrical influences upon bubble collapse (12, 140-143, eg) such as the presence of adjacent walls, pressure gradients, relative ("slip") velocity around the collapsing bubble, and multibubble effects (142, eg), but neglected real-fluid effects other than viscosity. Photographic studies here (12, 140-141) and elsewhere (39, 41, eg) had shown the controlling importance in many cases of these non-symmetric effects. Unfortunately it does not appear feasible at this point to include asymmetry and real-fluid effects, or the effects of multiple bubble in a completely general computer program together.

In summary (5,6, eg) the results of the above and other recent studies indicates the probable predominance of the liquid microjet mechanism in cavitation damage. It is possible from these studies to estimate the probable velocity (~ 300 m/s) and diameter ($\sim 1-10$ microns) of such microjets in typical cases. Hence, the microjet velocity magnitude is roughly typical of other droplet or jet impact applications, such as the steam turbine droplet erosion problem, but its diameter is orders of magnitude less, since droplet diameters of the order of 1 mm are typical in conventional droplet erosion problems. Hence it may be assumed that cavitation and conventional droplet erosion are very similar in mechanism as well as appearance, although the cavitation erosion may be generally of finer texture, and this has in fact been the general observation for many years. Full details of these and other computer studies are given in the appropriate sections,

3. Cavitation and Impact Erosion Prediction Techniques

a. General

The previous section has discussed computer modelling of the basic phenomena and high-speed photography as basic tools for developing the capability to predict cavitation or liquid impact erosion rates. It may eventually become possible using this approach to estimate realistically the stress-time regimes existing in the material as a result of liquid impact or cavitation. This capability is closer^{now} for impact than for cavitation, since the cavitation phenomenon is basically considerably more complex.

However, even if this capability should be attained, there would still remain the apparently even more difficult problem of accurately modelling the material removal process, given the pertinent time-dependent stress-strain values. Computer modelling of the erosion process would obviously depend upon the type of material, the relative importance of corrosive effects, as well as many other complicating factors, so that a general solution of this portion of the overall liquid erosion process seems even more remote than that of the fluid flow phenomena, previously discussed. Nevertheless, continued, though relatively gradual, progress from the side of computer modelling of the basic phenomena is certainly useful in increasing basic understanding of the phenomena involved, and gradually improving overall predicting capabilities.

b. Noise and Bubble Collapse Pulse Spectra

Since the capability for predicting erosion rates "a priori" from relatively basic principles does not presently exist, another possibility is to measure some easily and quickly measurable aspect of the cavitation or impact phenomenon, and then correlate this measurement with measured damage. The measurement of "noise" provides such a possibility, which appears to be of potential importance.

The use of noise for the detection of cavitation has been an accepted practice for years, and several recent attempts have been made to correlate overall noise with erosion (144-146, eg.).

Some success has been obtained in specific experiments with individual pumps or venturis. However, it appears that useful general correlations

cannot be attained in this way. Hence, we have here attempted to develop a technique whereby bubble collapse pressure pulse "spectra" are measured. If it is assumed that bubble collapse pressure pulse durations are roughly uniform (or at least

uniquely related to the pressure magnitude), then the area under such a spectrum curve provides a measure of the total impulse delivered to the damaged surface, or to a probe presumably located at a position equivalent to that of the surface to be damaged from the viewpoint of the cavitation field. Such a technique is sensitive to not only the number of "blows" delivered to the surface, but also to their strength. It thus appears to provide vital information beyond that provided either by a simple noise measurement or a noise frequency spectrum. Some relatively limited, successful experimentation with methods similar to those here suggested has been reported (27,29,146) using primarily vibratory cavitation damage facilities, as we have also in our work to date (30, 148,149, eg.).

Our experiments have included cavitation damage rate measurements in both water and molten sodium over a range of temperatures and suppression pressures in a _____ (38 μ m) vibratory horn cavitation damage facility, _____ (20 kHz). Detailed results are found elsewhere (30, 149,150) but Fig.26 illustrates the type of correlation obtained between measured bubble collapse pressure spectrum area and measured damage rate (MDPR = "mean depth of penetration", i.e., volume loss rate per unit exposed area). The best-fit relation is described by Eq.E-1

$$\text{MDPR} = C(\text{Spectrum Area})^n \text{-----} \quad (\text{E-1})$$

where C is a constant obtained empirically. The average value obtained for the exponent, n is ~ 5 for high intensity tests. and 1 for lower intensity results.

The pulse count energy spectrum area measurement will also allow computation of the "efficiency" of the delivery of energy to the damaged surface from the region of bubble collapse, as compared with the energy operative quantity in the erosion process. This latter, according to much previous work, can best be expressed in the form of an Ultimate Resilience, UR (see Section V-C), i.e., "strain energy to failure", if failures are of brittle (rather than ductile) nature, as generally appears to be the case for cavitation. Such a relationship would then be of the form:

$$\text{Spectrum Area} = C \cdot \eta \cdot \text{UR} \quad \text{-----} \quad \text{(E-2)}$$

This equation considers the erosion rate model discussed in Section C, where erosion energy efficiencies of this type are discussed. However, the measurement of Spectrum Area would allow the computation of the otherwise unknown "efficiency factor". In Eq.(E-2) C is a constant involving the calibration constant for the bubble collapse pulse measuring pressure probe, and η is the "efficiency" sought.

If found appropriate after additional research, material failure energy properties other than UR could be used in Eq. (E-1) above. If η were thus known for a class of cavitation regimes, then erosion rate, MDPR could be calculated from the pulse count measurement.

Figures 27 and 28 show respectively a typical bubble collapse pulse height spectrum for water in the U-M venturi and typical individual pulses measured by the U-M microprobe.

The standard percent error for the MDPR correlations (Eq. E-1) was only $\sqrt{20\%}$. This seems surprisingly small for experiments of this kind.

The required next step is to continue this type of experiment in a venturi facility with water, and eventually in field devices, but no such experiments had been reported by the time of writing.

Though the evidence yet available is relatively sparse, it appears that an "a priori" erosion rate predicting technique may be developed in the relatively near future for application to many field devices. Such a capability, within even very rough limits of possible engineering utility, is unfortunately virtually non-existent today.

While the pressure pulse spectrum technique has so far (148-150, eg.) been applied only to cavitation erosion, it appears applicable also to impact erosion cases, depending of course on geometrical considerations. Its eventual application to rotating components also seems feasible, but obviously involves geometric considerations pertinent to specific applications.

Figure 27 shows a typical bubble collapse pulse spectrum measured in our cavitating venturi, and Fig. 28 typical microprobe output from these tests. The rapid oscillations accompanying the initial pulse are believed to result from the probe "ringing" frequency.

c. Erosion "Acoustic Emission Noise"

"Acoustic emission" from material deformation (microcrack formation, etc.) is a well-known phenomenon, so that it is conceivable that this could be used to detect and measure erosion directly from an acoustic probe attached to the eroding surface. However, at the present time this appears to be improbable of success since it appears that the level of acoustic emission noise is orders of magnitude less than that of cavitation, so that the cavitation noise itself would mask the acoustic emission noise making it impossible to detect. However, since little or no pertinent research appears to have as yet been done, it is possible that this expectation may prove to be in error.

Somewhat pertinent to this possibility is an observation from a high-speed motion picture sequence taken here of an apparent ejected particle from so aluminum. It had an ejection velocity of ≈ 100 m/s normal to the surface, and was of elongated shape (≈ 1 mm length). If such high ejection energy is typical, the associated noise could be sufficient to detect, considering the good acoustic transmission to a probe attached to the surface, as compared to that from collapsing bubbles in the liquid.

d. Erosion Particle Size

Pertinent to the possibility of detecting erosion by its associated "emission noise" as discussed in the foregoing, is knowledge of eroded particle size and mode of removal from the eroded surface. Some information concerning the "ejection velocity" of such a particle was discussed in the last section. Very few studies exist as yet concerning the size distribution of cavitation debris. However, one such study was conducted some years ago here (151) where neutron irradiated stainless steel ^{test} specimens were used in a water venturi system. The irradiated eroded particles could thus be isolated from other miscellaneous particles in the system and sieved. It was found that particle diameters ranged up to ~ 0.1 mm, with the greatest number of particles much smaller. Typical results are shown in Fig. 29. It can thus be concluded from this study, and also whatever other fragmentary information exists, that the debris particle sizes are certainly not uniform, no doubt depend strongly upon the material and flow parameters, that no minimum size can be specified, and that the maximum in some cases could be the order of a millimeter.

References

1. F. G. Hammitt, "Erosive Wear Testing", Selection and Use of Wear Tests for Metals, ASTM STP 615, 45-67, 1975.
2. Y. C. Huang, "Numerical Studies of Unsteady, Two-Dimensional Liquid Impact Phenomena", Ph.D. thesis; ORA Report No. UMich 03371-8-T, June 1971; see also Y. C. Huang, F. G. Hammitt, W. J. Yang, "Hydrodynamic Phenomena During High-Speed Collision Between a Liquid Droplet and Rigid Plane," Trans. ASME, J. Fluids Engr., 1, 95, 2, 1973, p. 276-294.
3. J. B. Hwang, "The Impact Between a Liquid Drop and an Elastic Half-Space," Ph.D. thesis, Dept. of Mech. Engr., also available as ORA Rept. No. UMich 012449-8-T, Mar. 1975, Univ. of Michigan.
4. J. B. Hwang and F. G. Hammitt, "Transient Distribution of the Stress During the Impact Between a Liquid Drop and an Aluminum Body," BHRA Third International Symposium Jet Cutting Technology, Chicago, May 11-13, 1976); ORA Report No. UMich 012449-8-T, June 1975.
5. F. G. Hammitt and F. J. Heymann, "Liquid-Erosion Failures," Handbook, Vol 10, Ed. 8, 160-167, American Society of Metals, Metals Park, Ohio.
6. R. T. Knapp, J. W. Daily, F. G. Hammitt, Cavitation, McGraw-Hill, 1970
7. R. T. Knapp and A. Hollander, "Laboratory Investigations of the Mechanism of Cavitation," Trans. ASME, Vol 70, 1948, 419-435.
8. R. Hickling and M. S. Plesset, "Collapse and Rebound of a Spherical Bubble in Water," The Physics of Fluids, Vol 7, No. 1, 1964.
9. R. D. Ivany and F. G. Hammitt, "Cavitation Bubble Collapse in Viscous, Compressible Liquids--Numerical Analysis," Trans. ASME, J. Basic Engr., D, 87, n. 5, 1965, 977-985.
10. F. G. Hammitt, "Collapsing Bubble Damage to Solids," Cavitation State of Knowledge, ASME, 1969, 87-102.
11. M. J. Robinson and F. G. Hammitt, "Detailed Damage Characteristics in a Cavitating Venturi," Trans. ASME, J. Basic Engr., D, 89, 1967, 161-173.
12. C. L. Kling and F. G. Hammitt, "A Photographic Study of Spark-Induced Cavitation Bubble Collapse," Trans. ASME, J. Basic Engr., Dec. 1972, 825-833.
13. H. A. Wagner, J. M. Decker, J. C. March, "Corrosion-Erosion of Boiler Feed Pumps and Regulating Valves," Trans. ASME, May 1947, 389-403.

References (cont.)

14. J. M. Decker, H. A. Wagner, J. C. Marsh, "Corrosion-Erosion of Boiler Feed Pumps and Regulating Valves at Marysville, 2nd Test Program," Trans. ASME, 72, 1950, 19-36.
15. J. Ackeret and P. de Haller, "Untersuchen uber Korrosion durch Wasserstoss," Schwiez Bauzeitung, 98, 309-310, 1931.
16. D. E. Elliott, J. B. Marriott, A. Smith, "Comparison of Erosion Resistance of Standard Steam Turbine Blade and Shield Materials on Four Test Rigs," ASTM STP No. 474, Oct. 1970, 127-161.
17. N. E. Wahl, "Investigation of the Phenomena of Rain Erosion at Supersonic Speeds," AFML-TR-65-330, Air Force Materials Lab., WPAFB, Dayton, Ohio, October 1965.
18. G. F. Schmitt, Jr. and A. H. Krabill, "Velocity-Erosion Rate Relationships of Materials in Rain at Supersonic Speeds," AFML-TR-70-44, Air Force Materials Lab., WPAFB, Dayton, Ohio, October 1970.
19. G. F. Schmitt, Jr., W. G. Reinecke, G. D. Waldman, "Influence of Velocity, Impingement Angle, Heating, and Aerodynamic Shock Layers on Erosion of Materials at Velocities of 5500 f/s (1700 m/s)," ASTM STP No. 567, Dec. 1974, 219-238.
20. K. Steller, Personal Communication, Inst Fluid Flow Machines, Polish Acad. of Science, Gdansk, Poland, 1974.
21. H. N. Boetcher, "Failure of Metals due to Cavitation under Experimental Conditions," Trans. ASME, 58, 1936, 355-360.
22. A. Thiruvengadam, "A Comparative Evaluation of Cavitation-Damage Test Devices," Tech. Repts. 233-2, Hydronautics, Inc., Nov. 1963.
23. K. K. Shal'nev, "Experimental Study of the Intensity of Erosion due to Cavitation," Cavitation in Hydrodynamics, Nat'l Phys. Lab., October 1955, Teddington, England, 22 p. 1-37.
24. R. E. H. Rasmussen, "Some Experiments on Cavitation Erosion in Water Mixed with Air," Cavitation in Hydrodynamics, Nat'l Phys. Lab., 1955, London, England, 20 p. 1-25.
25. G. M. Wood, L. K. Knudson, and F. G. Hammitt, "Cavitation Studies with Rotating Disk," Trans. ASME, 89, D, J. Basic Engr., 98-110, 1967.
26. Anonymous, "Standard Method of Vibratory Cavitation Erosion Test," ASTM, G 32-72, 1974.

27. F. Numachi, "An Experimental Study of Accelerated Cavitation Induced by Ultrasound", Trans. ASME, J. Basic Engr., 87, 1965, 967-976.
28. F. Numachi, M. Hongo, "Ultrasonic Shock Waves Emitted by Cavitation at Perforation on Plate/Rept 1," Rept. Inst. High Speed Mech., 30, 277, 1974.
29. V. K. Makarov, A. A. Kortnev, S. G. Suprun, G. I. Okolelov, "Cavitation Erosion Spectra Analysis of Pulse-Heights Produced by Cavitation Bubbles," Proc. 6th Non-Linear Acoustics Conf., Moscow, July 1975, (Odessa Poly. Inst).

30. F. G. Hammitt, J-B. Hwang, M. K. De, et al, "Final Report for Argonne National Laboratory Project", ORA Rept. No. UMICH 013503-2-F, June, 1976.
31. Lord Rayleigh, "On The Pressure Developed in a Liquid During the Collapse of a Spherical Cavity", Phil. Mag., 34, 94-98, 1917.
32. F.G. Hammitt, "Collapsing Bubble Damage to Solids" in Cavitation State of Art Symposium, ASME, June 1969.

33. F. G. Hammitt, et al, "Initial Phases of Damage to Test Specimens in a Cavitating Venturi", Trans. ASME, J. Basic Engr., D, 87, 2, 453-464, 1965.
34. F. G. Hammitt, "Observations on Cavitation Damage in a Flowing System", Trans. ASME, J. Basic Engr. D, 85, 3, 347-359, 1963.

35. M. J. Robinson and F. G. Hammitt, "Detailed Damage Characteristics in a Cavitating Venturi", Trans. ASME, J. Basic Engr. D, 89, 1, 161-173, 1967.
36. R. T. Knapp, "Recent Investigations of the Mechanics of Cavitation and Cavitation Damage", Trans. ASME, 1045-1054, Oct. 1955.
37. C.L.Kling, "A High Speed Photographic Study of Cavitation Bubble Collapse", PhD Thesis, Nucl. Engr. Dept., Univ. of Mich., Ann Arbor, Mich. 1970; also available as ORA Rept. No. UMICH 03371-2-T, March 1970
38. E.E. Timm, "An Experimental Photographic Study of Vapor Bubble Collapse and Liquid Jet Impingement", PhD Thesis, Chem. Engr. Dept., University of Michigan, Ann Arbor, Mich., 1974; also available as ORA Report No. UMICH 01357-39-T, June 1974.
39. C. F. Naudé and A. T. Ellis, "On the Mechanism of Cavitation Damage by Non-hemispherical Cavities Collapsing in Contact with a Solid Boundary", Trans. ASME, J. Basic Engr., D, 83, 4, 648-656, 1961.
40. T. B. Benjamin and A. T. Ellis, "The Collapse of Cavitation Bubbles and the Pressures Thereby Produced Against Solid Boundaries", Phil. Trans. Roy. Soc., A, 260, 1110, 221-240, 1966.
41. N. D. Shutler and R. B. Mesler, "A Photographic Study of the Dynamics and Damage Capabilities of Bubbles Collapsing Near Solid Boundaries", Trans. ASME, J. Basic Engr., D, 87, 2, 511-517, 1965.
42. R. D. Ivany, F. G. Hammitt, and T. M. Mitchell, "Cavitation Bubble Collapse Observations in a Venturi", Trans, ASME, J. Basic Engr., D, 88, 3, 649-657, 1966.
43. A. Eller and H. G. Flynn, "The Equilibrium and Stability of a Translating Cavity in a Fluid", J. Fluid Mech., 30, pt. 4, 785-803, 1967.

- H. C. Yeh and W. J. Yang, "Dynamics of Bubbles Moving in Liquids with Pressure Gradient", J. Appl. Phys., 19, 7, 3156-3165, 1968.
- D. C. Gibson, "The Collapse of Vapor Cavities", Ph.D. Thesis, Churchill College, Cambridge Univ., July, 1967.
- M. Rattray, "Perturbation Effects in Cavitation Bubble Dynamics", Ph.D Thesis, Cal. Inst. Tech., Pasadena, Calif., 1952.
-
- A. N. Korovkin and Y. L. Levkovskiy, "Closing of Cavitation Caverns Close to a Solid Wall", (Russian), J. of Engr. Physics, XII, 2, 246-253, April, 1967.
- J. H. Brunton, "The Physics of Impact and Deformation: Single Impact", Phil. Trans. Roy. Soc. A, 260, 1110, 79-85, 1966.
- F. J. Barclay, T. J. Ledwidge, G. C. Cornfield, Discussion of F. G. Hammitt, "Damage Due to Cavitation and Sub-Cooled Boiling Bubble Collapse", Proc. I. Mech. E., 1968-69, Vol. 183, Part I.
- R. Hickling, "Some Physical Effects of Cavity Collapse in Liquids", Trans. ASME, J. Basic Engr., D., 88, 1, 229-235, 1966.
- T.M. Mitchell and F.G. Hammitt, "On the Effects of Heat Transfer Upon Collapsing Bubbles", Nucl. Sci. and Engr., 53, 3, 1974, 263-276.
- A.T. Ellis, "On Jets and Shock Waves from Cavitation", Proc. 6th Naval Symposium, Washington, D.C., 6-1, 6-19, Oct. 1966.
- W. Lauterborn and H. Bolle, "Experimental Investigations of Cavitation-Bubble Collapse in the Neighbourhood of a Solid Boundary", J. Fluid Mech., 72, 2, 1975, 391-399.
- A.T. Ellis, private communication, 1968.
- R. Canavelis, "Comparison of the Resistance of Different Materials with a Jet Impact Test Rig", HC/061-230-9, Electricité de France, Chatou, France, Nov. 1967.
- M. Delhaye, R. Semeria, and J.C. Flamand, "Void Fraction, Vapor and Liquid Temperature. Local Measurements in Two-Phase Flow Using a Micro-thermocouple.", J. Heat Transfer, Aug. 1973, 365-370.
- G. W. Sutton, "A Photo-Elastic Study of Strain Waves Caused by Cavitation", J. Appl. Mech., 24, 3, 340-348, 1957.
- A.T. Ellis, "Parameters Affecting Cavitation and Some New Methods for Their Study", California Institute of Technology Hydrodynamics Laboratory Report No. E-115.1, Oct. 1965.
-
- W. Bober, "An Analytical Investigation of the Pressure Field in a Cavitating Flow", ASME Paper No. 69-FE-34, 1969.
- V.E. Johnson and T. Hsieh, "The Influence of Entrained Gas Nuclei Trajectories on Cavitation Inception", Proc. 6th Naval Hydrodynamics Symp., Wash., D.C., Oct. 1966.

61. K. K. Shalnev, "Experimental Study of the Intensity of Erosion Due to Cavitation", Cavitation in Hydrodynamics, National Physical Laboratory, Teddington, Middlesex, England, 22 p. 1-22 p.37, Oct., 1955.
62. F.G. Hammitt, "Cavitation Damage Scale Effects - State of Art Summarization", J. Hyd. Research (IAHR), 13, 1975, 1-18.
63. S.G. Young and J.R. Johnston, "Effect of Cover Gas Pressures on Accelerated Cavitation Damage in Sodium", NASA TN, D-4235, 1967.
64. F.G. Hammitt and D.O. Rogers, "Effects of Pressure and Temperature Variation in Vibratory Cavitation Damage Test", J. Mech. Engr. Sci., 12, 6, 1970, 432-439.
65. F.G. Hammitt and N.R. Bhatt, "Cavitation Damage at Elevated Temperature and Pressure", 1972 ASME Polyphase Flow Forum, 11-13, 1972.
66. J. M. Hobbs, "Experience with a 20-KC Cavitation Erosion Test", ASTM STP No. 408, 159-179, 1967.
67. H.A. Stahl and A.J. Stepanoff, "Thermodynamic Aspects of Cavitation in Centrifugal Pumps", Trans. ASME, 78, 1691-1693, 1956.
68. J. Bonnin, "Theoretical and Experimental Investigations of Incipient Cavitation in Different Liquids", ASME Paper No. 72-WA/FE-31, 1972.
69. J. Bonnin, "Influence des Effects Thermiques sur L'Erosion de Cavitation (essais vibratoires)", Electricité de France, Direction des Etudes et Recherches, Chatou (Internal report), June 1972.
70. R. Garcia and F. G. Hammitt, "Cavitation Damage and Correlations with Material and Fluid Properties", Trans. ASME., J. Basic Engr., D, 89, 4, 753-763, 1967.
71. R. E. Devine and M. S. Plesset, "Temperature Effects in Cavitation Damage", C.I.T. Rept. No. 85-27, April, 1964, Calif. Inst. of Tech., Pasadena, Calif.

72. F.G. Hammitt, Y.C. Huang, etal, "A Statistically Verified Model for Correlating Volume Loss Due to Cavitation or Liquid Impingement", ASTM STP No. 474, 1969, 288-322.
73. F.J. Heymann, Discussion Ref. 72, ibid 72, 312-315.
74. F.J. Heymann, "Toward Quantitative Prediction of Liquid Impact Erosion", ASTM STP No. 474, 1969, 212-248.
75. B.C. Syamala Rao, N.S. Lakshmana Rao, and K. Seetharamiah, "Cavitation Erosion Studies with Venturi and Rotating Disk in Water", Trans. ASME, J. Basic Engr., Sept. 1970, 563-579.

F.G. Hammitt, "Damage to Solids Caused by Cavitation", Phil. Trans. Roy. Soc., A, 260, 1110, 245-255, 1966.

D.J. Kemppainen and F.G. Hammitt, "Effects of External Stress on Cavitation Damage", Proc. XIII Congress IAHR, Kyoto, Japan, August, 1969.

K.K. Shalnev, R.D. Stepanov and S.P. Kozyrev, "Effect of the Stressed State of Metals on Resistance to Cavitation", Soviet Physics-Doklady, 11, 9, 822-824, March, 1967.

G. Hott, G. Langbein, and H. Rieger, "Material Destruction Due to Liquid Impact", ASTM STP 408, 42-69, 1966.

A. Thiruvengadam, "A Unified Theory of Cavitation Damage", Trans. ASME, J. Basic Engr., D, 85, 3, 365-376, 1963.

ASTM Committee G-2, "Standard Definitions of Terms Relating to Erosion By Cavitation and Impingement", 1973.

F. G. Hammitt, et al, "Initial Phase of Damage of Test Specimens in a Cavitating Venturi as Affected by Fluid and Material Properties and Degree of Cavitation", Trans. ASME, J. Basic Engr., D, 87, 453-464, 1965.

R. Garcia and F.G. Hammitt, "Cavitation Damage and Correlations with Materials and Fluid Properties", Trans. ASME, J. Basic Engr., D, 89, 4, 753-763, 1967.

J.M. Hobbs, "Experience With a 20-Kc Cavitation Erosion Test", ASTM, STP 408, 159-185, 1967.

F.J. Heymann, "Erosion by Cavitation Liquid Impingement and Solid Impingement," Engineering Report E- 1460, Westinghouse Electric Corporation, March 15, 1968.

"Standard Method of Vibratory Cavitation Erosion Test", G 32-72, ASTM, 1972.

R. B. King, letter to F.G. Hammitt, June 13, 1968.

F.G. Hammitt, C. Chao, C.L. Kling, D.O. Rogers, "ASTM Round - Robin Test with Vibratory Cavitation and Liquid Impact Facilities of 6061-T 6511 Aluminum Alloy, 316 Stainless Steel, Commercially Pure Nickel", Materials Research and Standards, MTRSA, 10, 10, 16-36, 1970.

89. G. Petracchi, "Investigation of Cavitation Corrosion", (in Italian), Metallurgica Italiana, 41, 1-6, 1944. English summary in Engr's Digest, 10, 314-316, 1949.
90. M. S. Plesset, "On Cathodic Protection in Cavitation Damage", Trans. ASME, 82, D, J. Basic Engr., 808-820, 1960.
91. S. Nemeček, "K otázce urcovani kavitacni odolnosti" Konference o vodnich turbinach, Brno 1958; also
92. S. Nemeček, "K otázce mechaniky kavitace." I. sbornik praci Vysoké školy strojní v Liberci 1959, str. 128-146.
93. K. Steller, IFFM, Polish Academy Science, Gdansk, Poland, personal communications with F. G. Hammitt, 1976.
-
94. F. G. Hammitt, "Cavitation Damage Scale Effects-State of Art Summarization," J. Hyd. Research (IAHR), 13, 1, 1-18, 1975.
95. F. G. Hammitt, "Effects of Gas Content upon Cavitation Inception, Performance, and Damage", J. Hyd. Research (IAHR), 10, 3, 1972, 259-290
96. J. M. Hobbs and A. Laird, "Pressure Temperature and Gas Content Effects in the Vibratory Test", NEL Report No. 438, Oct. 1969; see also 1969 ASME Cavitation Forum, p. 3-4.
97. Stanley G. Young, and James R. Johnston, "Effect of Cover Gas Pressures on Accelerated Damage in Sodium", NASA TN D-4235, Nov. 1967.
-
98. Stanley G. Young and James R. Johnston, "Accelerated Cavitation Damage of Steels and Superalloys in Liquid Metals," NASA TN D-3226, May 1966.
99. F. G. Hammitt, and D. O. Rogers, "Effects of Pressure and Temperature Variation in Vibratory Cavitation Damage Test," J. Mech. Engr. Sci., 12, 6, 1970, 432-439.
100. F. G. Hammitt and N. R. Bhatt, "Cavitation Damage at Elevated Temperature and Pressure", ASME Polyphase Forum, 1972, 11-13.
101. M. J. Robinson, "On the Detailed Flow Structure and the Corresponding Damage to Test Specimens in a Cavitating Venturi", Ph.D. thesis, The Univ. of Mich., Nuclear Dept., 1965, Ann Arbor, Mich.
102. F. G. Hammitt, "Observations on Cavitation Damage in a Flowing System," Trans. ASME, J. Basic Engr., 85, D, 347-359, 1963.
103. F. G. Hammitt, et al., "Initial Phases of Damage to Test Specimens in a Cavitating Venturi," Trans. ASME, J. Basic Engr., 87, D, 453-464, 1965.
- 103a. B. C. Syamala Rao and D. V. Chandrasekhara, "Internal Report, Size and Velocity Scale Effects on Damage in a Venturi", Civil Engr. Dept., Bangalore Inst. of Tech., 1973.

4. P. Tullis, and R. Govindarajan, "Cavitation and Size Scale Effects for Orifices", J. Hyd. Div., ASCE, v. 99, No. HY3, Proc. paper 9605, Mar., 1973.
5. R. Canavelis, "Jet Impact and Cavitation Damage", Trans. ASME, J. Basic Engr., Sept. 1968, 355-367.
6. J. M. Hobbs, "Factors Affecting Damage Caused by Liquid Impact", NEL Report No. 262, Dec. 1966.
7. J. M. Hobbs, and W. C. Brunton, "Comparative Erosion Tests on Ferrous Materials, Part I: Drop Impact Test", NEL Report No. 205, Nov. 1965.
8. J. F. Ripken, "Comparative Studies of Drop Impingement Erosion and Cavitation Erosion," Univ. of Minn., St. Anthony Falls Hydraulic Lab., Project Report No. 105, April 1969; see also J. F. Ripken, A Test Rig for Studying Impingement and Cavitation Damage," ASTM STP-408, 1967.
-
9. J. Z. Lichtman and E.R. Weingram, "The Use of a Rotating Disk Apparatus in Determining Cavitation Erosion Resistance in Materials," ASME Symp. on Cavitation Research Facilities and Techniques, 185-196, 1964.
-
0. K. K. Shalnev, I. I. Varga and D. Sebestyen, "Investigation of the Scale Effects of Cavitation Erosion," Phil. Trans. Roy. Soc. London, Series No. 1110, Vol. 260, July 1966, 256-266.
1. A. Thiruvengadam, "Theory of Erosion", Hydronautics Inc., Technical Report 233-11, March 1967.
2. A. Thiruvengadam, "Cavitation Erosion", Applied Mechanics Reviews, 24, No. 3, March 1971, pp. 245-253.
3. A. Thiruvengadam, "Effects of Hydrodynamic Parameters on Cavitation Erosion Intensity," Hydronautics, Inc., Tech. Report 233-14, Nov. 1970.
4. A. Thiruvengadam, "Scaling Laws for Cavitation Erosion," Hydronautics, Inc., Tech. Report 233-15, Dec. 1971.
5. R. T. Knapp, "Recent Investigations of Cavitation and Cavitation Damage," Trans. ASME, 77, 1045-1054, 1955.
-
6. R. T. Knapp, "Accelerated Field Tests of Cavitation Intensity," Trans. ASME, 80, 91-102, 1958.
7. K. Steller, Z. Reymann, and T. Krzysztofowicz, "Evaluation of the Resistance of Materials to Cavitation Erosion," Proc. 5th Conf. on Fluid Machinery, Akademiai Kiado, Budapest, Hungary, 1975, 1081-1096.
8. K. Steller, T. Krzysztofowicz, and Z. Reymann, "Effects of Cavitation on Materials in Field and Laboratory Conditions," Erosion, Wear, and Interfaces with Corrosion, ASTM STP 567, 1974.
-
9. K. Steller, "Wstepne Wyniki Badan nad Odpornoscia Tworzyw Sztucznych na Dzialanie Kawitacji," Prace Instytutu Maszyn Przeplywowych, Zeszyt 61, 1973
0. W. Thuss (J. M. Voith GmbH), letters to F. G. Hammitt, 1972-1973.

121. H. Giraud, Etude Detaillee de la Comparaison entre Essais Industriels et Modèle dans Quelques Cas Bien Definis, La Houille Blanche, n. 3, 1966, pp. 299-312.
122. F. G. Hammitt and N. R. Bhatt, "Temperature and Pressure Effects in Vibratory Cavitation Damage Tests in Various Liquids, Including Molten Sodium," *ibid* ref. 29, 393-402.
123. S. P. Hutton and J. LoboGuerrero, "The Damage Capacity of Some Cavitating Flows," *ibid* ref. 29, 427-438.
124. J. W. Ball, J. P. Tullis and T. E. Stripling, "Predicting Cavitation in Sudden Enlargements," J. of Hyd. Div., ASCE, 101, No. HY7, July 1975, pp. 857-870, ; See also J. W. Ball, J. P. Tullis and T. Stripling, "Incipient Cavitation Damage and Scale Effects for Sudden Enlargement Energy Dissipators", presented ASCE Hyd. Div. Specialty Conf., Tenn, 1974
125. R. Canavelis, "Contribution a l'Etude de l'Erosion de Cavitation dans les Turbomachines Hydrauliques," Ph.D. thesis, U. of Paris, Faculty of Science, 1974
126. W. Meier and H. Grein, "Cavitation in Models and Prototypes of Storage Pumps and Pump Turbines," Trans. IAHR Symp., Stockholm, 1970, Paper H3.
127. O. Schiele and G. Mollenkopf, "Some Views on Different Cavitation Criteria of a Proc. Cavitation, I. Mech. E., Fluid Machinery Group, Heriot-Watt Univ., Sept. 1974, 177-18
128. V. Malyshev and N. Pylaev, "Influence of Hydroturbine Size on Cavitation Pitting Intensity," *ibid*, 38, 309-312.
129. S. G. Young and J. R. Johnston, "Accelerated Cavitation Damage of Steels and Superalloys in Sodium and Mercury," Erosion by Cavitation or Impingement, ASTM STP 408, p. 186-212.
130. L. W. Florschuetz and B. T. Chao, "On the Mechanics of Vapor Bubble Collapse- A Theoretical and Experimental Investigation," Trans. ASME, 87, Jr. Heat Transfer, 209-220, 1965.
131. T. M. Mitchell and F. G. Hammitt, "On the Effects of Heat Transfer Upon Collapsing Bubbles," Nucl. Sci. and Engr., 53, 3, Mar. 1974, p. 263-276.
132. J. Bonnin, "Incipient Cavitation in Liquids Other than Cold Water, Report No. 030, EdF, Chatou, France, Jan. 1971; also see 1971 ASME Cavitation Forum, p. 14-16.
133. J. Bonnin, "Debut de Cavitation dans des Liquides Differentes," EDF-Bulletin de la Direction Recherches-Serie A Nucleaire Hydraulique, Thermique, No. 4, 1970, p. 53-72.
134. J. Bonnin, "Influence de la Temperature sur le Debut de Cavitation dans l'Eau," Société France, XII Journées de l'Hydraulique, Paris, 1972.
135. H. Nowotny, Destruction of Materials by Cavitation (in German) , VDI Verlag, Berlin, 1942.

- F. J. Hevmann, Westinghouse Steam Turbine Division, "Preliminary Report on Liquid Impact Erosion, Round-Robin Test Program," Internal Report, July 1973.
- F. G. Hammitt, Y.C. Huang, "Liquid Droplet Impingement Studies at the University of Michigan," Proc. Warwick Conf., Conf. Pub. #3, Inst. of Mech. Engrs., U. of Warwick, Coventry, Apr. 3-5, 1973, pp. 237-243.
- J.B. Hwang, F. G. Hammitt, "High Speed Impact Between Curved Liquid Surface and Rigid Flat Surface," ASME paper no. 76-WA/FE-34, Trans. ASME, J. Fluids Engr., 1977.
- J. B. Hwang, F. G. Hammitt, W. Kim, "On Liquid-Solid Impact Phenomena," 1976 ASME Cavitation Forum, p. 24-27.
- C. L. Kling, "A High Speed Photographic Study of Cavitation Bubble Collapse," ORA Report No. UMich 03371-2-T, March 1970.
- E.E. Timm, "An Experimental Photographic Study of Vapor Bubble Collapse and Liquid Jet Impingement," ORA Rept. No. UMich 01357-39-T, 1974, Ph.D. thesis, Chem. Engr. Dept., Univ. of Mich., 1974.
- T.M. Mitchell, "Numerical Studies of Asymmetric and Thermodynamic Effects on Cavitation Bubble Collapse," ORA Report No. UMich 03371-5-T, Dec. 1970.
- T.M. Mitchell, F.G. Hammitt, "Asymmetric Cavitation Bubble Collapse," Trans. ASME, J. Fluids Engr., 95, 1, March 1973, p. 29-37.
- I.S. Pearsall, P.J. McNulty, "Comparisons of Cavitation Noise with Erosion," 1968 ASME Cavitation Forum, p. 6-7.
- J. J. Varga, Gy. Sebestyen, "Determination of Hydrodynamic Cavitation Intensity by Noise Measurement," Proc. 2nd International JSME Symposium on Fluid Machinery and Fluidics, Tokyo, Sept. 1972, p. 285-292; see also J. J. Varga, Gy. Sebestyen, A. Fay, "Detection of Cavitation by Acoustic and Vibration-Measurement Methods," La Houille Blanche, 2, 1969, p. 137-149.
- P. A. Lush and S. P. Hutton, "The Relation Between Cavitation Intensity and Noise in a Venturi-Type Section," Proc. Int'l Conf. on Pump and Turbines, NEL, Glasgow, 1-3, Sept. 1976.
- F. Numachi, "Transitional Phenomena in Ultrasonic Shock Waves Emitted by Cavitation on Hydrofoils," Trans. ASME, J. Basic Engr., June 1959, p. 153.
- F. G. Hammitt, J. B. Hwang, "Ultrasonic Cavitation Regime Pulse-Count Spectra as Related to Cavitation Erosion," Proc. 7th Int'l Non-Linear Acoustics Conf., Blacksburg, Va., Aug. 1976.
- F. G. Hammitt, S. A. Barber, M. K. De, A. N. El Hasrouni, "Predictive Capability for Cavitation Damage from Bubble Collapse Pulse Count Spectra," Proc. Conf. "Scaling for Performance Prediction in Rotodynamic Machines", I.Mech.E., 6-8 Sept., 1977, Univ. Stirling, U.K.
- F. G. Hammitt, S. A. Barber, M. K. De, A. N. El Hasrouni, "Cavitation Damage Prediction from Bubble Collapse Pulse Count Spectra," 1977 Cavitation and Polyphase Flow Forum, ASME, 1977.
- W. J. Walsh and F. G. Hammitt, "Cavitation and Erosion Damage Measurements with Radio-Isotopes," Nuc. Sci. and Engr., 14, 3, Nov. 1962, 217-223.

List of Tables

- Table 1 - Numerical Example of Fluid Stresses at High Velocities in Cold Water
- Table 2 - Comparative Damage Intensities for Different Types of Facilities
- Table 3 - Mechanical Properties of Materials in Data Set
- Table 4 - Summary of Statistical Correlation Data for Eq. C-4.
- Table 5 - Acoustical Impedance Correction
- Table 6 - Equations Using Non-Linear Parameters
- Table 7 - Recommended Correlating Equations
- Table 8 - Statistical Correlation Coefficients

Table 2

Comparative Damage Intensities for Different Types of
Facilities _____:

		<u>Intensity</u> (watts/cm ² x 10 ⁷)
1.	<u>Magnetostriction</u>	
	Devices #1 - #7	0.004 - 2.5
2.	<u>Venturis</u>	
	#8-#9 Boetcher type	0.1 - 0.1 x 10 ⁻²
	#10 Shalnev type	0.1
	#11 "	0.03
	#12 "	0.1
	#13 U-M	0.3 x 10 ⁻⁴
3.	<u>Rotating Disc</u>	
	#14	4
	#15	0.34
	#16	1.0

Ref. A. Thiruvengadam, "A Comparative Evaluation of Cavitation Damage Test Devices", Tech. Report 233-2, Hydronautics, Inc., Nov. 1963

TABLE 4 Summary of Statistical Correlation Data for Eq. C-4

MATERIAL & NORMALIZED EPSILON	C ₁ = 0.914		C ₂ = 2.875		C ₁ = 6.487		C ₁ = 1.633		C ₂ = 1.735		C ₂ = -1.173	C ₁ = 1.139	C ₂ = 0.889	C ₁ *C ₂ *UR	C ₁ *C ₂ *SE	C ₁ *C ₂ *TSE	C ₁ *UR+C ₂ *SE	C ₁ *UR+C ₂ *TSE	C ₀ +C ₁ *UR+C ₂ *SE	SOURCES	
	C ₁	C ₂	C ₁	C ₂	C ₁	C ₂	C ₁	C ₂	C ₁	C ₂											
BS1433 COPPER	1.000	2.811	4.699	6.931	2.522	1.102	1.102	1.102	1.102	1.102	1.102	1.102	1.102								
STAINLESS STEEL 316	21.482	7.611	18.664	12.474	13.464	14.218	14.218	14.218	14.218	14.218	14.218	14.218	14.218								
NICKLE 270	5.044	3.179	11.254	14.510	6.035	5.534	5.534	5.534	5.534	5.534	5.534	5.534	5.534								
AL 6061	1.482	7.446	5.817	7.103	7.057	6.040	6.040	6.040	6.040	6.040	6.040	6.040	6.040								
STAINLESS STEEL 304	19.594	9.026	19.845	13.565	15.258	16.250	16.250	16.250	16.250	16.250	16.250	16.250	16.250								
BRONZE #1	3.421	5.119	5.801	6.924	5.046	3.902	3.902	3.902	3.902	3.902	3.902	3.902	3.902								UM Vibratory
BRONZE #2	39.669	23.359	9.326	7.612	22.468	22.789	22.789	22.789	22.789	22.789	22.789	22.789	22.789								Cavitation Facility
BRONZE #3	29.391	22.556	7.895	7.278	21.079	21.161	21.161	21.161	21.161	21.161	21.161	21.161	21.161								
BRONZE #4	3.674	2.645	3.352	6.553	1.723	0.109	0.109	0.109	0.109	0.109	0.109	0.109	0.109								
BRONZE #5	1.959	2.601	3.567	6.581	1.789	0.202	0.202	0.202	0.202	0.202	0.202	0.202	0.202								
BRONZE #6	2.516	2.295	3.038	6.511	1.268	-0.408	-0.408	-0.408	-0.408	-0.408	-0.408	-0.408	-0.408								
STAINLESS STEEL #1	25.659	25.666	12.609	8.452	26.055	26.951	26.951	26.951	26.951	26.951	26.951	26.951	26.951								
STAINLESS STEEL #2	23.948	37.310	6.850	7.230	33.271	34.005	34.005	34.005	34.005	34.005	34.005	34.005	34.005								
STAINLESS STEEL #3	15.037	17.729	9.818	8.706	17.861	17.946	17.946	17.946	17.946	17.946	17.946	17.946	17.946								
COPPER	0.963	2.740	7.965	7.240	4.053	3.077	3.077	3.077	3.077	3.077	3.077	3.077	3.077								
BRASS (65-35)	3.801	7.056	9.267	7.455	8.550	8.076	8.076	8.076	8.076	8.076	8.076	8.076	8.076								
MILD STEEL 1020	8.002	9.091	9.910	7.571	10.470	10.102	10.102	10.102	10.102	10.102	10.102	10.102	10.102								
STAINLESS STEEL 304	19.476	9.889	7.575	7.017	10.018	9.374	9.374	9.374	9.374	9.374	9.374	9.374	9.374								
ASTM A141SAE660J	4.384	1.867	3.971	6.643	1.354	-0.217	-0.217	-0.217	-0.217	-0.217	-0.217	-0.217	-0.217								
MAGNESIUM	1.490	7.142	5.689	6.849	6.733	5.682	5.682	5.682	5.682	5.682	5.682	5.682	5.682								
ALUMINUM 3003-O	0.213	1.654	5.296	6.764	1.818	0.417	0.417	0.417	0.417	0.417	0.417	0.417	0.417								
COPPER	1.000	2.811	4.699	6.931	2.522	1.102	1.102	1.102	1.102	1.102	1.102	1.102	1.102								
CR-130 STEEL	1.391	6.441	9.022	7.654	7.755	7.123	7.123	7.123	7.123	7.123	7.123	7.123	7.123								
AL ALLOY	0.806	9.175	4.451	6.740	7.880	6.769	6.769	6.769	6.769	6.769	6.769	6.769	6.769								
ALUMINUM	0.254	1.663	3.100	6.523	0.755	-0.946	-0.946	-0.946	-0.946	-0.946	-0.946	-0.946	-0.946								
COPPER	0.785	2.403	7.238	7.320	3.409	2.315	2.315	2.315	2.315	2.315	2.315	2.315	2.315								
PHOSPHOR BRONZE	1.470	3.953	4.163	6.787	3.244	1.812	1.812	1.812	1.812	1.812	1.812	1.812	1.812								
BRASS	3.228	2.027	6.754	7.323	2.849	1.669	1.669	1.669	1.669	1.669	1.669	1.669	1.669								
MILD STEEL	2.739	4.889	3.973	6.724	3.957	2.549	2.549	2.549	2.549	2.549	2.549	2.549	2.549								
STAINLESS STEEL	9.902	9.051	17.795	9.383	14.280	14.992	14.992	14.992	14.992	14.992	14.992	14.992	14.992								
STAINLESS STEEL 316	9.069	7.611	18.664	12.474	13.464	14.218	14.218	14.218	14.218	14.218	14.218	14.218	14.218								
NICKLE 270	5.111	3.179	11.254	14.510	6.035	5.534	5.534	5.534	5.534	5.534	5.534	5.534	5.534								
AL 6061	1.482	7.446	5.817	7.103	7.057	6.040	6.040	6.040	6.040	6.040	6.040	6.040	6.040								

CORRELATION COEFFICIENT 0.808
STANDARD ERROR OF ESTIMATE 5.914

0.236 0.854 0.856
9.744 5.254 5.191

TABLE. 5
Acoustic Impedance Correction

<u>$f(AI)^n$</u>	<u>AI + 1</u>		<u>$\frac{(AI + 1)^2}{4AI}$</u>	
	<u>Correlation Coefficient</u>	<u>Standard Error of Estimate</u>	<u>Correlation Coefficient</u>	<u>Standard Error of Estimate</u>
0	0.808	2.007	0.808	2.007
1	0.807	2.005	0.807	2.101
2	0.807	2.003	0.782	2.324
3	0.806	2.001	0.743	2.668
-1	0.808	2.009	0.781	2.070
-2	0.808	2.011	0.721	2.431
-3	0.809	2.014	0.582	3.745

TABLE 6
Equations Using Non-linear Parameters

<u>Equation</u>	<u>Correlation Coefficient</u>	<u>Standard Error of Estimate</u>
$\Sigma = 2.330 \text{ UR}$	0.808	2.007
$\Sigma = -2.681 + 3.343 \text{ UR} - 0.087 \text{ UR}^2$	0.870	5.616
$\Sigma = 0.266 \text{ UR} + 0.412 \text{ UR}^2 - 0.019 \text{ UR}^3$	0.919	4.459
$\Sigma = 3.685 \text{ UR} \times E^2$	0.678	5.714
$\Sigma = 1.147 + 1.444 \text{ UR} \times E^2$	0.678	4.271

Tool Steel
1/MDPR = 1

$\frac{1}{MDPR}$ (hr/mil)

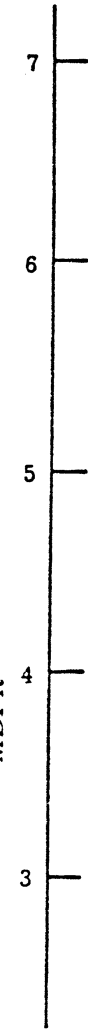


Table 7 Recommended Correlating Equations

MATERIAL & NORMALIZED	EPSILON	$C_1 = 0.463$		$C_2 = 2.330$		SOURCES
		$C_1 \cdot C_2 \cdot UR$	$+ C_2 \cdot UR$	$C_1 \cdot UR$	$+ C_2 \cdot UR$	
BS1433 COPPER	1.000	2.462	1.981	2.330	2.007	
STAINLESS STEEL 316	21.482	7.520	6.993	8.225	7.086	UM Vibratory Cavitation Facility
NICKLE 270	5.044	2.850	2.365	2.782	2.396	
AL 6061	1.482	7.346	6.820	8.022	6.911	
STAINLESS STEEL 304	19.594	9.011	8.471	9.964	8.584	
BRUNZE #1	3.421	4.894	4.391	5.164	4.449	
BRUNZE #2	39.669	24.115	23.438	27.568	23.750	
BRUNZE #3	29.391	23.269	22.603	26.582	22.900	
BRUNZE #4	3.674	2.288	1.808	2.127	1.832	
BRUNZE #5	1.959	2.240	1.761	2.071	1.784	
BRUNZE #6	2.516	1.918	1.442	1.696	1.461	
STAINLESS STEEL #1	25.659	26.547	38.817	30.402	26.191	
STAINLESS STEEL #2	23.948	38.817	38.007	44.704	38.513	
STAINLESS STEEL #3	15.037	18.182	17.559	20.653	17.792	
COPPER	0.963	2.387	1.906	2.242	1.932	
BRASS (65-35)	3.801	6.935	6.413	7.543	6.499	
MILD STEEL 1020	8.002	9.080	8.539	10.043	8.653	UM Vibratory Cavitation Facility with Stationary Specimen
STAINLESS STEEL 304	19.476	9.921	9.372	11.024	9.497	
ASTM 0144 (SAE660)	4.384	1.467	0.995	1.170	1.008	
MAGNESIUM	1.490	7.026	6.503	7.649	6.590	
ALUMINUM 3003-O	0.213	1.243	0.773	0.909	0.783	
COPPER	1.000	2.462	1.981	2.330	2.007	
CR-130 STEEL	1.391	6.287	5.771	6.788	5.848	
AL ALLUOY	0.806	9.169	8.627	10.147	8.742	RAE-Dornier Rotating Arm Facility
ALUMINUM	0.254	1.253	0.782	0.920	0.793	
COPPER	0.785	2.032	1.555	1.829	1.576	
PHOSPHOR BRUNZE	1.470	3.666	3.174	3.733	3.216	
BRASS	3.228	1.636	1.162	1.367	1.178	Venturi Facility
MILD STEEL	2.739	4.652	4.151	4.882	4.206	
STAINLESS STEEL	9.902	9.038	8.497	9.994	8.610	
STAINLESS STEEL 316	9.069	7.520	6.993	8.225	7.086	
NICKLE 270	5.111	2.850	2.365	2.782	2.396	
AL 6061	1.482	7.346	6.820	8.022	6.911	Rotating Wheel Impact Facility

CORRELATION COEFFICIENT 0.808
PERCENTAGE STANDARD ERROR OF ESTIMATE 1.981

Table 8 - Statistical Correlation Coefficients

Correlating Relation	n (Where Applicable)	Sample Correlation Coefficient	95% Confidence Limits for Population Correlation Coefficients		Factorial Standard Error of Estimate
$\frac{1}{\text{MDPR}} = C(\text{UR})^n$	0.998	0.811	0.64 - 0.91	2.52	
$\frac{1}{\text{MDPR}} = C(\text{UR})$	--	0.811	0.64 - 0.91	2.52	
$\frac{1}{\text{MDPR}} = C(\text{UR} \times \text{BHN})^n$	0.720	0.798	0.62 - 0.89	2.25	
$\frac{1}{\text{MDPR}} = C(\text{UR} \times E^2)^n$	0.659	0.744	0.52 - 0.86	2.35	
$\frac{1}{\text{MDPR}} = C(\text{BHN})$	--	0.742	0.52 - 0.86	2.75	
$\frac{1}{\text{MDPR}} = C(\text{BHN})^n$	1.788	0.734	0.52 - 0.85	2.38	
$\frac{1}{\text{MDPR}} = C(\text{UR} \times \text{BHN})$	--	0.716	0.49 - 0.84	2.57	
$\frac{1}{\text{MDPR}} = C(\text{UR} \times E^2)$	--	0.684	0.44 - 0.82	2.86	
$\frac{1}{\text{MDPR}} = C(\text{SE})^n$	0.738	0.517	0.21 - 0.73	3.24	
$\frac{1}{\text{MDPR}} = C(\text{SE})$	--	0.498	0.17 - 0.72	3.30	

List of Figures

- Fig. 1. Leading edge of a series 400 stainless steel impeller for a boiler feed pump, exhibiting deep local damage caused by cavitation erosion.
- Fig. 2. Processes by which a material is damaged by liquid-impingement erosion.
- Fig. 3. Schematic representation of successive stages of nonsymmetrical cavity collapse with microjet impingement against a metallic surface.
- Fig. 4. (a) Schematic representation of successive stages of growth, collapse and rebound of a single traveling cavity. (b) Graph of cavity diameter as a function of time for the cavity in (a).
- Fig. 5. Individual-blow cavitation craters on stainless steel.
- Fig. 6. Jet-impact damage device (schematic).-
- Fig. 7. Venturi device for cavitation-damage tests at the University of Michigan.
- Fig. 8. Holtwood Laboratory cavitation-damage test section.
- Fig. 9. Diagram of experiments on the erosion of metal specimens caused by the cavitation beyond a circular profile: 1. - walls of the experimental chamber. 2. - model. 3. - test piece. 4. - the ties of the test piece.
- Fig. 10. Rotating disk with drill ducts for air supply.
- Fig. 11. Water rotating-disk cavitation-damage test device at Pratt and Whitney Aircraft, CANEL. Wood, et. al. (25).
- Fig. 12. Liquid-metal vibratory facility at the University of Michigan.

List of Figures cont'd

- Fig. 13 - Hypothesized Bubble Energy Spectra for Various Cavitation Conditions
- Fig. 14 - High-Speed Motion Pictures (500,000 frames/s) of Spark-Generated Cavitation Bubble near Wall in Venturi
- Fig. 15 - Water Droplet Impact Crater on Plexiglass
- Fig. 16 - Cavitation Crater in Venturi on Plexiglass
- Fig. 17 - Cavitation Craters in Water on Cadmium-Plated Stainless Steel
- Fig. 18 - Temperature Effect on Cavitation Damage Rate for 304 Stainless Steel in Vibratory Facility
- Fig. 19 - Best Fit Correlation for Erosion Resistance and Ultimate Resilience, Hammitt, et al.
- Fig. 20 - Erosion Resistance versus Ultimate Resilience: Comparison of Hammitt's and Heymann's Correlations
- Fig. 21 - Cavitating Venturi Flow Geometry - University of Michigan Facility, Indian Institute of Science, Bangalore, India.
- Fig. 22 - Cavitating Venturi Facility, Indian Institute of Science, Bangalore
- Fig. 23 - Damage Rate vs. Cavitation Sigma in Venturi (Water and Mercury)
- Fig. 24 - University of Michigan Damage Venturi-Schematic
- Fig. 25. Typical Cavitation Wall Pressure Profiles, University of Michigan Venturi
- Fig. 26 - Correlation of Bubble Collapse Pulse Spectrum and Cavitation Erosion Rate
- Fig. 27 - Typical Bubble Collapse Pulse Height Spectrum for Water in U-M Venturi
- Fig. 28 - Typical Individual Cavitation Bubble Collapse Pulses: U-M Microprobe Output in Water Venturi (Oscilloscope Photos)
- Fig. 29 - Cavitation Damage Particle Distributions; % Stainless Steel Permeating Filter vs. Filter Rating.



1185

Fig. 1. Leading edge of a series 400 stainless steel impeller for a boiler feed pump, exhibiting deep local damage caused by cavitation erosion. (Ref. 6)

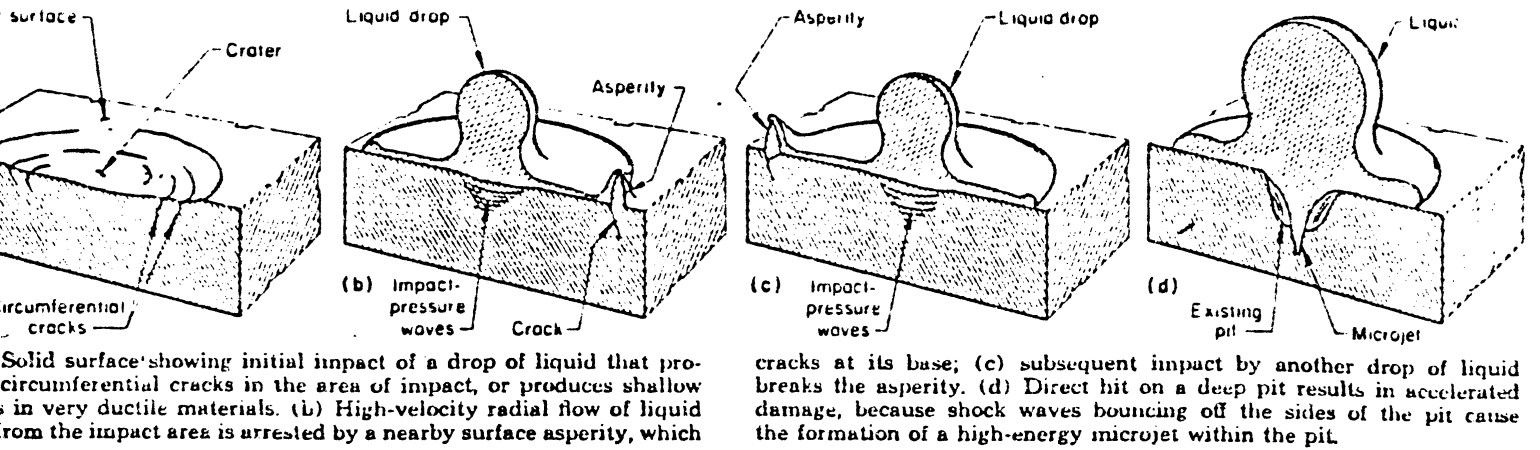


Fig. 2. Processes by which a material is damaged by liquid-impingement erosion. (Ref. 5).

cracks at its base; (c) subsequent impact by another drop of liquid breaks the asperity. (d) Direct hit on a deep pit results in accelerated damage, because shock waves bouncing off the sides of the pit cause the formation of a high-energy microjet within the pit.

Fig. 2. Processes by which a material is damaged by liquid-impingement erosion. (Ref. 5).

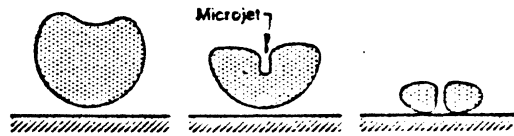


Fig. 3. Schematic representation of successive stages of nonsymmetrical cavity collapse with microjet impingement against a metallic surface. (Ref. 5)

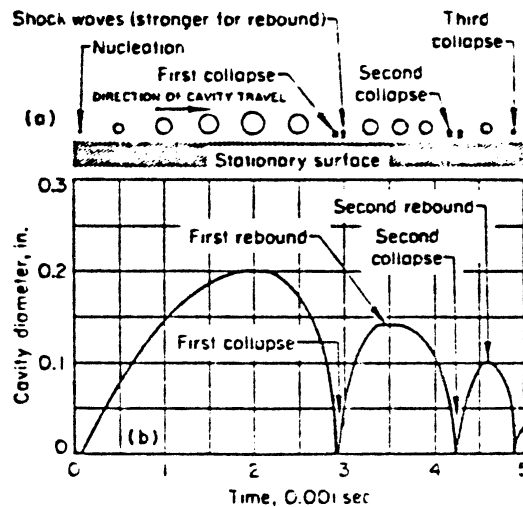


Fig. 4. (a) Schematic representation of successive stages of growth, collapse and rebound of a single traveling cavity. (b) Graph of cavity diameter as a function of time for the cavity in (a). (Refs. 5,7).

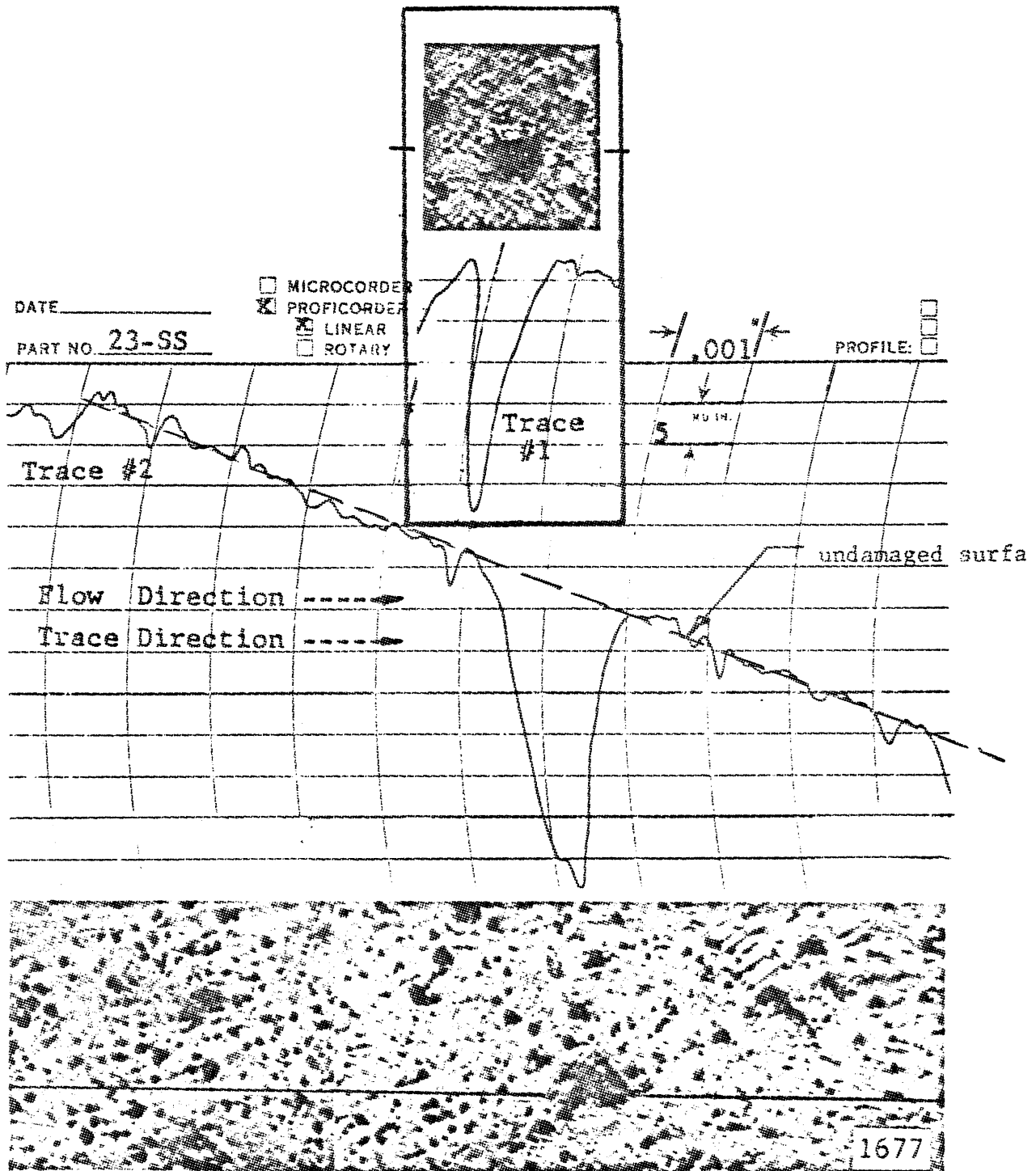


Fig. 5. Individual-blow cavitation craters on stainless steel.

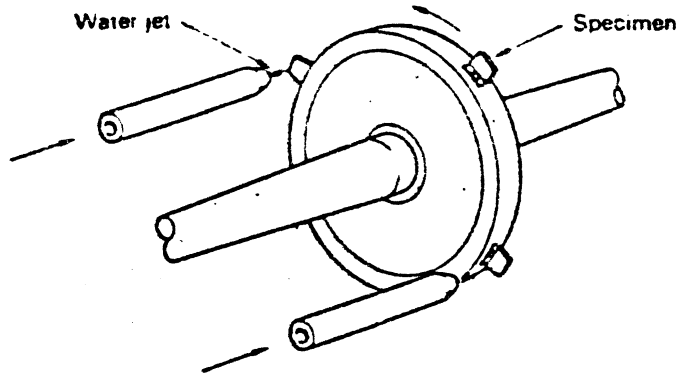
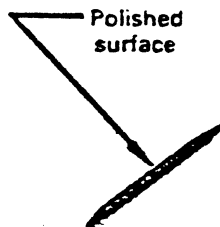
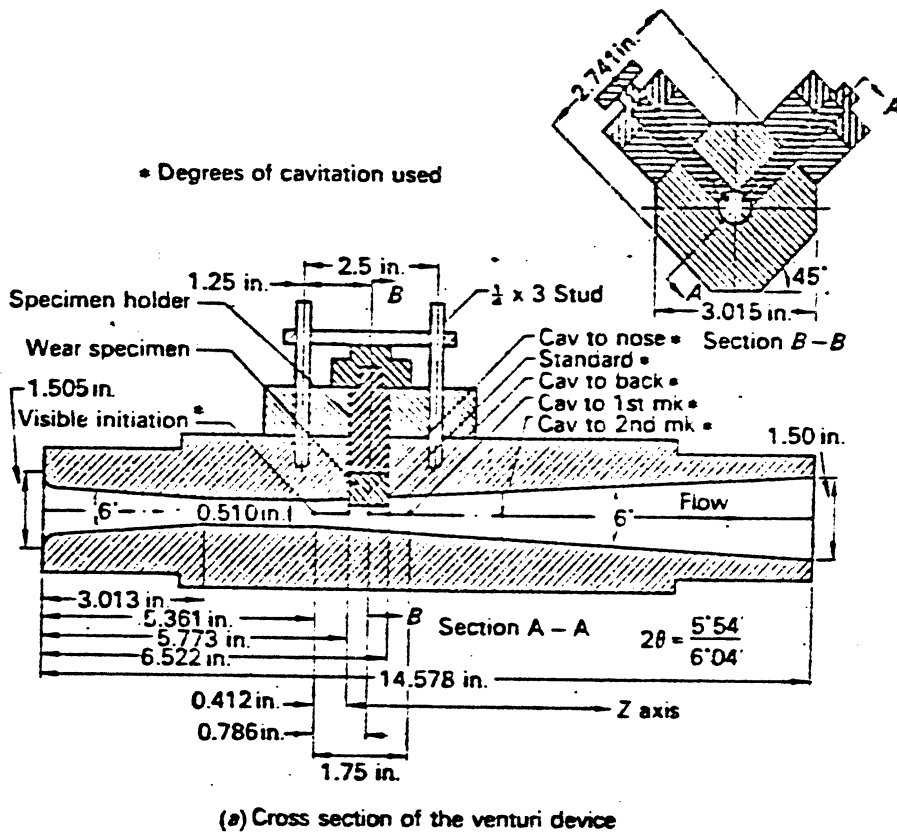


FIG. 6. Jet-impact damage device (schematic). (Ref. 6)



(b) Test specimen from the venturi device.

FIG. 7. Venturi device for cavitation-damage tests at the University of Michigan.

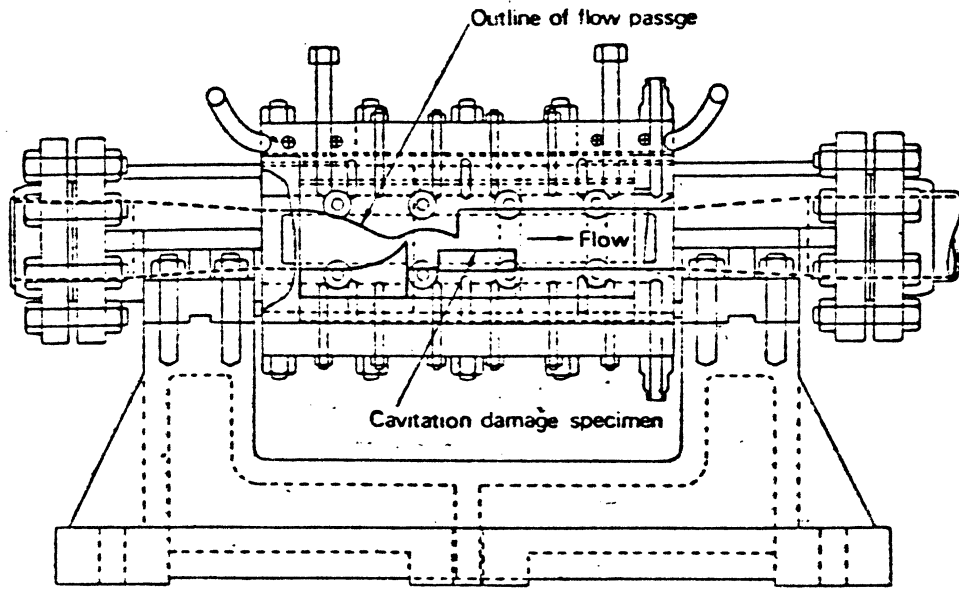


FIG. 8. Holtwood Laboratory cavitation-damage test section. Boetcher, Ref. 21

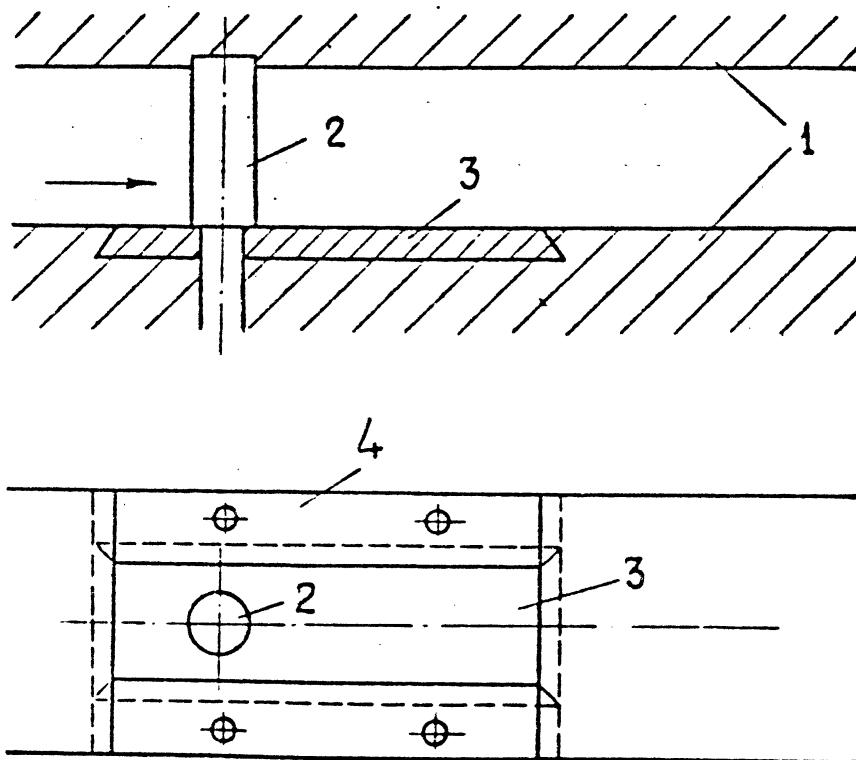


Fig. 9. Diagram of experiments on the erosion of metal specimens caused by the cavitation beyond a circular profile: 1.-walls of the experimental chamber. 2.-model. 3.-test piece. 4.-the ties of the test piece. Ref. 23

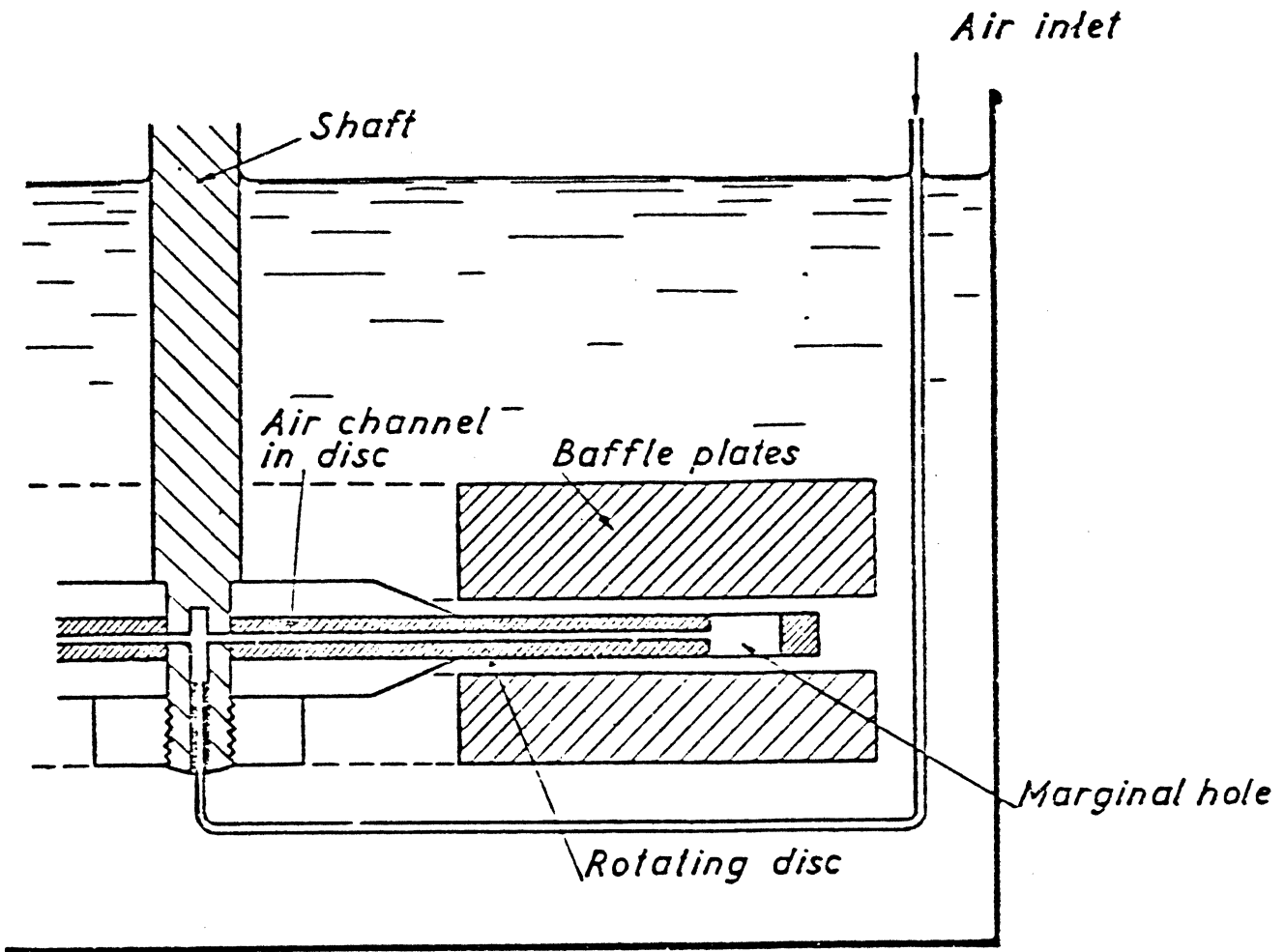
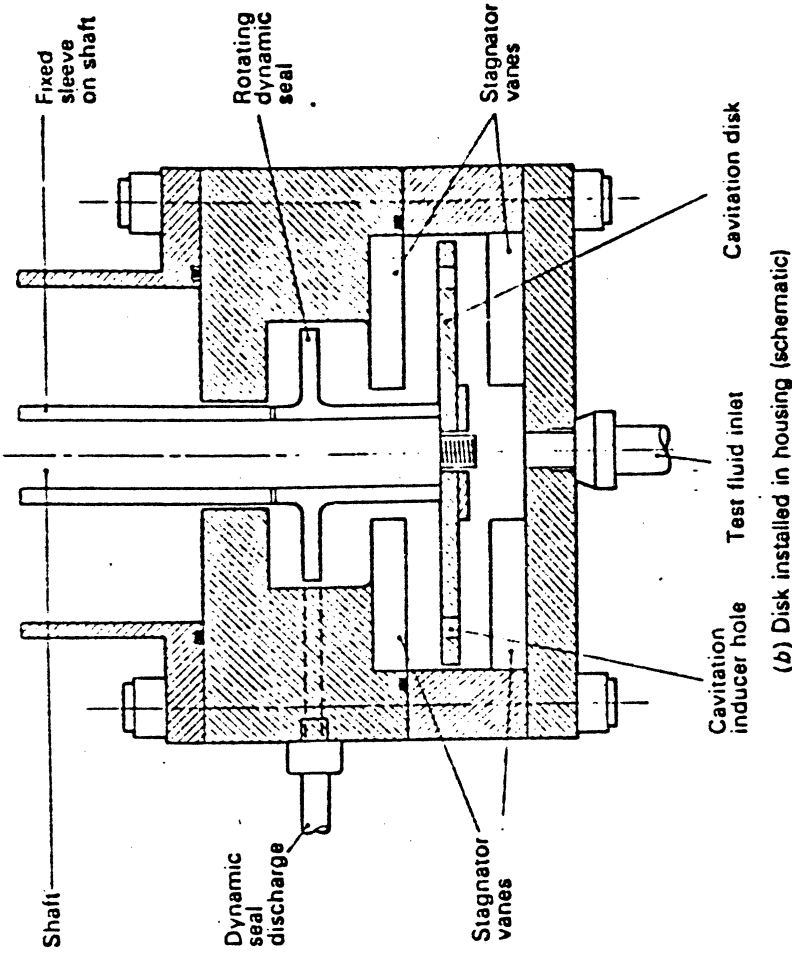
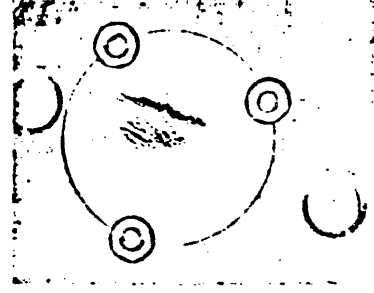


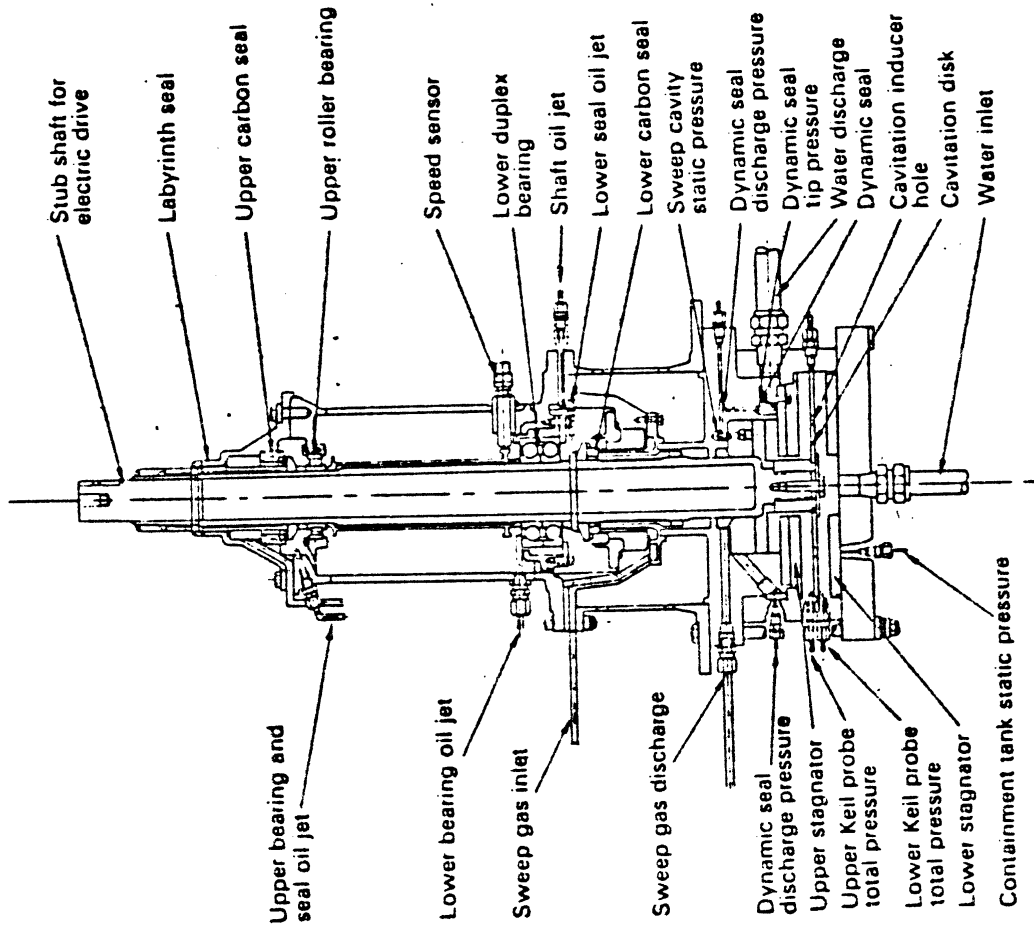
Fig. 10. Rotating disc with drill ducts for air supply. (24)



(b) Disk installed in housing (schematic)



(c) Damaged specimen (Cb-12r alloy) after 30 hr. Cavitation is generated from the hole above the specimen.



(a) Cross section of the PWA rotating disk device

Fig. 11. Water rotating-disk cavitation-damage test device at Pratt and Whitney Aircraft, CANEL. Wood, et. al. (25)

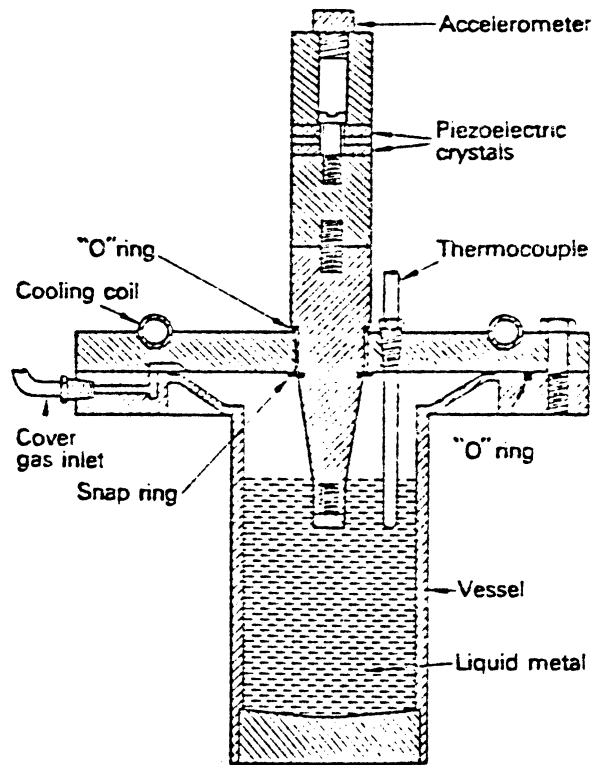


Fig. 12. Liquid-metal vibratory facility at the University of Michigan.

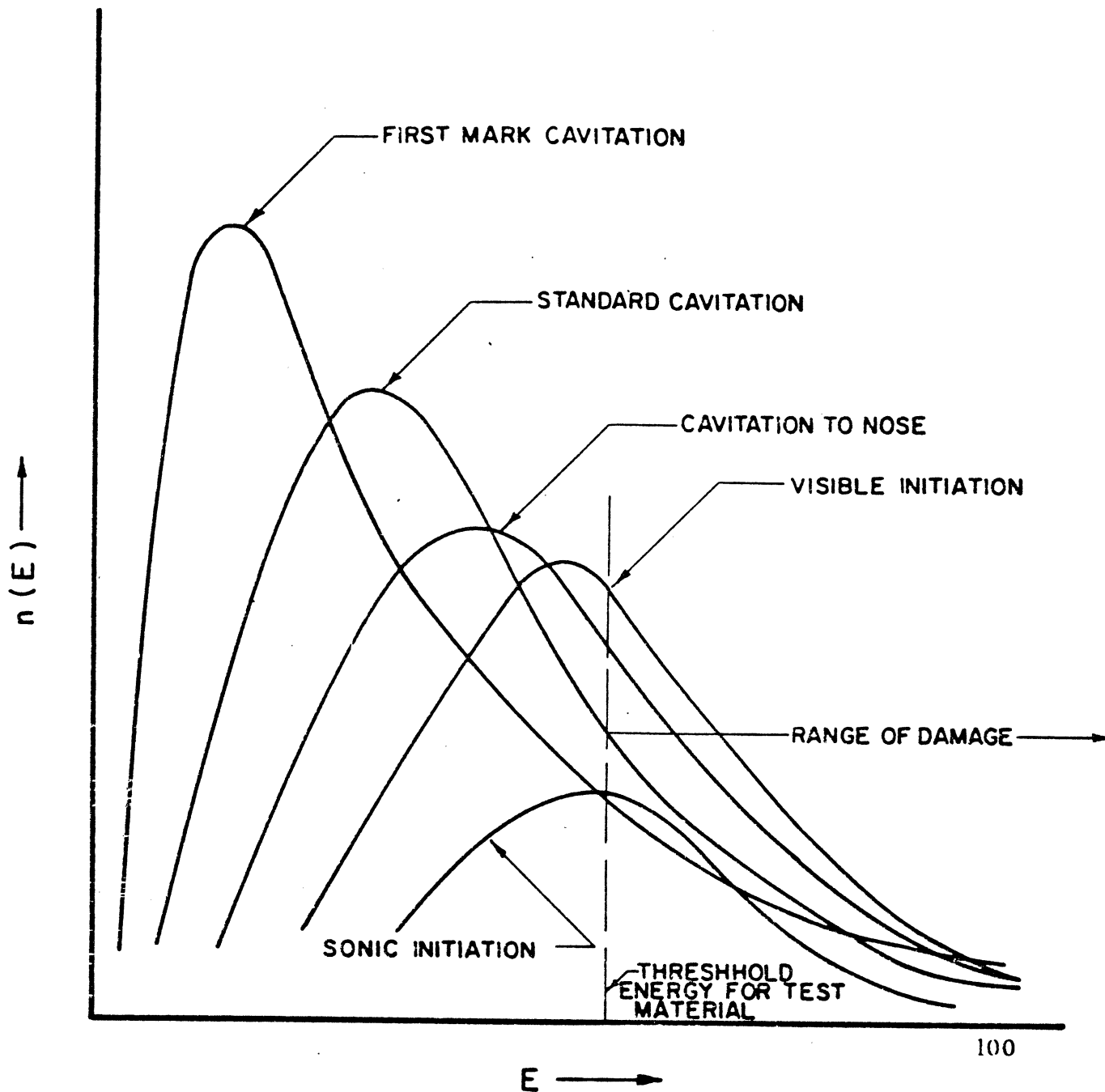


Figure 13- Hypothesized bubble energy spectra for various cavitation conditions at a constant velocity, for a given material.

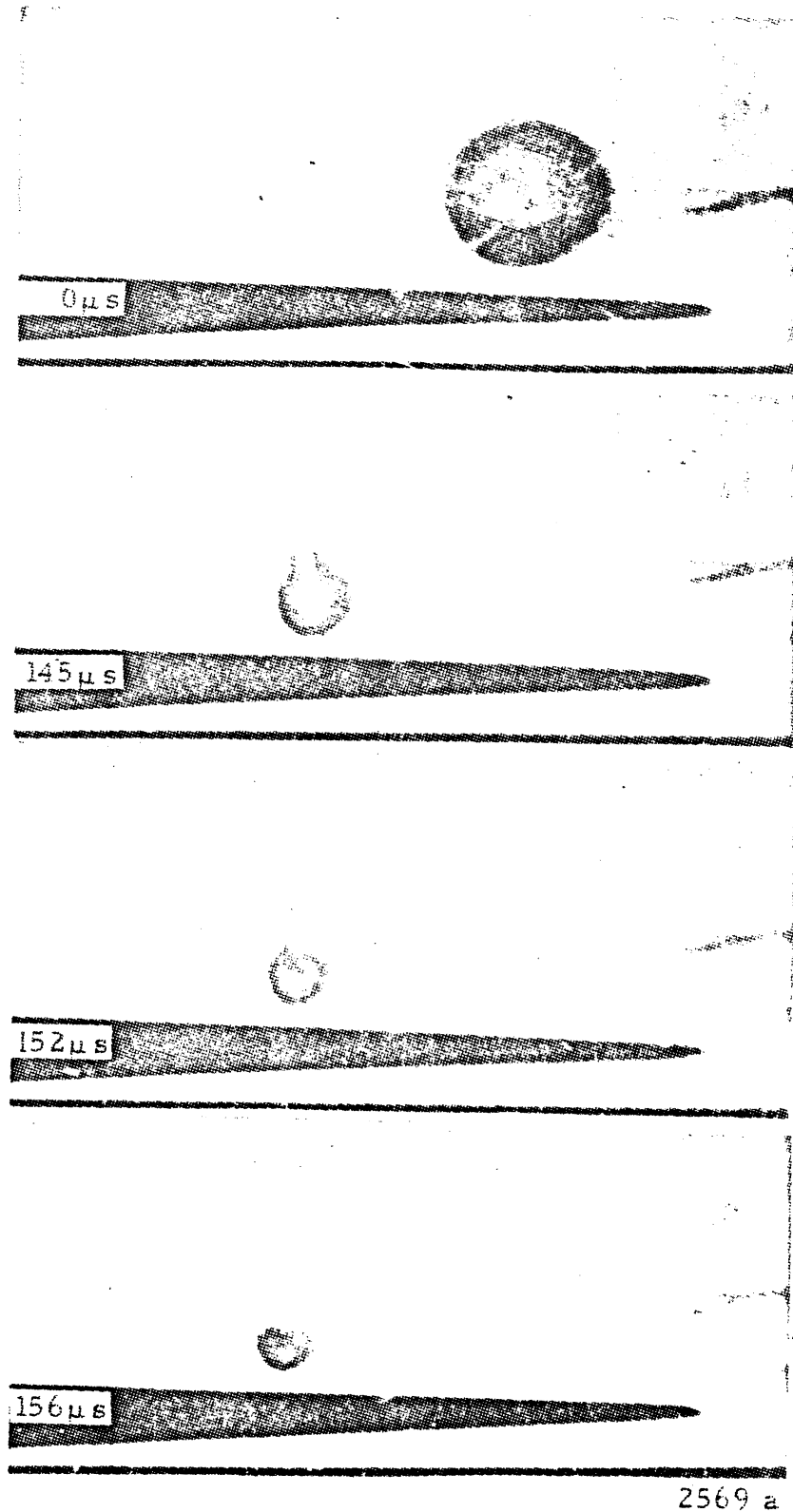
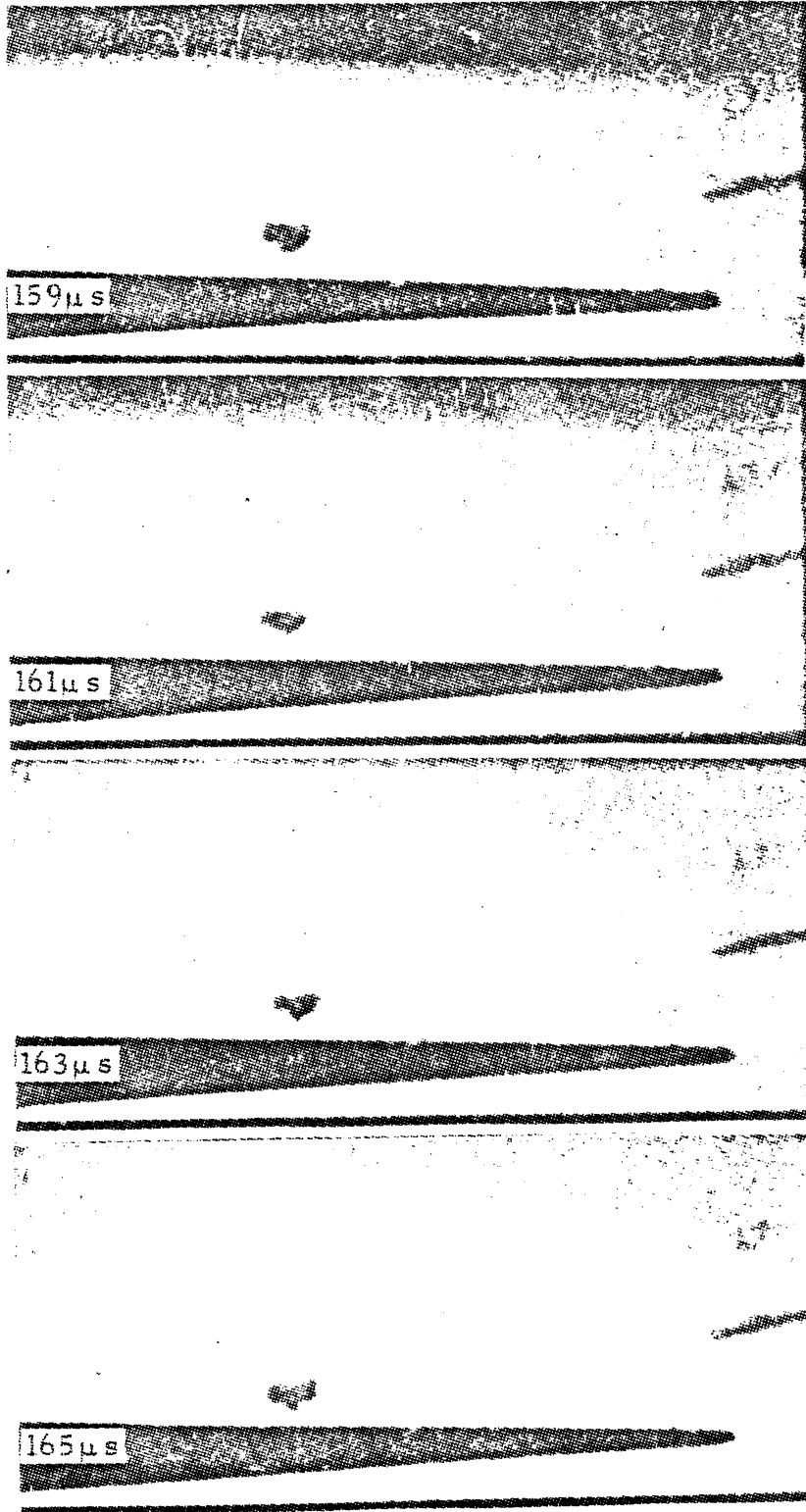


Figure 14 - Selected frames from a sequence taken at 550,000 frames per second of a spark generated cavitation bubble near a splitter in a venturi, exposure 1.8 μ sec per frame, flow right to left, magnification 5 x.



2569 b

Figure 14 (Cont.)

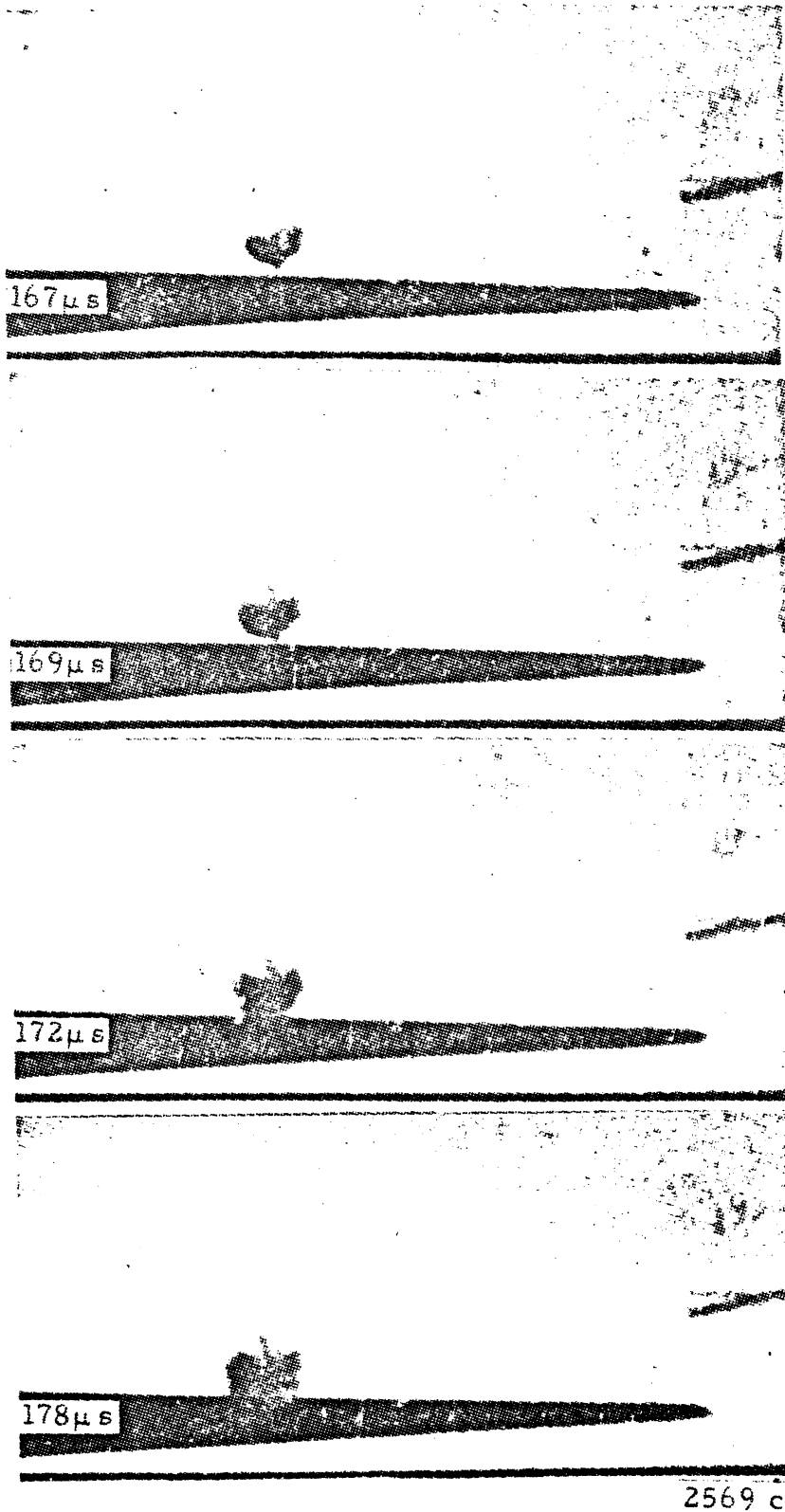


Figure 14 (Cont.)

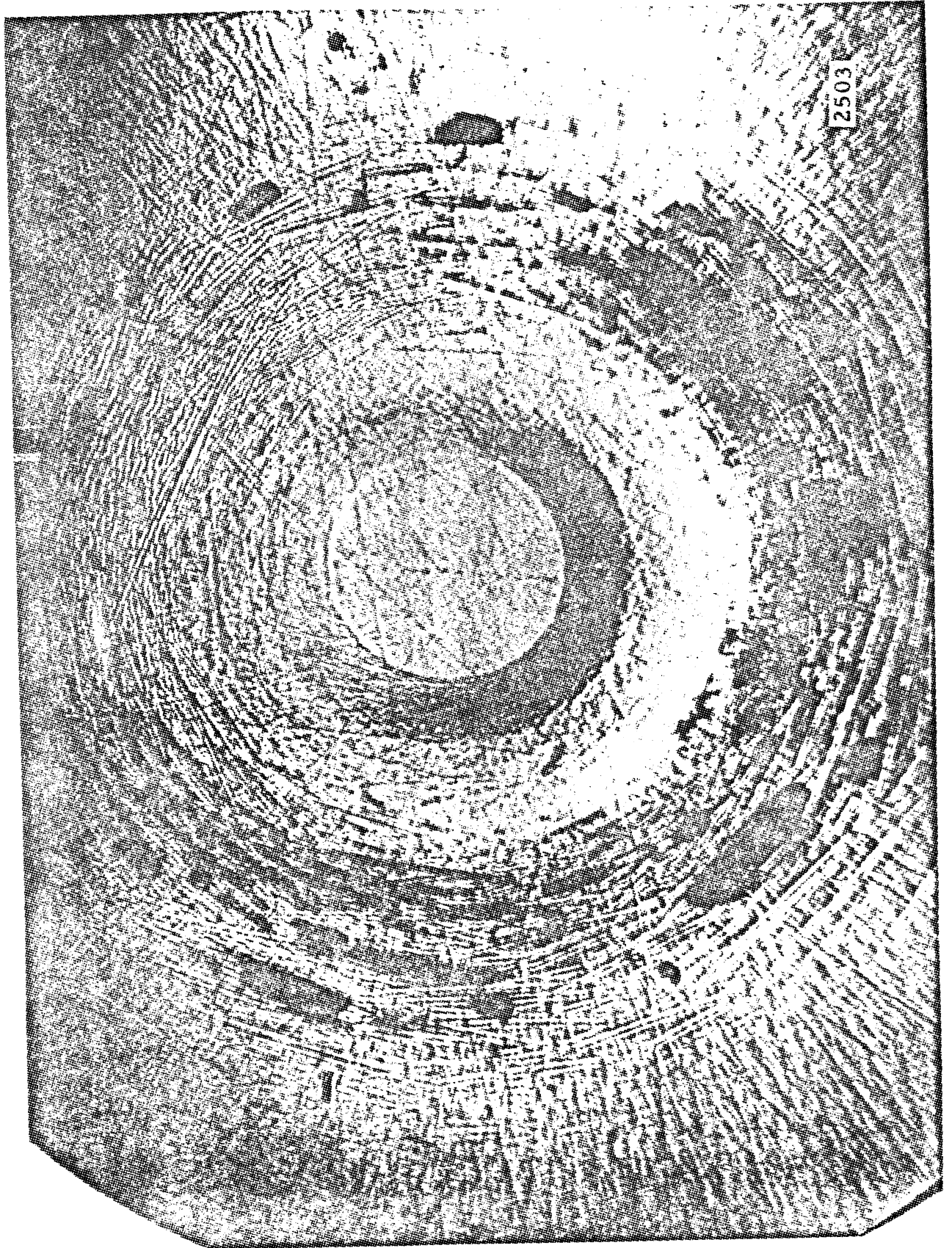


Figure 15 - Water droplet impact crater on
micrograph magnification 100 x. (After A. Fyall,

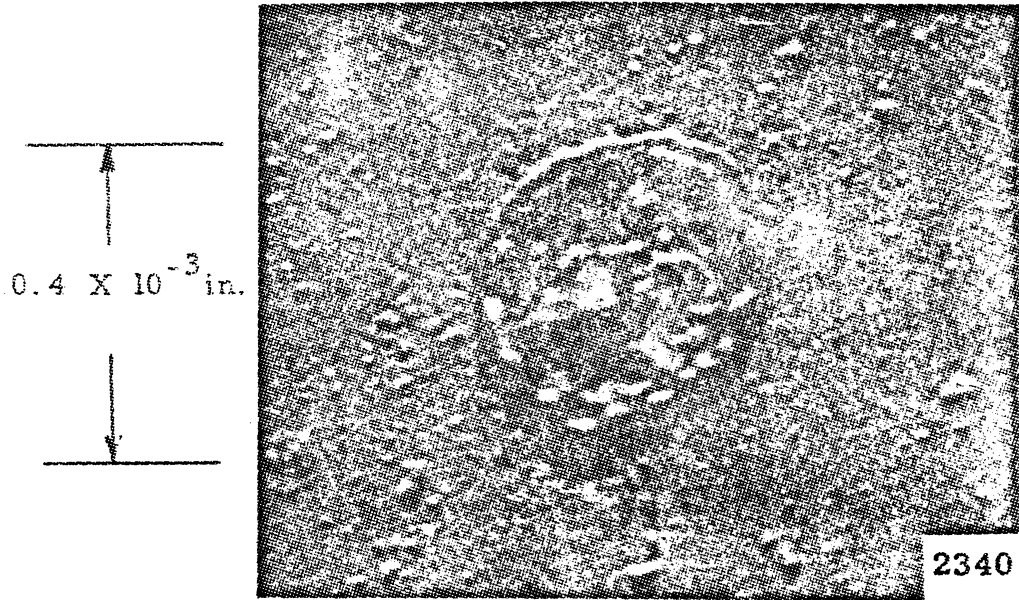
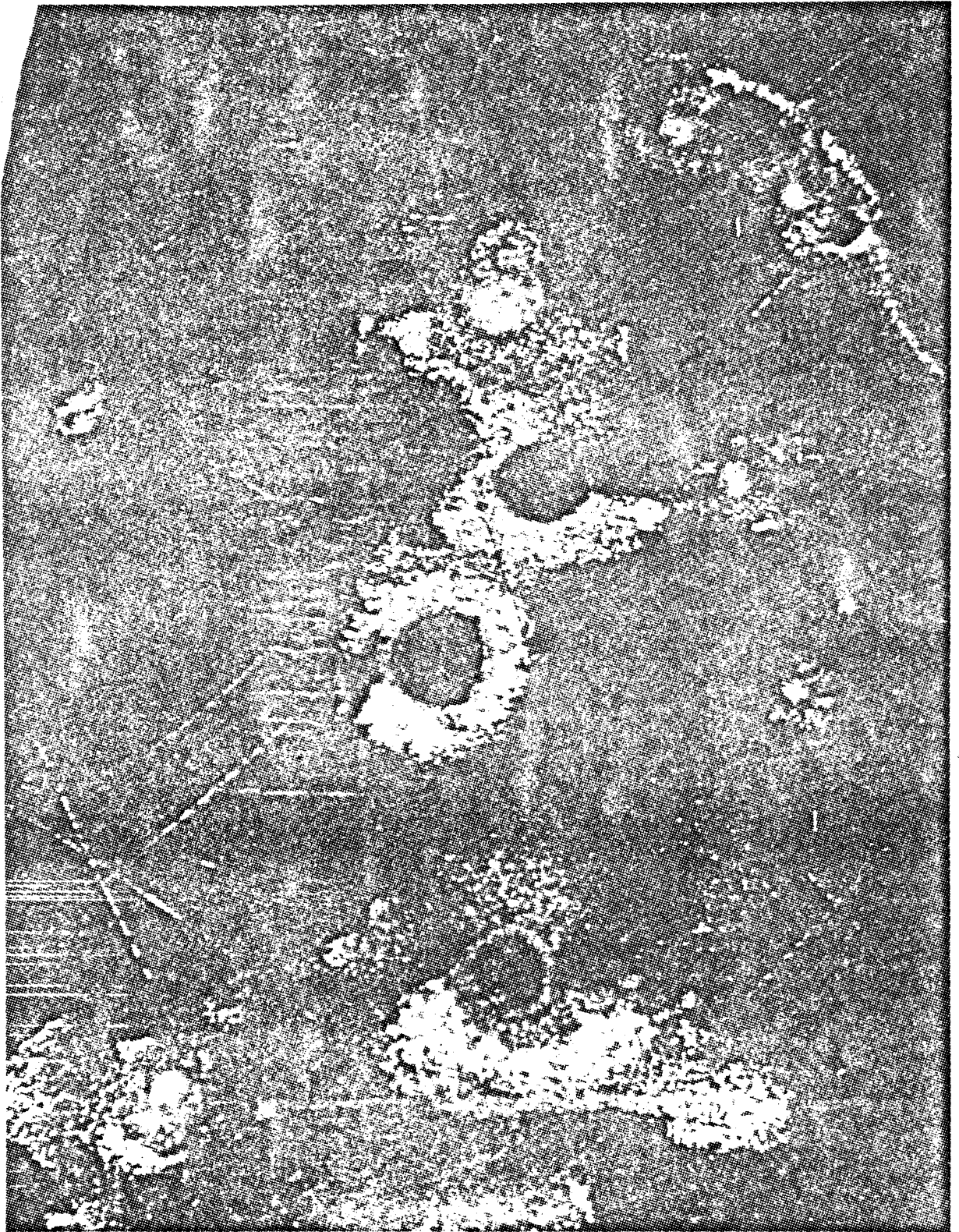


Figure 16- Crater produced by cavitating water in a venturi on plexiglass, magnification 4,000 x.



5 X

Figure 17 - Craters produced by cavitating water on 0.6 μm cadmium-plated stainless steel, magnification 180 x.

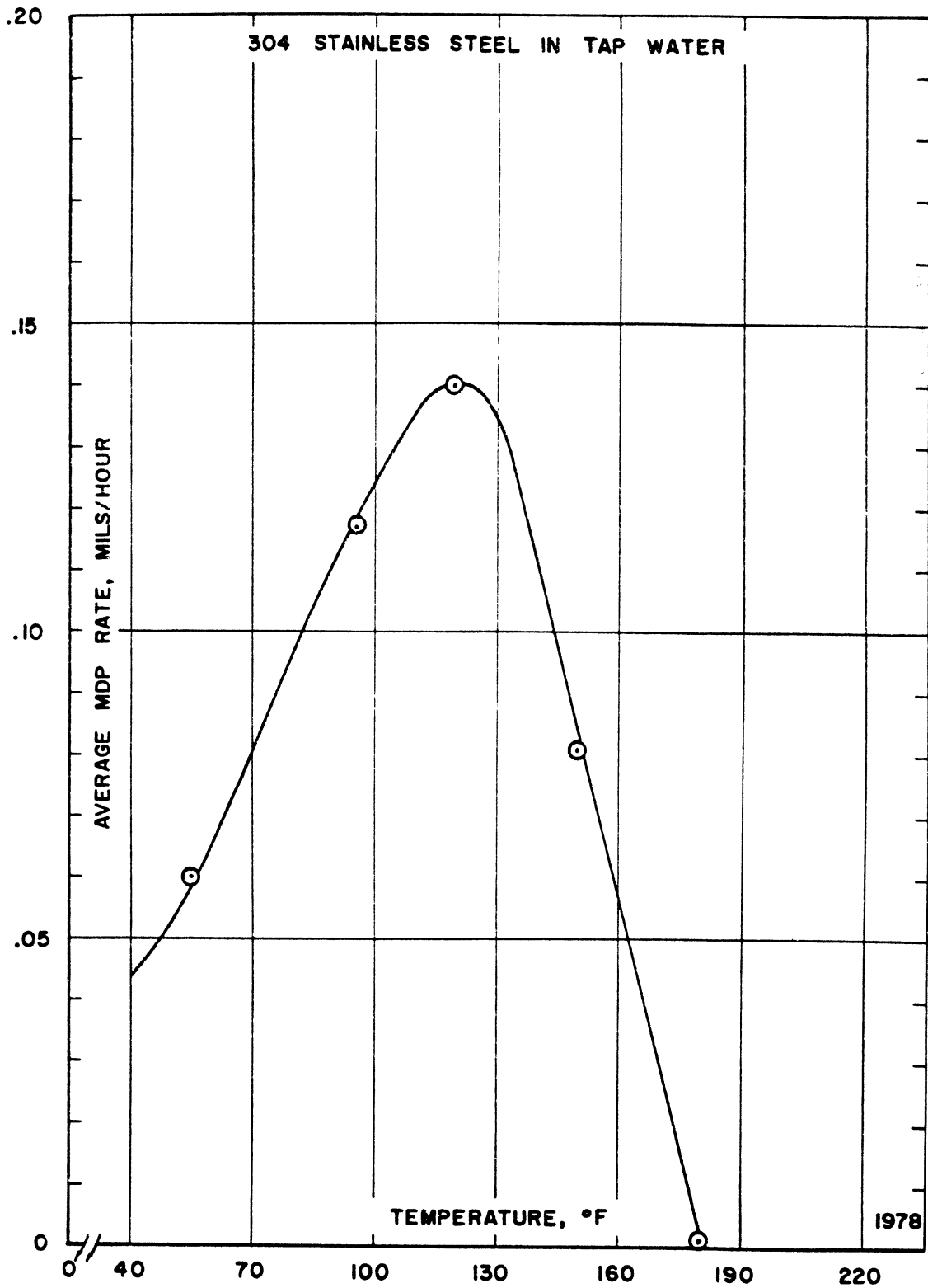


Figure 18-a Effect of temperature on average damage rate for 304 stainless steel cavitared in water at one atmosphere pressure, University of Michigan tests. (45) (Open beaker test)

3) Increased NPSH causes a strong increase of damage in this type of facility up to at least 4 atm. NPSH. Obviously, damage must maximize at some higher NPSH and then decrease to near zero, since the number and size of bubbles decreases with increasing NPSH (though their collapse violence increases), reaching zero at sufficiently high NPSH, depending upon facility frequency and amplitude.

Acknowledgements

Financial support provided by: National Science Foundation, Grant No. GK 1889, Westinghouse Electric Corporation, and Worthington Pump International.

References

1. F. G. Hammitt and D. O. Rogers, "Effects of Pressure and Temperature Variation in Vibratory Cavitation Damage Test", Journal Mech. Engr. Sci., 12, 6, 1970, 432-439.

- 2. R. Garcia, "Comprehensive Cavitation Damage of Water and Various Liquid Metals Including Conditions with Material and Fluid Properties", Thesis, Nucl. Engr. Dept., University of Michigan, 1966; see also Garcia-Hammitt, Trans. ASME, Engr., 89, 1967.
- 3. F. G. Hammitt, discussion of Reference 4.
- 4. S. G. Young and J. R. Johnston, "Effect of Temperature and Pressure on Cavitation Damage in SAE-660", ASTM STP 474, 67-103, 1967.
- 5. J. M. Hobbs and A. Laird, "Pressure, Temperature, Gas Content Effects in the Vibratory Cavitation Erosion Test", 1969 Cavitation Forum, ASME

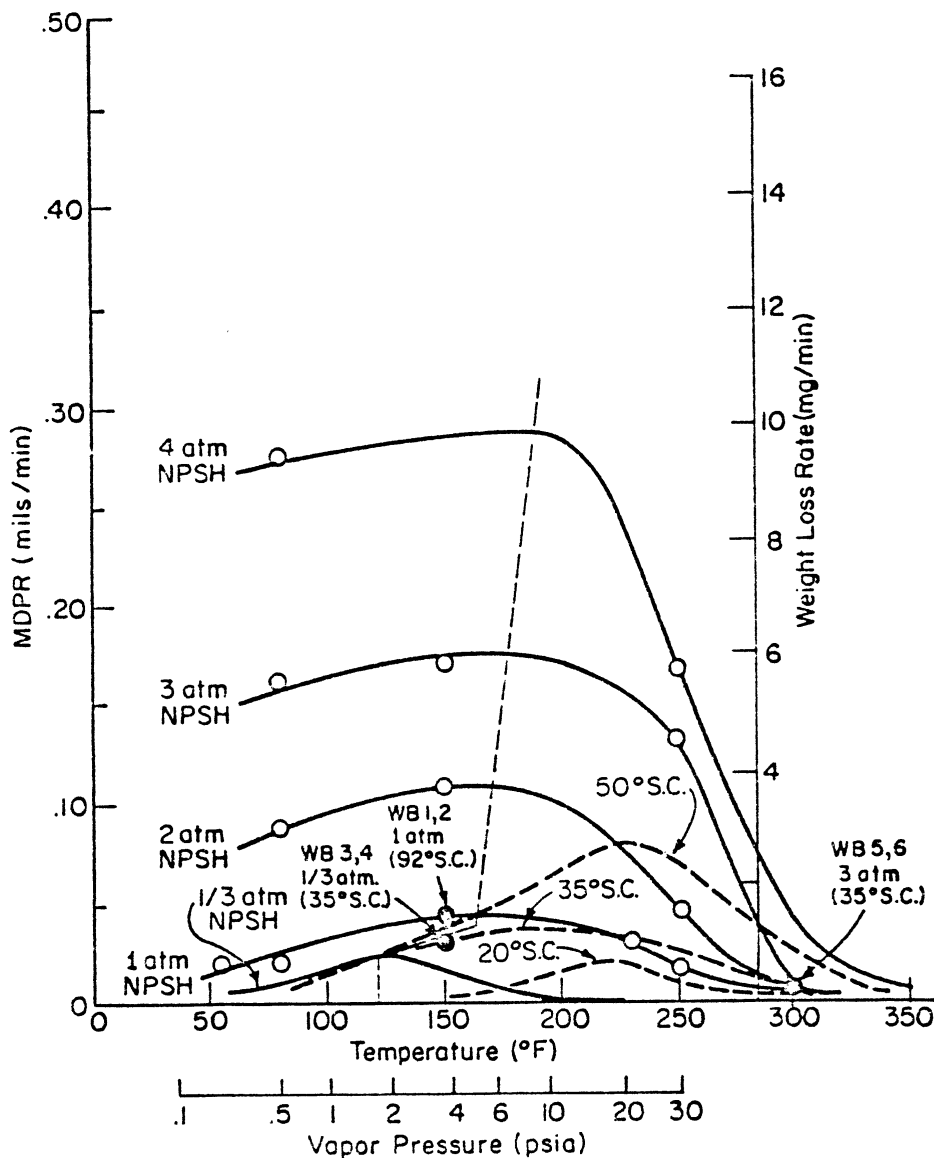


Figure 18b Maximum MDPR Versus Temperature and Vapor Pressure for Bearing Brass (SAE-660)

Fig 19, Chap. 5

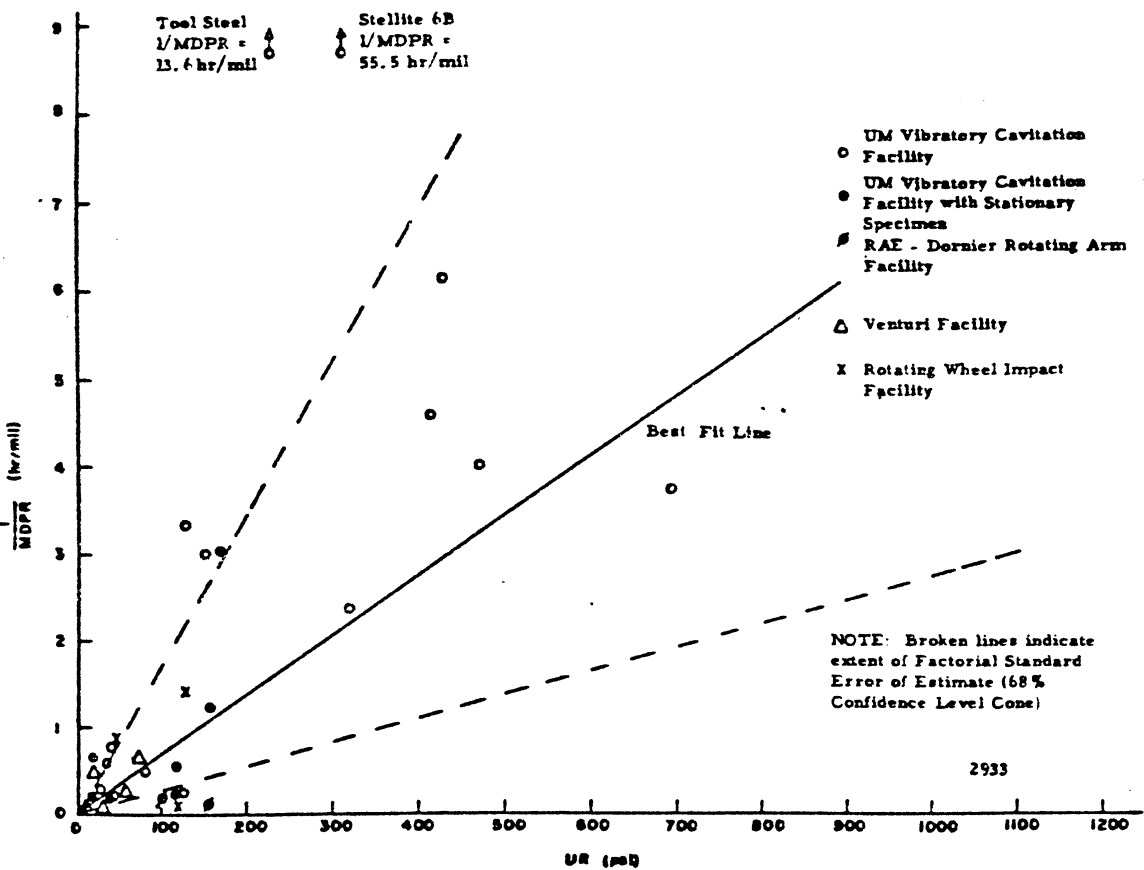


Fig 19 - Best fit correlation and standard deviation cone for 1/MDPR versus ultimate resistance for 23 materials

Conclusions

It is postulated that the most likely form for an equation relating material, liquid, and test parameters with impingement or cavitation erosion rates with good hope for general applicability, is one which is based on a clear physical model with dimensional consistency. For the evaluation of impingement erosion rates, consistent with the previous suggestion of Kad et al [7] the equation has been chosen:

$$MDPR = \left(\frac{\eta \eta_0}{\epsilon} \right) \left(\frac{A_p}{A_s} \right) \left(\frac{\rho_{oil} V^2}{2} \right) \dots \dots \dots (1a)$$

where η represents factors affecting energy transfer efficiency not included in η_0 .
 A statistical evaluation of ϵ , which must have units of energy per volume, has shown the best fit with a comprehensive data set including both impingement and cavitation data, in the form:

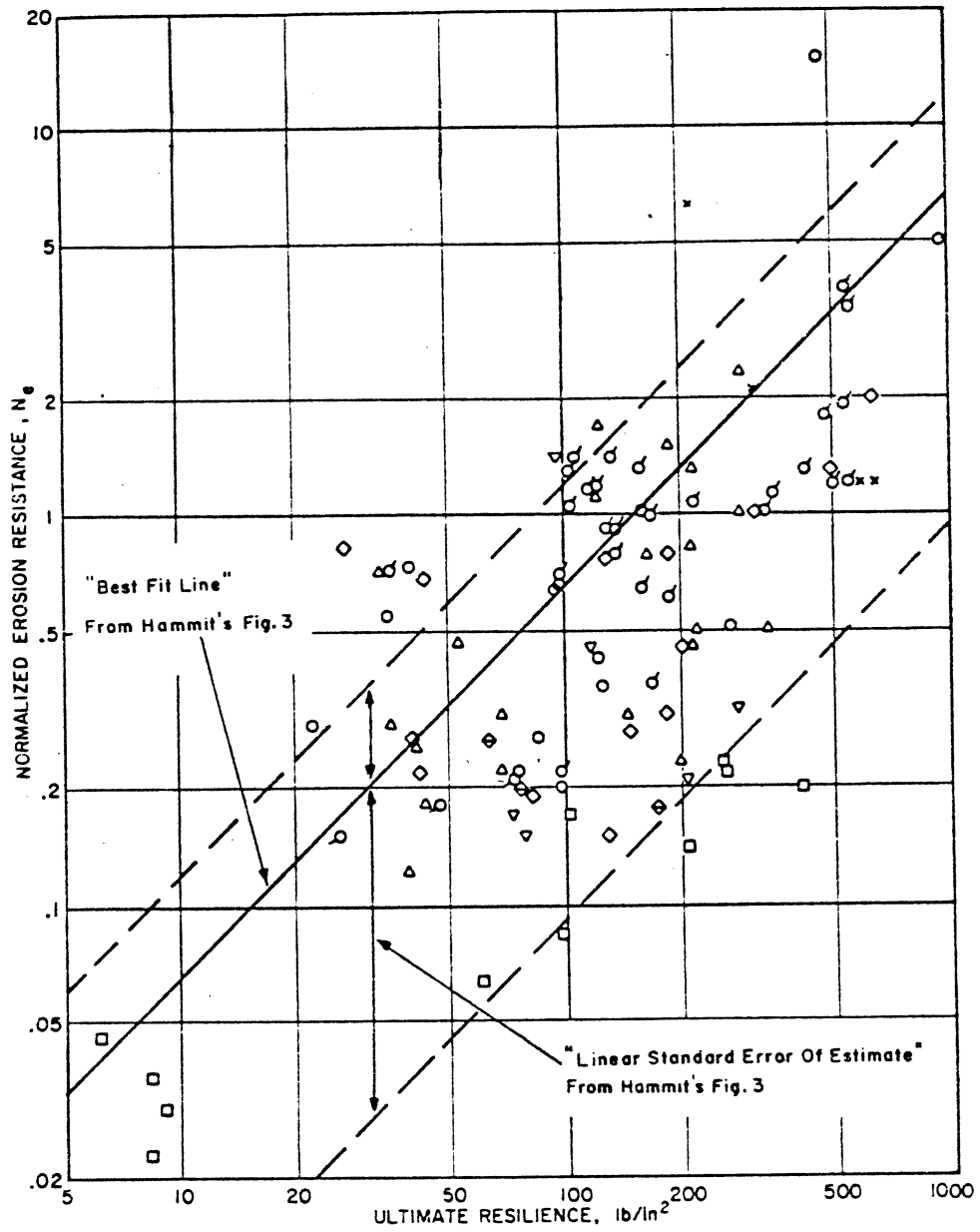
$$\epsilon = C_1 UR \dots \dots \dots (10b)$$

Rather higher power terms in UR or terms in SE improved the statistics of the fit substantially, and the fit in terms only of SE was relatively very poor. Thus it is concluded that for the large group of metals here used the best linear energy per volume mechanical property correlation for volume loss rate under droplet impingement or cavitation attack is the expression Eq 10b in ultimate resilience alone.

Rocket sled rain erosion data have been statistically evaluated to find best values for threshold velocity and velocity exponent, as well as the coefficient n in the Eqs 4 and 5:

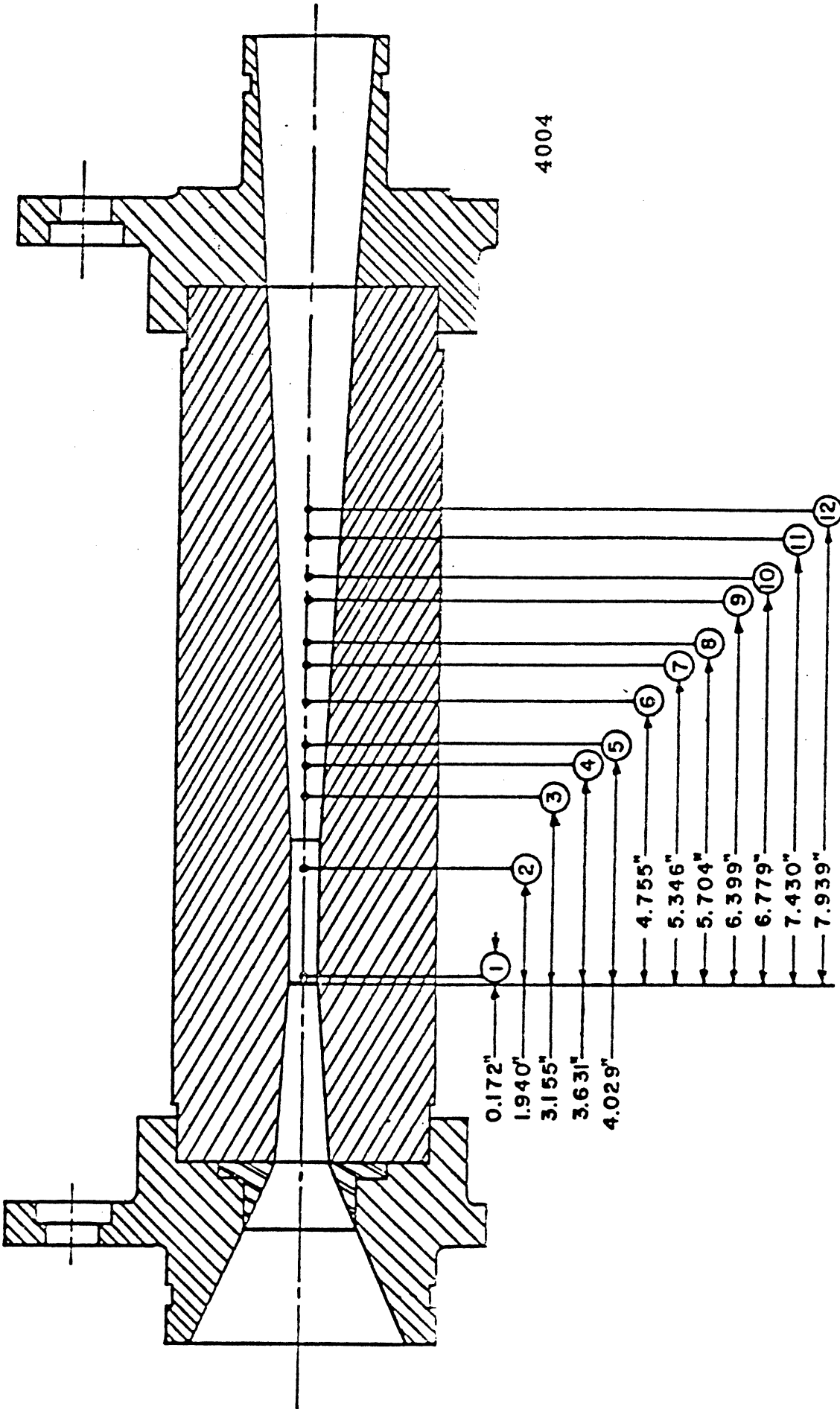
$$MDPR = K (V \sin \theta - V_0)^n / \sin^m \theta \dots \dots \dots (1a)$$

It was found that the statistical fit is relatively insensitive to n so that $n=1$ is a suitable value. It was also found that for many materials, the statistical fit is also insensitive to the choice of a threshold velocity V_0 , so that only slight reduction in the "goodness" of the fit occurs for most materials if it is assumed that $V_0=0$. However, the best fit values for K and α are sensitive to the choice of V_0 and n . It was found that there is a weak correlation between best fit K and α , with K decreasing approximately linearly with increasing α . Thus, it might be possible to characterize a material by a single figure of merit in terms of Eq 4a, if a best fit relation between K and α is determined, so that either may be eliminated in terms



Erosion resistance versus ultimate resilience: comparison of Hammit's and Heymann's correlations.

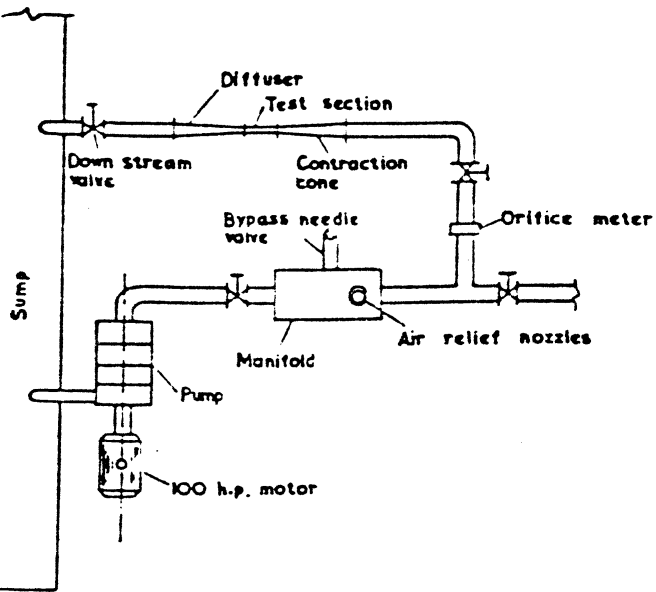
FIGURE 20



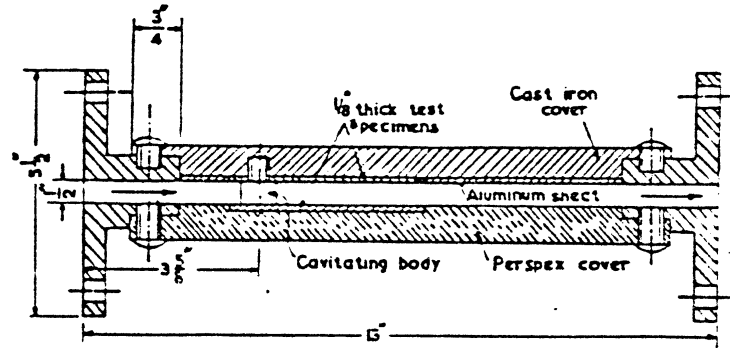
4004

Pressure tap locations and water loop installation geometry for 3/4" plexiglas venturi.

Fig. 21 - Cavitating Venturi Flow Geometry, University of Michigan



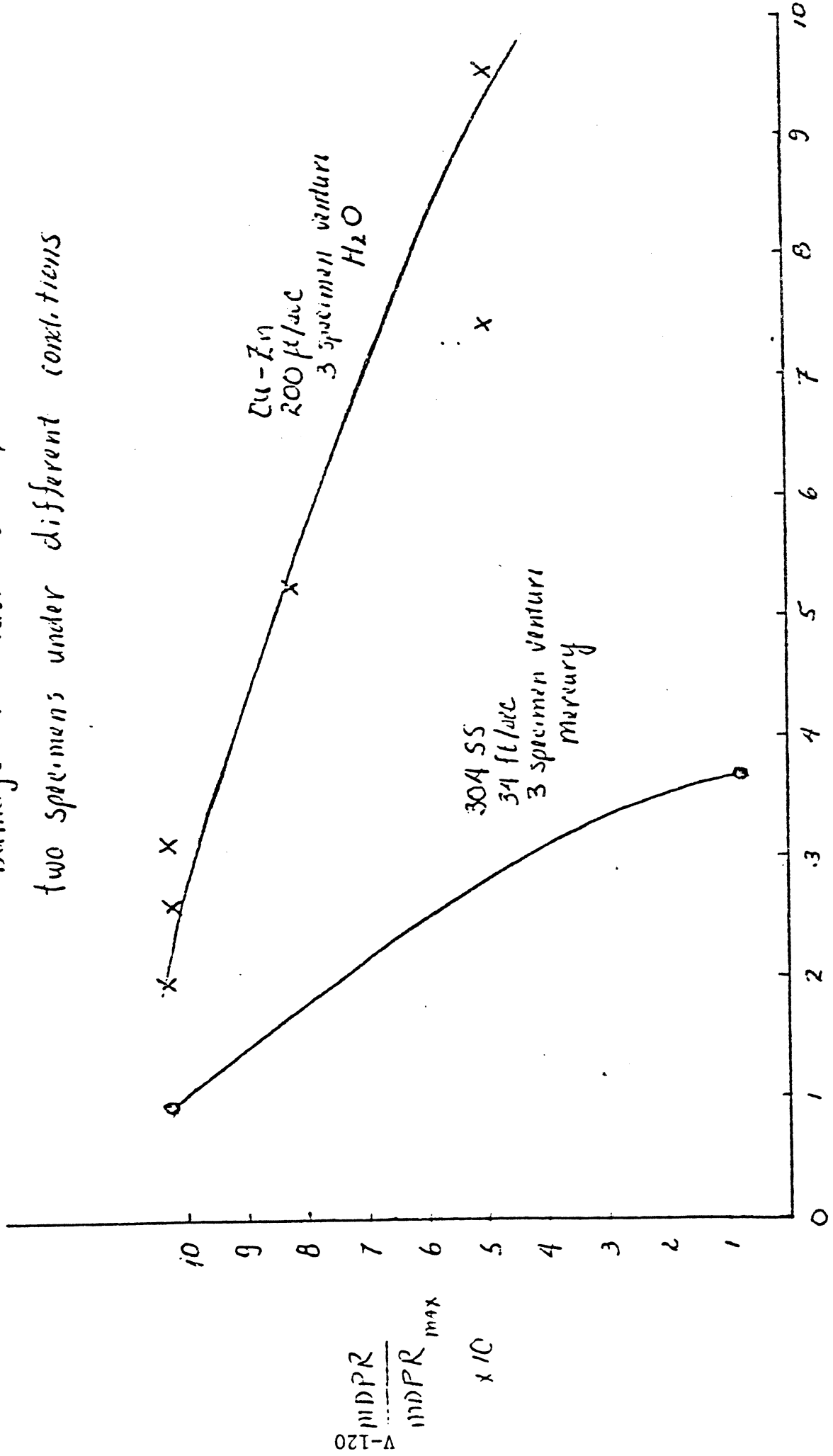
Lay-out of the two-dimensional water tunnel.



Sectional plan of the water tunnel test section.

Fig. 22 - Cavitating Venturi Facility, Indian Institute of Science, Bangalore

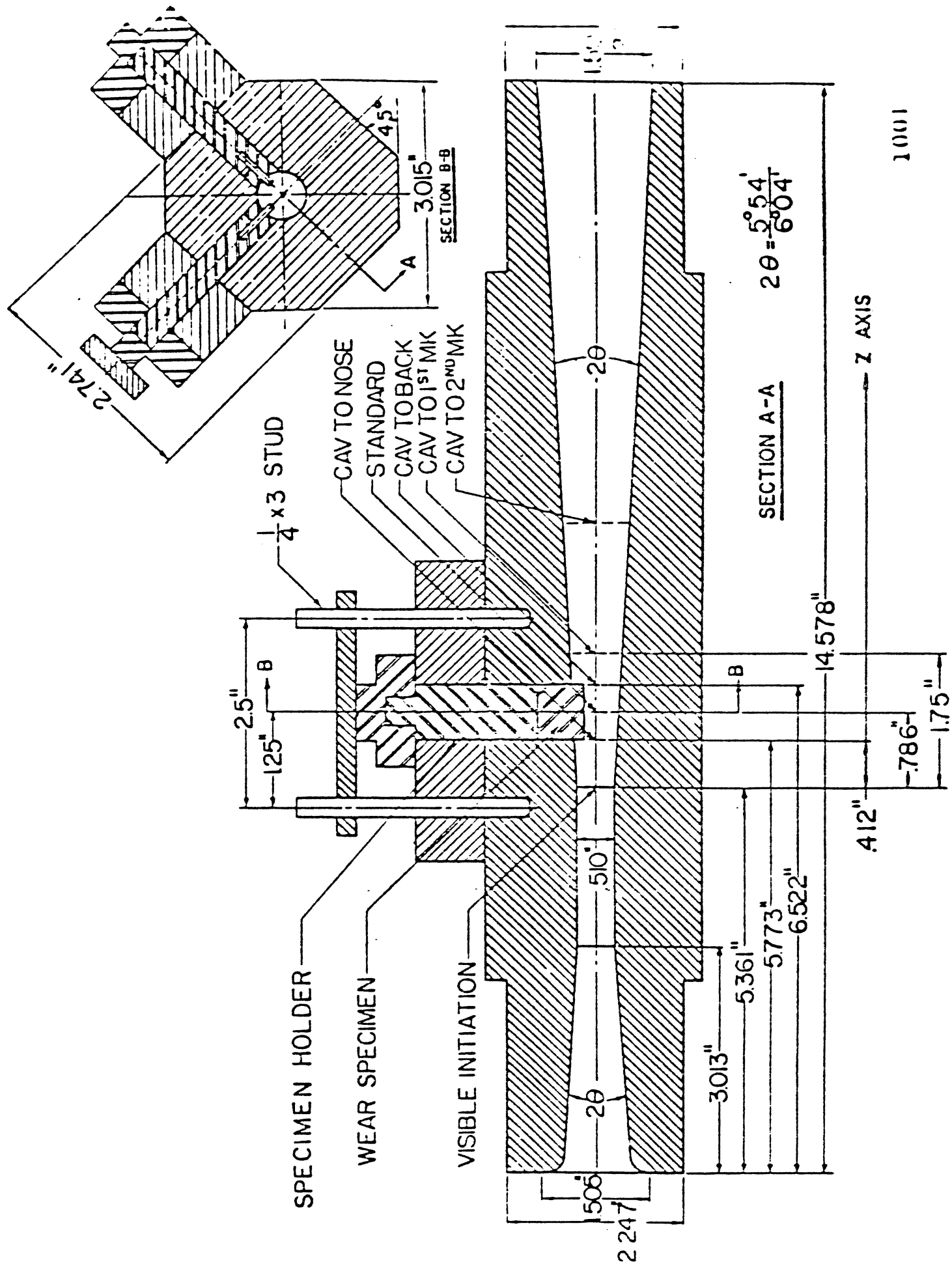
Damage vs Cavit. σ for
two specimens under different conditions



$$\text{CAVIT. } \sigma = \frac{P - P_v}{\rho V^2 / \text{kg}} \times 10^2$$

Fig. 23 - Normalized MDPR vs. Sigma

KIT



1001

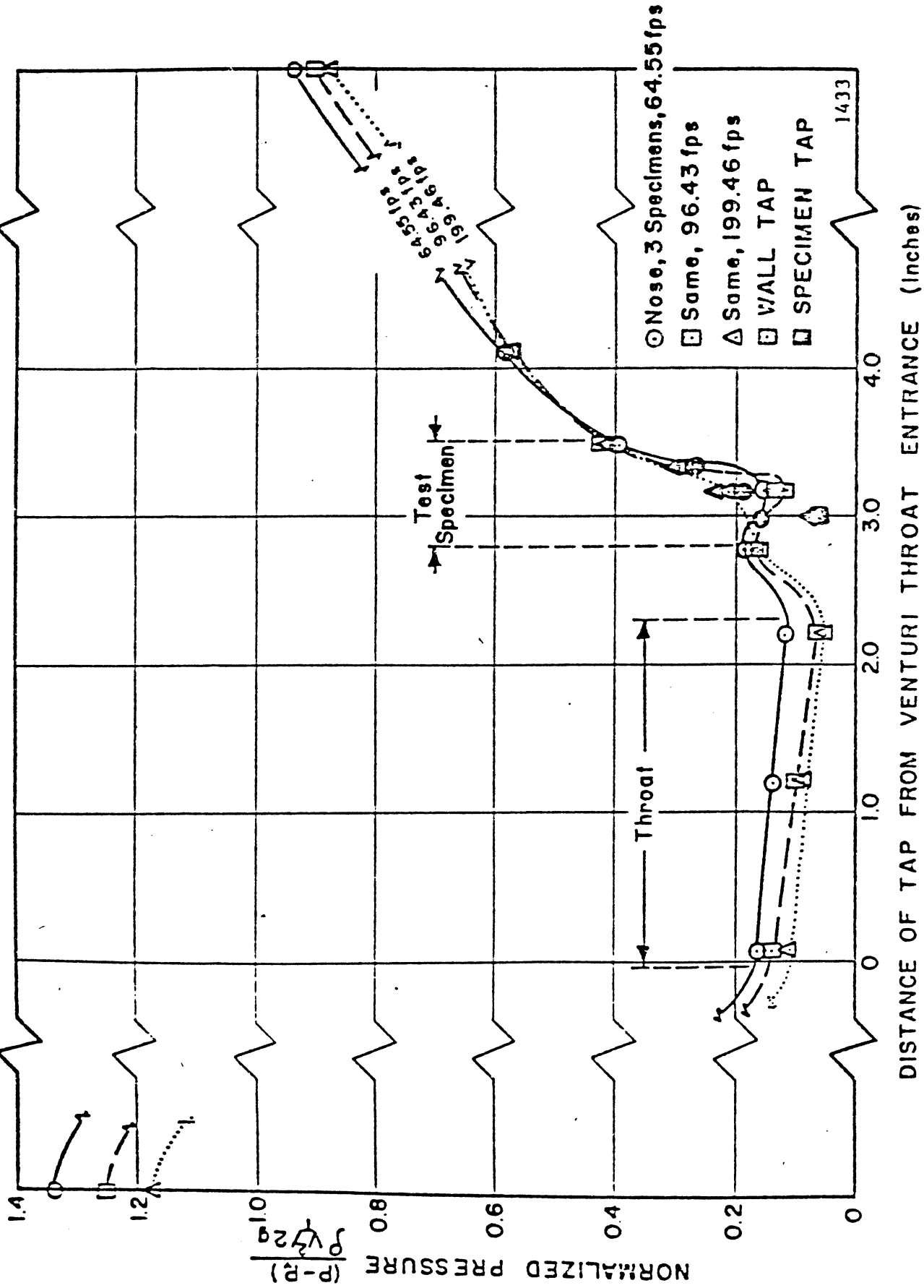


Fig. 25 -- Normalized pressure profile for 'cavitation to nose' with three specimens in water at various velocities.

(From ANL Final)
Reports

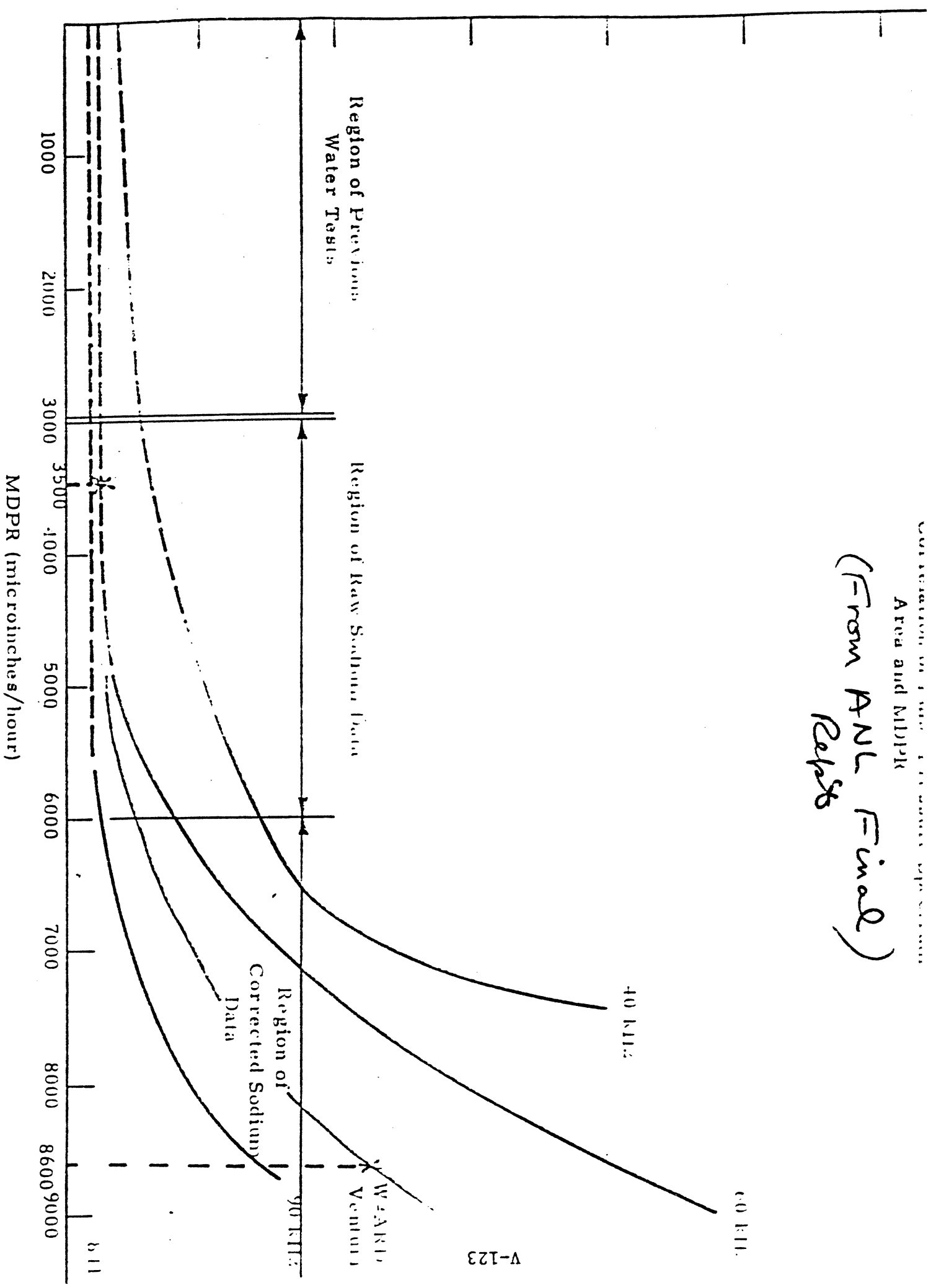


Fig. 27

"Typical Bubble Collapse Pulse Height Spectrum for Water in U-M Venturi"

(Actual ~~photo~~ plot from Veil paper to be substituted when available)

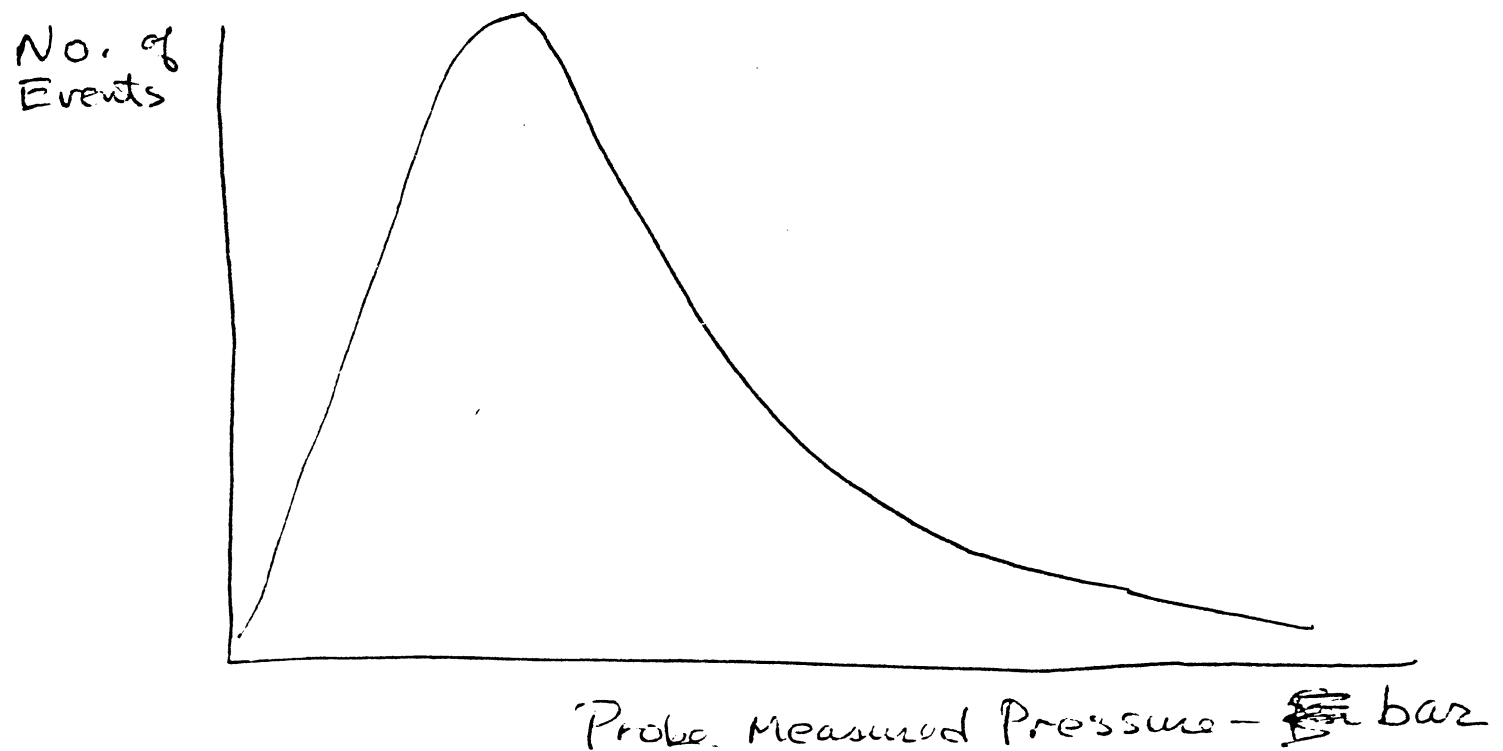
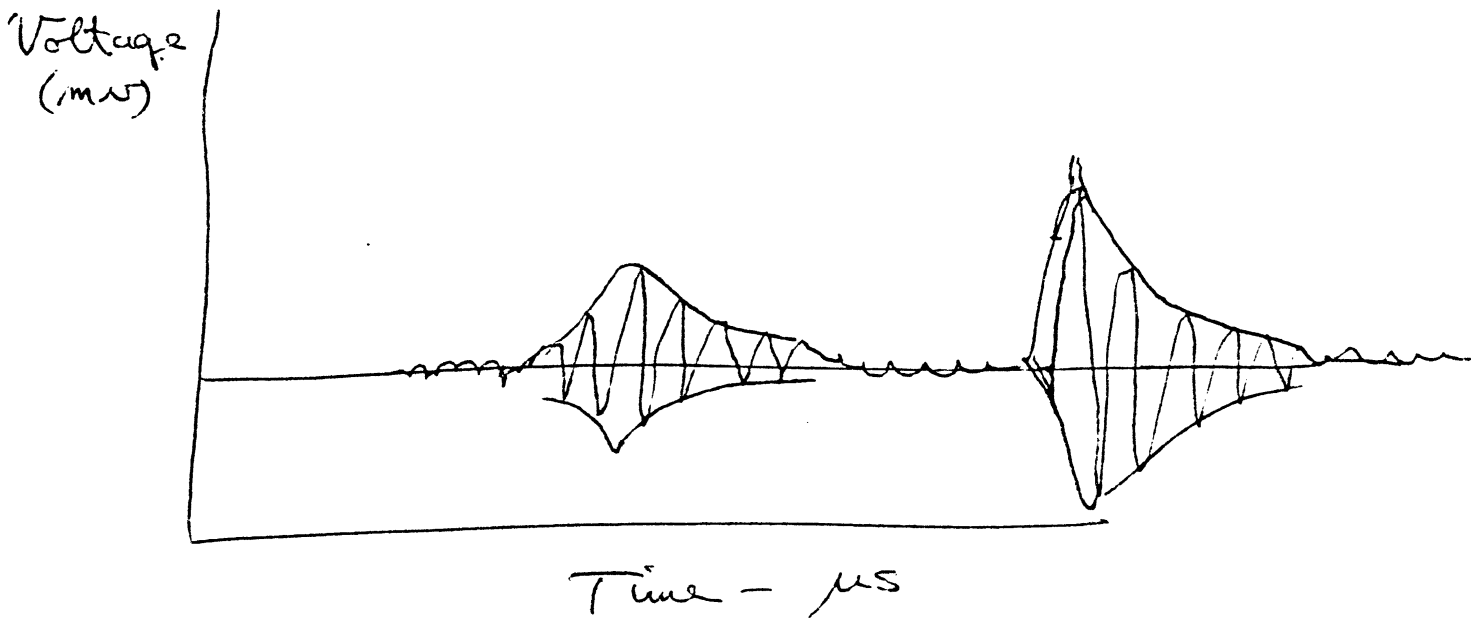


Fig 28

" Typical Individual Cavitation Bubble Collapse Pulses: U-M Microprobe Output in Water Venturi (Oscilloscope)



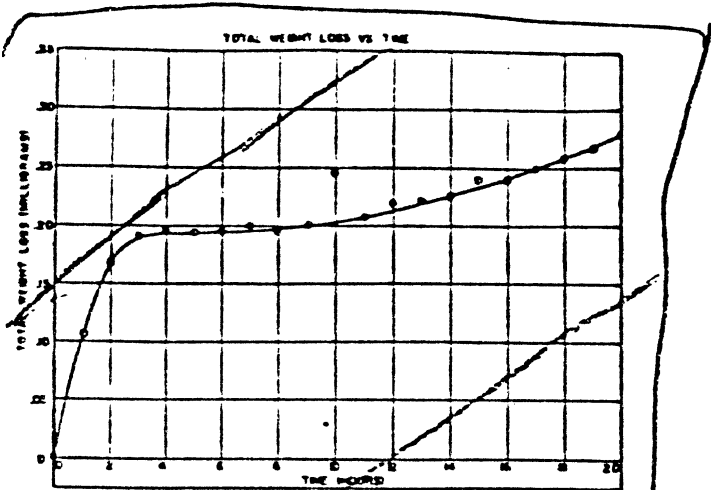


Fig. 5. Total weight loss vs time

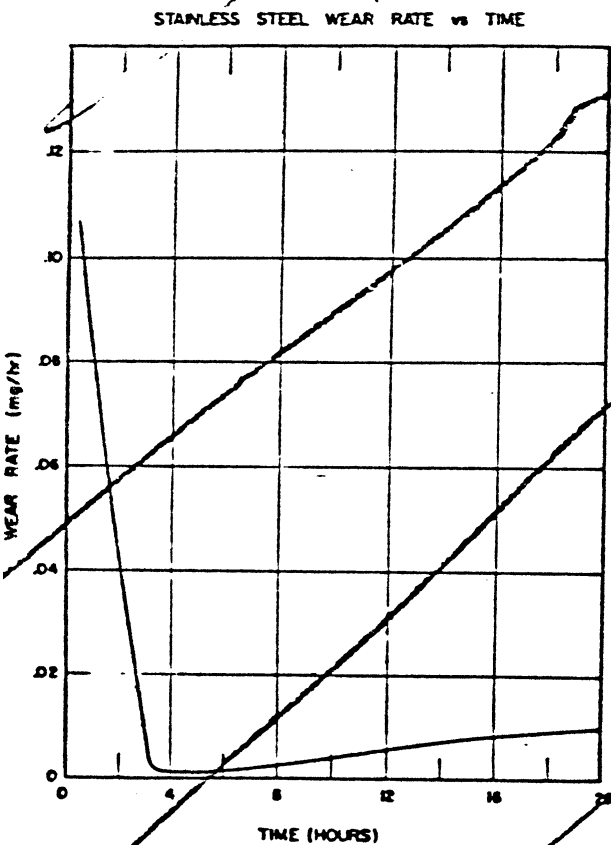


Fig. 6. Stainless steel wear rate vs time

grams of metal and counts per minute was determined (4).

VI. EXPERIMENTAL RESULTS

RADIOACTIVE WEAR RUN

Figure 5 shows the total weight loss from the wear specimens as a function of time. Cavitation damage was extensive during the first three hours with a total of 0.19 mg worn off in that time. By the fourth hour, the damage rate had become much less with the weight loss per unit time only

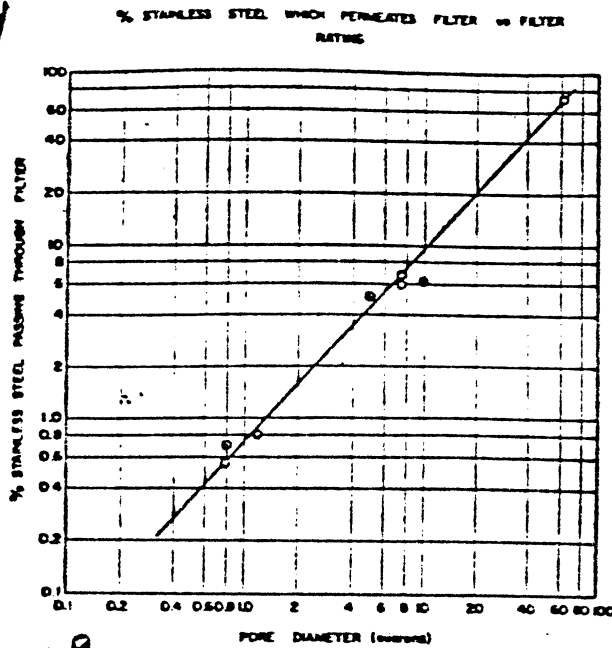


Fig. 7. Percentage stainless steel which permeates filter vs. filter rating.

1/10 of that observed initially. After the fourth hour the damage rate increased slowly and by the end of the experiment, it had reached a level which was about 1/5 of the initial wear rate. At the completion of the 20-hr experiment, a total of 0.28 mg had been lost from the stainless steel wear specimens.

Figure 6 is a differential plot of Fig. 5 and shows the damage rate as a function of time.

The effect of particles settling in the circulating stream was determined to be negligible by comparison of the first and third filter runs. As seen in Fig. 7, where data from all the runs are plotted, the cavitation particles in the stagnant stream had approximately the same size distribution as in the turbulent runs. If settling had occurred, the filter measurements would indicate a smaller percentage of large particles in the system.

The data were corrected for a small rate of random entrapment³ which was observed. The entrapment rate was assumed to be a function of the total activity present in the water, since the filter tests demonstrated the particle-size distribution to be constant with time:

$$\text{Rate of entrapment} = k \times \text{Activity (cpm/hr)}$$

The value of k was determined by measuring the slight decrease in activity of the circulating water with time after the radioactive specimens were

³ Entrapment refers to the phenomenon by which some particles are removed from the circulating stream by surface adsorption, lodging in crevices, etc.

Fig 29

29

Nucl. Sci + Engr., 14, 3, Nov, 1952
Walsh + Hammit

CAVITATION WEAR WITH RADIOISOTOPES

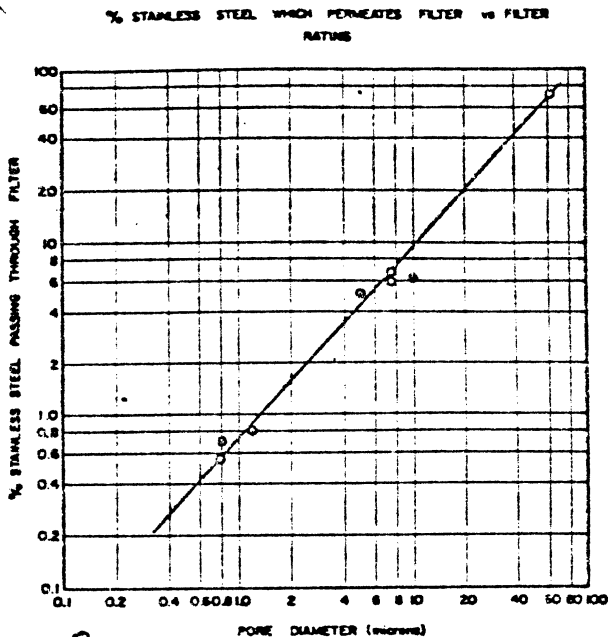


Fig 29
C. Walsh

29
FIG. 7. Percentage stainless steel which permeates filter vs. filter rating.